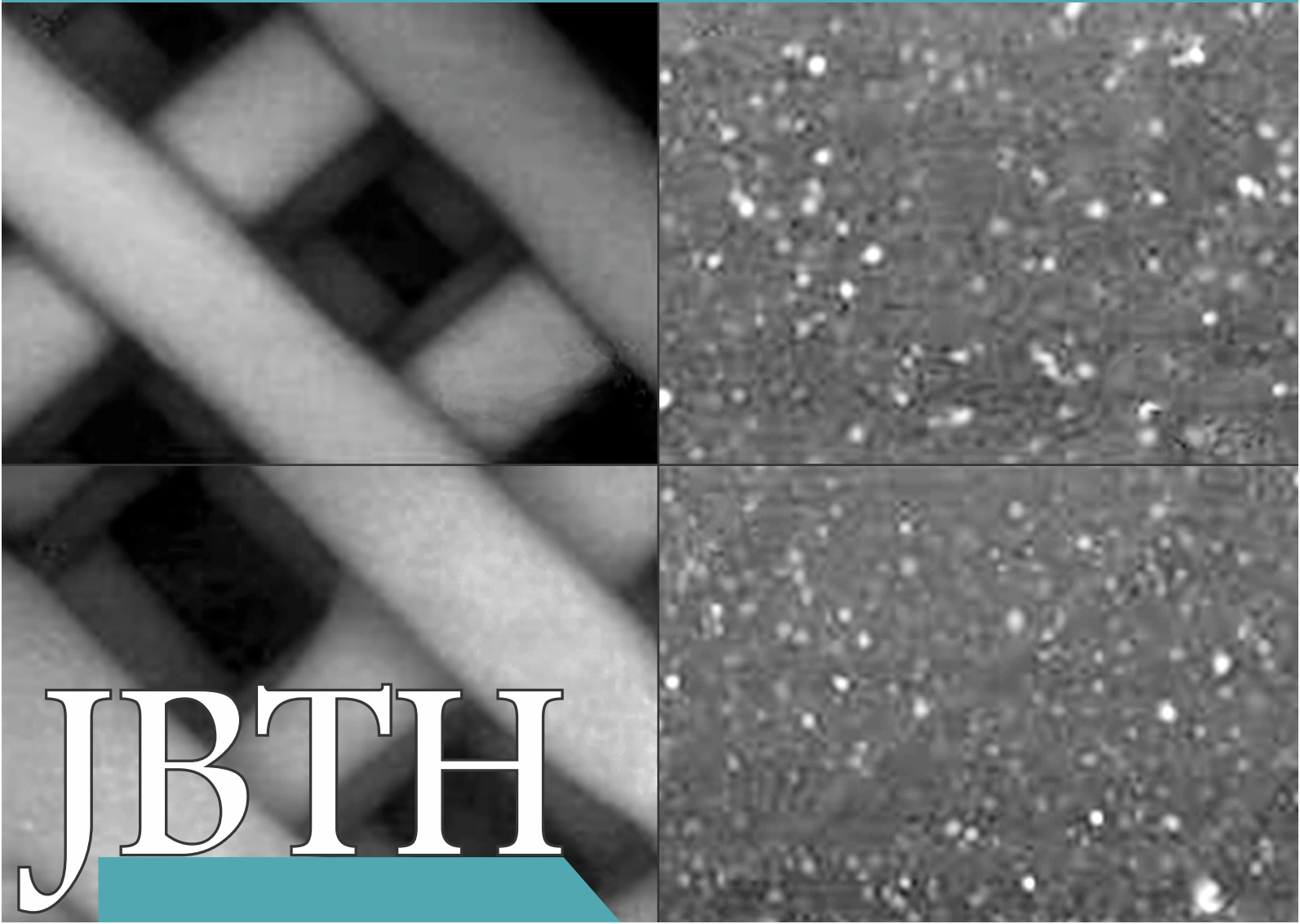




# Journal of Bioengineering, Technologies and Health

An Official Publication of  
SENAI CIMATEC



ISSN: 2764-5886 / e-ISSN 2764-622X

---

Volume 7 • Number 4 • December 2024

---



# **JOURNAL OF BIOENGINEERING TECHNOLOGIES AND HEALTH**

---

**An Official Publication of SENAI CIMATEC**

EDITOR-IN-CHIEF  
Leone Peter Andrade

PUBLISHED BY SENAI CIMATEC

Sistema FIEB



December 2024  
Printed in Brazil

# **JOURNAL OF BIOENGINEERING TECHNOLOGIES AND HEALTH**

---

An Official Publication of SENAI CIMATEC

## **EDITOR-IN-CHIEF**

Leone Peter Andrade

## **DEPUTY EDITOR**

Roberto Badaró

## **ASSISTANT DEPUTY EDITORS**

Alex Álisson Bandeira Santos (BR)

Josiane Dantas Viana Barbosa (BR)

Lilian Lefol Nani Guarieiro (BR)

Valéria Loureiro (BR)

## **ASSOCIATE EDITORS**

Alan Grodzinsky (US)

Bruna Aparecida Souza Machado (BR)

Carlos Coimbra (US)

Eduardo Mario Dias (BR)

Frank Kirchner (DE)

Jorge Almeida Guimarães (BR)

Milena Soares (BR)

Preston Mason (US)

Sanjay Singh (US)

Steven Reed (US)

Valter Estevão Beal (BR)

## **STATISTICAL ASSOCIATE EDITOR**

Valter de Senna (BR)

## **EDITORIAL BOARD**

Carlos Augusto Grabois Gadelha (BR)

Durvanei Augusto Maria (BR)

Eliane de Oliveira Silva (BR)

Erick Giovani Sperandio Nascimento (BR)

Fernando Pellegrini Pessoa (BR)

Francisco Uchoa Passos (BR)

George Tynan (US)

George Tynan (US)

Gilson Soares Feitosa (BR)

Gisele Olímpio da Rocha (BR)

Hercules Pereira (BR)

Herman Augusto Lepikson (BR)

Hermano Krebs (US)

Idelfonso Bessa dos Reis Nogueira (NO)

Immanuel Lerner (IR)

Ingrid Winkler (BR)

James Chong (KR)

Jeancarlo Pereira dos Anjos (BR)

José Elias Matieli (BR)

Joyce Batista Azevedo (BR)

Larissa da Silva Paes Cardoso (BR)

Lusiada Portugal (PT)

Luzia Aparecida Tofaneli (BR)

Maria Lídia Rebello Pinho Dias (BR)

Mario de Seixas Rocha (BR)

Maximilian Serguei Mesquita (BR)

Regina de Jesus Santos (BR)

Renelson Ribeiro Sampaio (BR)

Roberto de Pinho (BR)

Rodrigo Santiago Coelho (BR)

Sanjay Mehta (US)

Vidal Augusto Zapparoli Castro Melo (BR)

Vilson Rosa de Almeida (BR)

## **PRODUCTION STAFF**

Luciana Knop, Managing Editor

Valdir Barbosa, Submissions Manager

## Original Articles

**Strengthening Entomological Surveillance in Rio de Janeiro: Analysis and Control of Arboviroses Using the LIRAA Toll from 2015 to 2019 ..... 320**

Cristina Conceição Rocha Guedes, Maria de Lourdes Ferraz Heleodoro, Carlos Augusto Correia Lima Reis, Charles da Silva Bezerra, Rodrigo Gomes Marques Silvestre, Aloisio Santos Nascimento Filho, Hugo Sabab

**Development and Characterization of a PLA/NHA Composite Scaffold Manufactured by 3D Printing ..... 327**

Arthur João Reis Lima Rodovalho, Willams Teles Barbosa, Jaqueline Leite Vieira, Caio Athayde de Oliva, Ana Paula Bispo Gonçalves, Sabrina Arcaro, Josiane Dantas Viana Barbosa

**Development Process of a Medicinal Cannabidiol Dosing Pen ..... 333**

José Santos Damasceno, Gabriel Barreto Teles Fonseca

**Development of a Sunscreen Formulation Enriched with *Camellia sinensis* Extract in the Treatment of Melasma ..... 337**

Amanda Cerqueira Ribeiro Santos, Esther Gabrielle Ribeiro Nascimento, Isis Santos Silva, Júlia Alves Gribel de Oliveira, Rainy Teixeira Gonzaga, Tatiana Oliveira do Vale, Érica Patrícia Lima Pereira

**Influence of the Defects in a Graphene Oxide on the Reduction via Ascorbic Acid for Structuring Aerogels ..... 342**

Camila Miranda Fonseca Duarte, Eliel Gomes da Silva Neto, Iara de Fatima Gimenez

**Evaluating the Influence of Processing Conditions on Colloidal Stability and Particle Size in Fibrillated Nanocellulose ..... 348**

Marina Andrade, Ana Paula Gonçalves, Lucas Horiuchi, Vinícius Oliveira, Rodrigo Polkowski

**Hybrid Polyamide Membranes Obtained by the Immersion Precipitation Method ..... 352**

Joanne Graziela Andrade Mendes, Damares Oliveira de Jesus Ferreira, Airan Magalhães Moura, Carlos Antônio Pereira de Lima, Arthur de Sousa Ferreira, Keila Machado de Medeiro

**Ecotoxicity Study Using Dibenzothiophene and Mercury Chloride in "Brine Shrimp" ..... 358**

Melise Lemos Nascimento, Madson Moreira Nascimento, Gisele Olímpio da Rocha, Jailson Bittencourt de Andrade

**Rare Earth Elements in Bahia, Brazil: Potential for Global Production ..... 363**

Alexandre Pereira Wentz, Maria das Graças Andrade Korn, Jeancarlo Pereira dos Anjos, Fabiano Ferreira de Medeiros, Paulo Henrique Marques Modesto, Fabrício Dias Rodrigues, Sara Silva Alves, Alexandre Porto, Caio Silva Assis Felix, Eduarda de Lima Guimarães, Lilian Lefon Nani Guarieiro

**Application of a Preprocessing Pipeline to VIS-NIR Data for Predicting Soil Nutrient Concentration Values ..... 369**

Eduardo Menezes de Souza Amarante, Julian Santana Liang, Carlos Alberto Campos da Purificação, Rômulo Alexandrino Silva

**An Adjusted Model of Proton Conductivity in Nafion® Membranes ..... 375**

Artur Santos Bispo, Chrislaine do Bomfim Marinho, Fernando Luiz Pellegrini Pessoa, José Luis Gonçalves de Almeida

## Systematic Review / Bibliometric Articles

**Anaerobic Digestion of *Agave sisalana*: Existing Data, Trends, and Potential Applications ..... 380**

Julio C.A. Toqueiro, Otanéa B. Oliveira, Oscar F.H. Adarme, Gustavo Mockaitis

**Sustainable AI Applied to Project Management: A Literature Review ..... 386**

Hérica de Souza Araújo, Thiago Barros Murari, Anusio Menezes Correia, Erick G. Sperandio Nascimento

Game Theory to Promote the Sustainable Development of the Pharmaceutical Industry .....392  
Rosivaldo Cardoso Santiago, Aloísio Santos Nascimento Filho, Bruna Aparecida Souza Machado, Hugo Saba Pereira Cardoso

## **Case Study**

3D Modeling of Hospital Environments: Case Study to Improve Patient Safety ..... 399

Luciane Oliveira Lima, Marcelly Ribeiro Bulcão Macêdo, Laura Ferreira Morais de Souza, Camille Pereira Guimarães, Andressa Clara Barbosa de Araujo, Sabrina Cortiana Rodrigues Lima, Cristiane Agra Pimentel

## **Instructions for Authors**

## **Statement of Editorial Policy**

## **Checklist for Submitted Manuscripts**

**The Journal of Bioengineering, Technologies and Health (JBTH)** is an official publication of the SENAI CIMATEC (Serviço Nacional de Aprendizagem Industrial - Centro Integrado de Manufatura e Tecnologia). It is published quarterly (March - June - September - December) in English by SENAI CIMATEC – Avenida Orlando Gomes, 1845, Piatã, Zip Code: 41650-010, Salvador-Bahia-Brazil; phone: (55 71) 3879-5501. The editorial offices are at SENAI CIMATEC.

### Editorial Office

Correspondence concerning subscriptions, advertisements, claims for missing issues, changes of address, and communications to the editors should be addressed to the Deputy Editor, Dr. Roberto Badaró, SENAI CIMATEC (Journal of Bioengineering, Technologies and Health – JBTH) – Avenida Orlando Gomes, 1845, Piatã, Zip code: 41650-010, Salvador-Bahia-Brazil; phone: (55 71) 3879-5501; or sent by e-mail: [jbth@fieb.org.br](mailto:jbth@fieb.org.br) / [jbth.cimatec@gmail.com](mailto:jbth.cimatec@gmail.com).

### Permissions

The permissions should be asked to the Editor in Chief of the Journal of Bioengineering, Technologies and Health and SENAI CIMATEC. All rights reserved. Except as authorized in the accompanying statement, no part of the JBTH may be reproduced in any form or by any electronic or mechanic means, including information storage and

retrieval systems, without the publisher's written permission. Authorization to photocopy items for internal or personal use, or the internal or personal use by specific clients is granted by the Journal of Bioengineering, Technologies and Health and SENAI CIMATEC for libraries and other users. This authorization does not extend to other kinds of copying such as copying for general distribution, for advertising or promotional purposes, for creating new collective works, or for resale.

### Postmaster

Send address changes to JBTH, Avenida Orlando Gomes, 1845, Piatã, Zip Code: 41650-010, Salvador-Bahia-Brazil.

### Information by JBTH-SENAI CIMATEC

Address: Avenida Orlando Gomes, 1845, Piatã, Zip Code: 41650-010, Salvador-Bahia-Brazil

Home-page: [www.jbth.com.br](http://www.jbth.com.br)

E-mail: [jbth@fieb.org.br](mailto:jbth@fieb.org.br) / [jbth.cimatec@gmail.com](mailto:jbth.cimatec@gmail.com)

Phone: (55 71) 3879-5501 / 3879-5500 / 3879-9500



DOI:10.34178

ISSN: 2764-5886 / e-ISSN 2764-622X

### Copyright

© 2024 by Journal of Bioengineering,  
Technologies and Health  
SENAI CIMATEC  
All rights reserved.

---

**COVER:** SEM of scaffolds (c-d) PLA/nHA-A1 and (e-f) PLA/nHA-A2. Development and Characterization of a PLA/NHA Composite Scaffold Manufactured by 3D Printing by Arthur João Reis Lima Rodovalho et al. J Bioeng. Tech. Health 2024;7(4):330.



## Strengthening Entomological Surveillance in Rio de Janeiro: Analysis and Control of Arboviroses Using the LIRAA Toll from 2015 to 2019

Cristina Conceição Rocha Guedes<sup>1,2\*</sup>, Maria de Lourdes Ferraz Heleodoro<sup>1,2</sup>, Carlos Augusto Correia Lima Reis<sup>1,2</sup>, Charles da Silva Bezerra<sup>2</sup>, Rodrigo Gomes Marques Silvestre<sup>3</sup>, Aloisio Santos Nascimento Filho<sup>2</sup>, Hugo Sabab<sup>4</sup>

<sup>1</sup>Fundação Oswaldo Cruz, Rio de Janeiro, Rio de Janeiro; <sup>2</sup>SENAI CIMATEC University; Salvador, Bahia; <sup>3</sup>Federal University of Paraná; Curitiba, Paraná; <sup>4</sup>State University of Bahia; Salvador, Bahia, Brazil

The triple arboviruses—Dengue, Zika, and Chikungunya—pose significant challenges for public managers. This study aimed to demonstrate the strengthening of entomological surveillance to control arboviruses using LIRAA as a tool, with an analysis of Rio de Janeiro from 2015 to 2019. The method used was quantitative and exploratory, analyzing data from LIRAA Epidemiological Reports and relevant legislation. Results indicated that LIRAA effectively identifies mosquito infestation hotspots and guides vector control actions. The conclusion underscores that entomological surveillance is critical for preventing arbovirus transmission, emphasizing the importance of continuing such practices to safeguard public health and ensure a safer environment.

**Keywords:** Rapid Infestation Survey of *Aedes aegypti*. Entomological Surveillance. Triple Arboviruses. Rio de Janeiro.

The arboviruses Dengue, Chikungunya, and Zika are viral diseases caused by Flaviviruses and Alphaviruses. Dengue virus and its serotypes have circulated in Brazil since the 1980s, while Chikungunya and Zika emerged around 2014 and 2015. Classified as neglected diseases, these arboviruses are a significant global public health threat due to their similar clinical symptoms, progression to severe conditions, maternal-fetal contamination syndromes, and increased lethality during epidemic outbreaks [1–4].

Arboviruses are primarily transmitted to humans through the bite of arthropod vectors, specifically mosquitoes of the *Culicidae* family belonging to the genus *Aedes* (*Aedes aegypti* and *Aedes albopictus* females). Additional modes of viral transmission include transfusion routes and, for Zika, sexual and transplacental transmission, which caused a surge in microcephaly cases among babies born to infected mothers [2,5].

Certain factors increase vulnerability to arboviruses, including climatic conditions, environmental challenges, socioeconomic factors, and unplanned urban growth. These factors contribute to structural deficiencies in essential public services such as sanitation, garbage collection, and access to clean water [4–8].

### Public Policies to Combat Arboviruses

In 1996, the *Aedes aegypti* Eradication Plan (PEAA) was implemented with a decentralized, multisectoral approach. Actions focused on combating adult mosquitoes using vector control, water treatment of breeding sites, and insecticide applications. However, the plan was discontinued due to health and environmental risks associated with prioritizing insecticides. Measures such as breeding site elimination, environmental education, and sanitation were overlooked [9].

In response to rising dengue cases, the Ministry of Health launched the National Plan to Combat Dengue (PNCD) in 2002, revised in 2006.

Updates included strengthened information campaigns, social mobilization, epidemiological and entomological surveillance, sanitation measures, integration with primary care services, training for endemic agents, and indicators to evaluate action effectiveness [1,10,11].

Received on 20 September 2024; revised 28 November 2024.  
Address for correspondence: Cristina Conceição Rocha Guedes. Fundação Oswaldo Cruz. Av. Brasil, 4365 - Manguinhos. Zipcode: 21040-900. Rio de Janeiro, RJ, Brazil.  
E-mail: cristina.guedes@fiocruz.br.

With the emergence of new arboviruses in 2015, additional guidelines were introduced for early diagnosis, case management, and public health service reinforcement. That year's Zika virus outbreak highlighted the need for mass vaccination or specific antivirals [12]. Collaborative efforts across the Ministry of Health and state and municipal health departments demonstrated the importance of support networks to mitigate public health impacts [13,14].

This study aimed to present an analysis of the entomological indicator LIRAA in the 92 municipalities of Rio de Janeiro from 2015 to 2019 during outbreaks of the triple arboviruses.

## Materials and Methods

This research employed a quantitative, descriptive, and exploratory approach, analyzing data from 92 municipalities in Rio de Janeiro between 2015 and 2019. The method involved numerical data extracted from LIRAA Epidemiological Reports for the defined years. These reports facilitated an analysis of the magnitude of arbovirus-related challenges during this period.

The study also involved bibliographic and documentary research, utilizing scientific articles, technical documents, federal legislation, and data from sources such as Gov.br, the Health Surveillance System Panel, and the Brazilian Institute of Geography and Statistics (IBGE).

### LIRAA: An Entomological Surveillance Tool

Since 2003, LIRAA (Rapid Infestation Survey of *Aedes aegypti*) has played a critical role in combating arboviruses. Known as the "Dengue Map," this tool enables municipal managers to plan vector control actions such as breeding site elimination, insecticide application, and public awareness campaigns. In 2017, LIRAA became mandatory for municipalities, linking report submission to financial resource allocation [15–17].

The method, revised in 2013, evaluates infestation using Breteau and Predial indices, with

standardized procedures for simplified diagnosis. Table 1 outlines key methodological aspects of LIRAA.

## Results and Discussion

We analyzed the variables extracted from the LIRAA Reports from 2015 to 2019 from the state of Rio de Janeiro using: number of municipalities that delivered the LIRAA Report and percentage; the results of the Building Infestation Index, demonstrated by the number of municipalities that had satisfactory results, at risk and on alert and their respective percentages; number of municipalities with simultaneous presence of *Aedes aegypti* and *albopictus*; predominant types of deposits; number of strata visited and the percentages of municipalities that presented their Breteau Indexes with satisfactory, alert and risk results.

Teams of endemic disease control agents (ACE) are responsible for all fieldwork and define the visitation strata, which are geographically delimited areas within a municipality or region previously selected for sampling and data collection. Neighborhoods, census sectors, blocks, or other territorial divisions can be listed and segmented into smaller parts, facilitating the assessment and analysis of the infestation and allowing a more practical approach to combating diseases transmitted by mosquitoes [19].

The strata are important in the *Aedes aegypti* Infestation Index Survey (LIRAA), allowing a more detailed and specific assessment of the transmitting mosquito's presence in different parts of a municipality. The classification of strata as satisfactory, at risk, or at risk based on infestation rates collected in these areas helps to identify where vector foci are concentrated and guides control and prevention actions [15,18].

Rio de Janeiro hosted several international sporting events in 2014, 2016 and 2018. In the second half of 2015, the first cases of Chikungunya and Zika were recorded, in addition to dengue [4]. During this period, its municipalities carried out LIRAA systematically and continuously. They recorded for



**Table 1.** LIRAA methodological aspects.

Methodological Aspects	Goal
Geographic Recognition (RG)	As a preliminary and essential activity for programming the index survey. It involves the identification and delimitation of the areas to be evaluated, considering geographic and population aspects.
Property inspections	Endemic disease control agents conduct inspections of selected properties, checking for the presence of breeding sites, such as containers with stagnant water.
Data collect	During inspections, information is collected about the presence of mosquito larvae, the number of containers with standing water, and other characteristics relevant to assessing the infestation.
Calculation of Infestation Rates	Based on the data collected, infestation rates are calculated, such as the Breteau Index (number of containers with mosquito larvae/100 properties inspected), and the Building Index (percentage of properties with the presence of larvae).
Data Analysis and Consolidation	To identify areas with a higher risk of disease transmission and guide vector control actions. Allowing reliable estimates of <i>Aedes aegypti</i> infestation rates to be obtained quickly and economically, contributing to entomological surveillance and the fight against arboviruses

health authorities local epidemiological conditions, detailing the types of deposits and breeding sites found in the strata of the municipalities, defined as satisfactory, alert, and at risk, according to data obtained from inspections of properties, vacant land, and possible sources that could be potential mosquito breeding grounds.

Table 2 presents the results of the Reports and variants analyzed; there was no adherence to delivery of the LIRAA for 100% of the municipalities, which could harm the state's actions, as it does not describe the actual situation of the municipalities that did not present the results. However, from 2018 onwards, the number of participating municipalities increased due to mandatory delivery. Reflecting about the application of the management tool and as agreed by the Rio de Janeiro Bipartite Commission, the method became a mandatory and routine activity in arbovirus prevention and control actions, as well as the understanding that decentralization of management actions combat, allowed greater autonomy and capacity for municipalities to conduct monitoring and report infestation rates, according

to data from the Reports, varying in delivery results during the established periods of 2015:68–82 municipality; 2016: 73–75 municipalities; 2017: 64–88 municipalities; 2018: 89–91 municipalities and 2019: 88–90 municipalities An increase in the number of municipalities with satisfactory results can be observed over the years: 2015: Ranged from 29.3% (March) to 57.5% (October); 2016: Ranged from 59.5% (May) to 86.03% (July); 2017: Ranged from 52.4% (March) to 76.1% (October); 2018: Ranged from 35.6% (January) to 61.8% (May) and 2019: Ranged from 45.5% (May) to 68.5% (August).

Variations in the percentage of municipalities at different infestation levels are observed over the months and years due to the increase in the percentage of municipalities at satisfactory levels. There was also an increase in the strata evaluated, indicating higher percentages of alert or risk in the municipalities during the period evaluated. Demonstrating the possibility of each region expressing seasonal variations within the same state implies mosquito infestation within the region.

**Table 2.** Results of variables by health regions from 2015 to 2019 in Rio de Janeiro, Brazil.

Year	LIRAA	LIRAA Report (%) <sup>1</sup>	Number of Municipality (%)	Number of Municipality Alert (%)	Number of Municipality at Risk (%)	Number of Municipality with <i>Aedes aegypti</i> and <i>albopictus</i>	Deposits <sup>2</sup>	Strata (N) <sup>3</sup>	S (%) <sup>4</sup>	Alert (%)	Risk (%)
2015	January	76 (82.61)	32 (42.11)	44 (57.89)	0 (0)	49	A2 B	843	52.0	43.80	3.50
	March	82 (89.10)	23 (29.30)	52 (63.40)	6 (7.30)	56	A2 B	874	37.30	51.10	11.60
	May	68 (73.90)	29 (42.60)	37 (54.40)	2 (2.90)	49	A2 B	819	52.63	43.22	4.15
	October	80 (86.96)	46 (57.50)	33 (41.25)	1 (1.25)	45	A2 B	891	57.35	38.95	3.70
2016	May	74 (80.40)	44 (59.50)	29 (39.20)	1 (1.40)	52	A2 B	844	61.50	36.30	2.30
	July	73 (79.03)	63 (86.03)	10 (13.07)	0 (0)	31	A2 B	815	75.58	23.44	0.98
	October	75 (81.50)	54 (72.0)	20 (26.70)	1 (1.30)	44	A2 B	880	66.90	30.80	2.30
2017	January	64 (69.60)	39 (60.90)	24 (37.50)	1 (1.60)	39	C, A2 D2, B	808	58.50	38.0	3.50
	March	84 (91.30)	44 (52.40)	35 (41.60)	5 (6.0)	63	C, A2 D2, B	950	56.40	39.10	4.50
	May	85 (92.40)	47 (55.30)	34 (40.0)	4 (4.70)	62	C, A2 D2, B	884	61.50	30.50	8.0
	October	88 (94.60)	67 (76.10)	21 (23.86)	0 (0)	38	C, A2 D2, B	875	69.50	29.50	1.20
2018	January	90 (97.80)	32 (35.60)	51 (56.70)	7 (7.80)	73	C, A2 D2, B	934	44.80	46.0	9.20
	February	89 (96.70)	35 (39.30)	49 (55.10)	5 (5.60)	68	C, A2 D2, B	922	49.10	43.50	7.40
	May	90 (97.80)	51 (56.70)	34 (37.80)	5 (5.60)	67	C, A2 D2, B	935	61.80	33.70	4.50
	August	89 (96.70)	48 (53.90)	40 (44.90)	1 (1.10)	52	C, A2 D2, B	692	55.50	40.50	4.0
	October	91 (98.90)	45 (49.50)	43 (47.30)	3 (3.30)	59	C, A2 D2, B	929	49.70	44.20	6.0
2019	February	90 (97.80)	53 (58.90)	36 (40.0)	1 (1.10)	58	C, A2 D2, B	938	64.60	32.90	2.50
	May	88 (95.70)	40 (45.50)	46 (52.30)	2 (2.30)	61	C, A2 D2, B	909	50.10	43.20	6.70
	August	89 (96.70)	61 (68.50)	25 (28.10)	3 (3.40)	48	C, A2 D2, B	915	69.20	28.60	2.20
	October	89 (96.70)	55 (61.80)	32 (36.0)	2 (2.20)	53	C, A2 D2, B	916	57.90	37.0	5.10

Source: LIRAA Rio de Janeiro reports from 2015 to 2019.

1: Number of municipality that delivered the LIRAA Report.

2: Types of deposits predominant.

3: Number strata.

4: Satisfactory.

However, it must also be analyzed whether all the combat measures adopted by the municipalities are effective, causing a reduction in the risk and alert strata. Regarding the simultaneous presence of the two vectors *Aedes aegypt* and *albopictus*, a significant increase in samples was observed, according to the results analyzed: 2015: Ranged from 45 to 56 municipalities; 2016: Ranged from 31 to 52 municipalities; 2017: Ranged from 38 to 63 municipalities; 2018: Ranged from 52 to 73 municipalities; 2019: Ranged from 48 to 61 municipalities. *Aedes albopictus* is highlighted as a vector for transmission of the Chikungunya virus.

This increase is related to urban infrastructure, environmental changes, and deforestation, as wild mosquitoes have adapted to artificial breeding sites, making it necessary to intensify vector management.

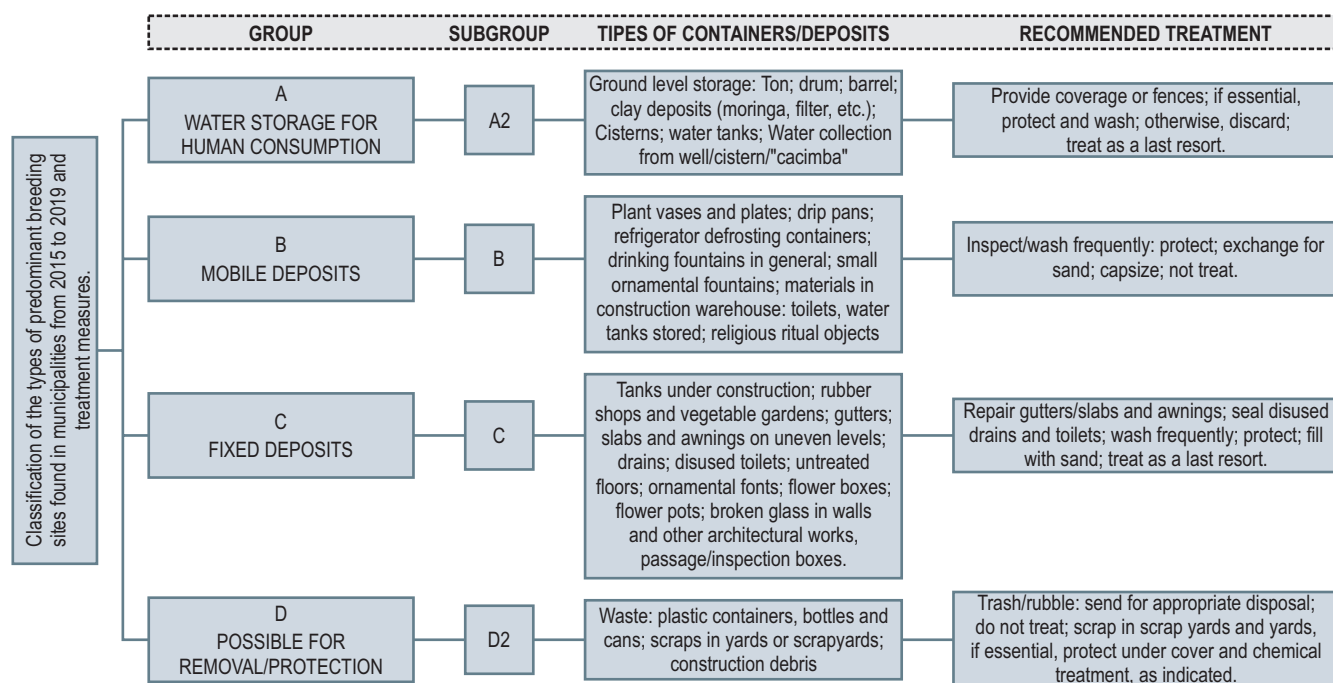
In the diagnosis of the LIRAA tool, the breeding sites found were also highlighted, with a predominance of types of deposits A2, B, C, D2 throughout the analyzed period, determining the need for multidisciplinary actions involving

sanitation actions, water supply, disposal of waste, with the participation of government bodies and the Master Plans of each municipality. It also demonstrates the need for ACEs to guide the population in creating continuous and regular monitoring of possible water storage locations and potential breeding sites for the two mosquito species (Figure 1). Classification and actions indicated regarding *Aedes aegypt* breeding sites.

These observations suggest progress in the management of infestation rates but also highlight the need for continuous and adaptive strategies to face persistent challenges in the fight against *Aedes aegypti* and *Aedes albopictus*, mainly focusing on areas that presented alert and risk situations and municipalities that share borders, which can increase the spread of vectors and diseases, through the movement of people and interconnected transport networks.

The strategy public managers adopt involves establishing an intersectoral integration network among the health, environment, education, and sanitation sectors. Key actions include intensifying

**Figure 1.** Classification of the types of predominant breeding sites found in municipalities from 2015 to 2019 and treatment measures.



Source: Adapted from the LIRAA Manual, (2013) [15].

education and public awareness campaigns, particularly during peak disease seasons, and enhancing monitoring efforts through the adoption of advanced technologies for vector control. This strategy also focuses on preventing outbreaks in urban and rural areas by regularly inspecting high-risk locations such as abandoned buildings, garbage dumps, and containers used for plants and animals.

Additionally, the plan emphasizes significant investments in basic sanitation infrastructure and waste management systems, including efficient garbage collection processes. Training and capacity-building programs for ACE teams are prioritized, alongside support for research and development of innovative technologies and tools. Climate monitoring is also integrated into this approach to predict and mitigate risks effectively.

## Conclusion

Entomological surveillance in Rio de Janeiro from 2015 to 2019 demonstrated the effectiveness of LIRAA in identifying mosquito infestation hotspots and guiding strategic public health actions. The tool proved essential for continuous monitoring, vector elimination, and timely intervention.

The results underscore the importance of ACE professionals, whose roles include inspecting properties, eliminating outbreaks, and educating the public on water storage and waste management. The regular use of LIRAA has significantly contributed to reducing the burden of arboviruses on public health systems in Rio de Janeiro, emphasizing its value as a practical and impactful tool.

## Acknowledgments

We acknowledged the Oswaldo Cruz Foundation for supporting this study.

## References

1. Brasil. Lei nº 13.596, de 8 de janeiro de 2018. Altera a Lei nº 7.670, de 8 de setembro de 1988, para definir as doenças negligenciadas e estabelecer diretrizes para ações de vigilância, controle e eliminação dessas doenças. D.O. República Federativa do Brasil, Brasília, DF, 9 jan. 2018.
2. Martins M, Prata-Barbosa A, da Cunha A. Arboviral diseases in pediatrics. *Jornal de Pediatria* 2020;96:2–11.
3. de Moraes SSF, Neto JC, da Silva MGC. Aspectos epidemiológicos das arboviroses em anos epidêmicos e não epidêmicos em uma metrópole brasileira. *Saúde e Pesquisa* 2022;15(2):1–13.
4. Guedes CCR, Araújo MLV, Saba HSP, Nascimento Filho AS. Epidemiological outbreaks of dengue, chikungunya and zika from 2015 to 2019: Rio de Janeiro case: surtos epidemiológicos da dengue, chikungunya e zika no período de 2015 a 2019: caso Rio de Janeiro. *Concilium* 2023;23(20):124–138.
5. Causa R et al. Emerging arboviruses (dengue, chikungunya, and Zika) in Southeastern Mexico: influence of socio-environmental determinants on knowledge and practices. *Cadernos de Saúde Pública* 2020;36.
6. Zara AL, Santos SM, Fernandes-Oliveira ES, Carvalho RG, Coelho G. *Aedes aegypti* control strategies: a review. *Epidemiologia e Serviços de Saúde* 2016;25(2):391–404.
7. Lagrotta MTF, Silva WC, Souza-Santos R. Identificação de áreas chaves para o Controle de *Aedes aegypt* por meio de geoprocessamento em Nova Iguaçu, estado do Rio de Janeiro, Brasil. *Caderno de Saúde Pública* 2008;24(1):70–80.
8. Oliveira JB, Murati TB, Nascimento Filho AS, Saba H, Moret MA, Cardoso CAL. Paradox between adequate sanitation and rainfall in dengue fever cases. *Science of The Total Environment* 2023;860:160491.
9. Brasil. Ministério da Saúde. Plano Diretor de Erradicação do *Aedes aegypti* no Brasil. Brasília: OPAS, 1996.
10. Brasil. Ministério da Saúde. Secretaria de Vigilância em Saúde. Departamento de Vigilância Epidemiológica. Diretrizes nacionais para prevenção e controle de epidemias de dengue / Ministério da Saúde, Secretaria de Vigilância em Saúde, Departamento de Vigilância Epidemiológica. – Brasília: Ministério da Saúde, 2009.
11. Brasil. Ministério da Saúde. Secretaria de Gestão Estratégica e Participativa. Departamento de Articulação Interfederativa. Caderno Diretrizes, Objetivos, Metas e Indicadores: 2016. Brasília: Ministério da Saúde, 2016.
12. Raafat N, Blacksel SD, Maude RJ. Uma revisão dos diagnósticos de dengue e implicações para vigilância e controle. *Transações da Sociedade Real de Medicina Tropical e Higiene* 2019;113(11):653–660.
13. Brasil. Ministério da Saúde. Portaria nº 3.129, de 28 de dezembro de 2016. Estabelece diretrizes para o controle das arboviroses. *Diário Oficial da República Federativa do Brasil*, Brasília, DF, 28 dez. 2016. Portaria nº 3.129 de 28 de dezembro de 2016.
14. Brasil. Lei nº 13.301, de 27 de junho de 2016. Dispõe sobre a adoção de medidas de vigilância em saúde para

- a prevenção e o controle de doenças transmitidas pelo *Aedes aegypti* e dá outras providências. Diário Oficial da República Federativa do Brasil, Brasília, DF, 27 jun. 2016.
15. Brasil. Ministério da Saúde. Secretaria de Vigilância em Saúde. Departamento de Vigilância das Doenças Transmissíveis. Levantamento Rápido de Índices para *Aedes aegypti* (LIRAA) para vigilância entomológica do *Aedes aegypti* no Brasil: metodologia para avaliação dos índices de Breteau e Predial e tipo de recipientes / Ministério da Saúde, Secretaria de Vigilância em Saúde, Departamento de Vigilância das Doenças Transmissíveis – Brasília: Ministério da Saúde, 2013.
  16. Vieira JS. Avaliação da efetividade do LIRAA como instrumento de monitoração da dengue. 2021. Dissertação (Mestrado em Economia) – Universidade Federal de Pernambuco, Caruaru, 2021.
  17. Comissão Intergestores Tripartite. Resolução nº12, de 26 de janeiro de 2017.
  18. Brasil. Ministério da Saúde. Diagnóstico rápido nos municípios para vigilância entomológica do *Aedes aegypti* no Brasil – LIRAA. Metodologia para avaliação dos índices de Breteau e Predial. Brasília: Ministério da Saúde, 2005. 62 p.
  19. Oliveira ES. Os desafios no trabalho dos agentes de combate à dengue no município de Assis Chateaubriand-PR. Revista ISSN, Belford Roxo 2014;2179:5037.



## Development and Characterization of a PLA/nHA Composite Scaffold Manufactured by 3D Printing

Arthur João Reis Lima Rodovalho<sup>1\*</sup>, Willams Teles Barbosa<sup>1</sup>, Jaqueline Leite Vieira<sup>2</sup>, Caio Athayde de Oliva<sup>1</sup>, Ana Paula Bispo Gonçalves<sup>1</sup>, Sabrina Arcaro<sup>3</sup>, Josiane Dantas Viana Barbosa<sup>1</sup>

<sup>1</sup>SENAI CIMATEC University; <sup>2</sup>Gonçalo Moniz Institute, Oswaldo Cruz Foundation (FIOCRUZ); Salvador, Bahia;

<sup>3</sup>University of Extreme South of Santa Catarina (UNESC); Criciúma, Santa Catarina, Brazil

**The use of 3D bioprinting techniques for scaffold production represents an innovative approach, enabling the development of biomimetic structures that serve as matrices for new tissue formation. This study investigated the influence of varying nanohydroxyapatite (nHA) particle sizes on the properties of PLA/nHA scaffolds. The results obtained from nanocomposites containing 3% wt. nHA indicated that particle size does not significantly affect surface morphology, mobility, thermal behavior, handling, or cytotoxicity in the analyzed scaffolds.**

**Keywords:** Biocomposite. Scaffold. PLA/nHA. 3D Printing.

The regeneration and repair of bone tissue lesions remain significant challenges in tissue engineering. Consequently, 3D printing has emerged as a promising production technique. By leveraging additive manufacturing, it is possible to achieve high precision and greater freedom in customizing the geometries of extracellular matrices and scaffolds [1].

Studies on materials for bone implants, including metals, ceramics, and polymers, have identified biopolymers as the most widely used material in biomedicine, offering good mechanical support. However, biopolymers exhibit limitations such as low osteogenesis activity, histocompatibility, and an inadequate degradation rate, often leading to unsatisfactory results in bone regeneration [2].

Combining biocompatible materials to mimic bone tissue is essential to address these shortcomings. Hydroxyapatite (hydrated calcium phosphate, Ca/P ratio = 1.67) is a suitable candidate due to its similarity to the mineral phase of bone tissue. In this study, poly(lactic acid) (PLA), a biopolymer, and hydroxyapatite

nanoparticles (nHA), a bioceramic, were combined to fabricate PLA/nHA biocomposite scaffolds.

nHA possesses osteoconductivity, osteoinductivity, and bioactivity [3], making it a valuable component in bone tissue engineering. Therefore, this study aimed to develop and characterize PLA/nHA biocomposite scaffolds with varying nHA particle sizes and crystallinity using 3D bioprinting. The resulting scaffolds were analyzed through scanning electron microscopy (SEM), thermogravimetric analysis (TGA), wettability tests, degradation tests, and cytotoxicity assays.

## Materials and Methods

### Materials

The polymer matrix used was PLA Luminy® from Corbion (Amsterdam, The Netherlands), with the following properties: density of 1.24 g/cm<sup>3</sup>, melt flow index of 3–8 g/10 min, stereochemical purity of 96% L-isomer, crystalline white pellet appearance, melting temperature (T<sub>m</sub>) of 155 °C, and glass transition temperature (T<sub>g</sub>) of 55–60 °C. Chloroform (99.8%, Êxodo Científica, Brazil) was used as a solvent for fabricating the PLA/nHA composite.

The hydroxyapatite used was synthesized from the spines of tilapia fish. The synthesized hydroxyapatite underwent heat treatment, and milling time was varied to modify surface area, crystallite size, and crystallinity [4].

Received on 17 September 2024; revised 12 November 2024.  
Address for correspondence: Arthur João Reis Lima Rodovalho. SENAI CIMATEC University Center. Av. Orlando Gomes, 1845 - Piatã, Salvador, Bahia, Brazil. E-mail: rodovalhoarthur13@gmail.com.

J Bioeng. Tech. Health 2024;7(4):327-332  
© 2024 by SENAI CIMATEC. All rights reserved.



### Preparation of PLA/nHA Nanocomposite

The nanocomposite was prepared by incorporating 3% wt of nHA relative to the PLA weight. nHA was dissolved in 100 mL of chloroform under magnetic stirring for 30 minutes, followed by dispersion in an ultrasonic bath for 1 hour. The solution was then stirred again while 10 g of PLA was gradually added until completely dissolved (Figure 1).

The resulting solution was poured into a Petri dish and dried at room temperature in an exhaustion hood for 24 hours. The dried composite films were then cut into smaller pieces for 3D printing. Two types of composites, PLA/nHA-1 and PLA/nHA-2 were produced, differing in nHA particle sizes of 6.06 nm and 9.42 nm, respectively [5].

### Method

**3D Printing of Composite Scaffolds**  
Scaffolds were printed using an Octopus™ 3D bioprinter (3D Biotechnology Solutions, 3DBS). Designs were created using SolidWorks CAD software, and G-code for printing was generated with Simplify3D. Tab 1 provides the printing parameters.

### Thermogravimetric Analysis (TGA)

TGA was performed using a TA Instruments Q50 analyzer (TA Instruments, New Castle, USA) in a temperature range of 25–600 °C, with a heating rate of 10 °C/min under a nitrogen atmosphere. This

**Table 1.** 3D printing parameters.

Parameters of print	
Scaffold size	12x12x5 mm
Printing temperature	195 °C
Nozzle diameter	1 mm
Build platform temperature	60 °C
Scaffold fill	90% ( $\pm 45^\circ$ )
Layer Size	0.8 mm
Print speed	45 mm/min

analysis evaluated the degradation temperature and residue percentage of the samples.

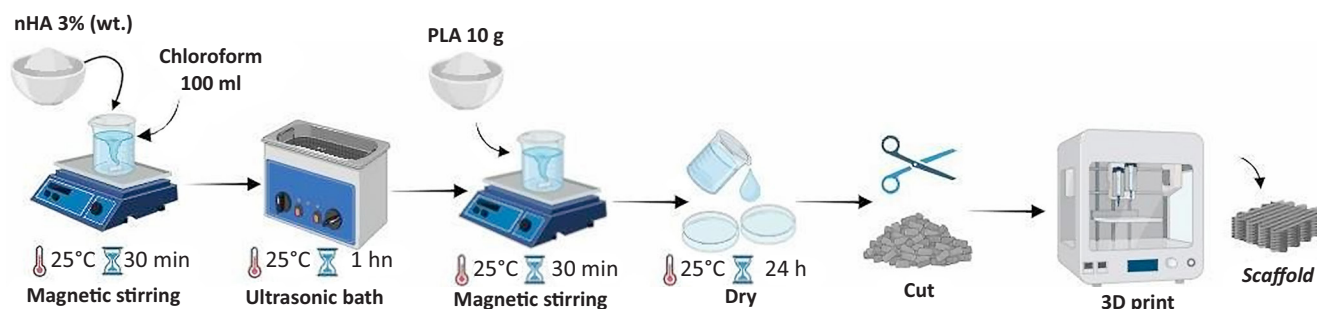
### Scanning Electron Microscopy (SEM)

Surface morphology was analyzed using a JSM-6510LV SEM (JEOL, Tokyo, Japan) at an acceleration voltage of 20 kV. Samples were metalized with gold to enhance electron beam dispersion across the scaffold surface.

### Wettability Test

Wettability was assessed by measuring the contact angle of water droplets (5  $\mu$ L) on the sample surfaces using a DSA-25 goniometer (Krüss, Hamburg, Germany). Photos were taken to measure the angles, with tests performed five times at different locations on each sample.

**Figure 1.** Composite scaffold manufacturing.



### In vitro Scaffold Degradation Test

Scaffolds were submerged in a 0.1 M phosphate-buffered solution (PBS) at pH 7.4 (Sigma-Aldrich, Missouri, USA). The PBS volume was calculated using Equation 1, where  $V$  is the volume and  $S_a$  is the surface area.

$$V = \frac{S_a}{10} \quad (1)$$

Scaffolds were submerged for three months, with weekly weight measurements. Samples were dried at 90 °C before weighing. Weight loss was calculated using Equation 2, where  $W_0$  is the initial mass and  $W_F$  is the final mass.

$$WL (\%) = \frac{W_0 - W_F}{W_0} \times 100 \quad (2)$$

### Cytotoxicity

Cytotoxicity was evaluated using the AlamarBlue® assay (Invitrogen, Carlsbad, CA, USA). Mouse fibroblast L929 cells were cultured in DMEM (Life Technologies) supplemented with 10% FBS and 1% penicillin/streptomycin in a 5% CO<sub>2</sub> incubator at 37 °C.

Sterilized scaffolds were incubated in DMEM for 24 hours before cell seeding at  $5 \times 10^5$  cells/well. After 72 hours of incubation, resazurin sodium salt was added at 10% v/v, followed by a 4-hour incubation. The supernatant was transferred

to a 96-well plate, and metabolic activity was measured at 570 and 600 nm using a multi-plate reader [6]. Tests were conducted in triplicate.

## **Results and Discussion**

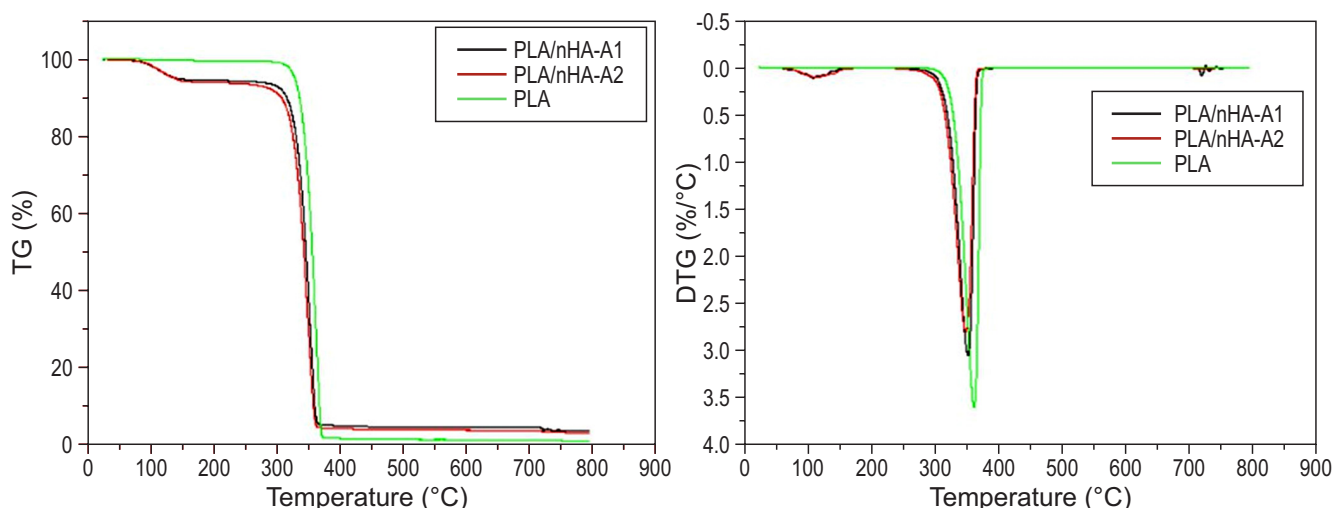
### Thermal Analysis

The analysis of TGA was done to assess and validate the method of fabrication of the composite. Figure 2 shows, respectively, the TG (a) and DTG (b), which represent the curves from the samples of PLA, PLA/nHA-A1, and PLA/nHA-A2. In Figure 2 (a), the PLA curve shows only one thermic event, which is the loss of mass of the polymer, and Figure 2 (b) shows that this occurs at approximately 360 °C.

The composites have the same thermic behavior between each other and can be observed in two thermal events. The first one is approximately 140 °C, and this loss of mass is because of the evaporation of water from the material, justified because of the hydrophilic properties of the material determined in the wettability test. The second thermal event is approximately 350 °C, representing the loss of mass in the material.

Also, it is possible to observe that the composites have a residue of approximately 3 % wt. Which is equivalent to a concentration of nHA from the

**Figure 2.** Thermal analysis of the sample, TGA Curves (a), and DTG curves (b).



fabrication of the composite. The TGA analysis proved that there was an efficient fabrication of the composite without considerable waste of nHA. Furthermore, in comparison with the analysis from Rodovalho and colleagues [5], who have made a study with 10 % wt. nHA, the fabrication of composites is effective independent of the concentration because there isn't considerable loss of bioceramics.

### Scanning Electronic Microscopy

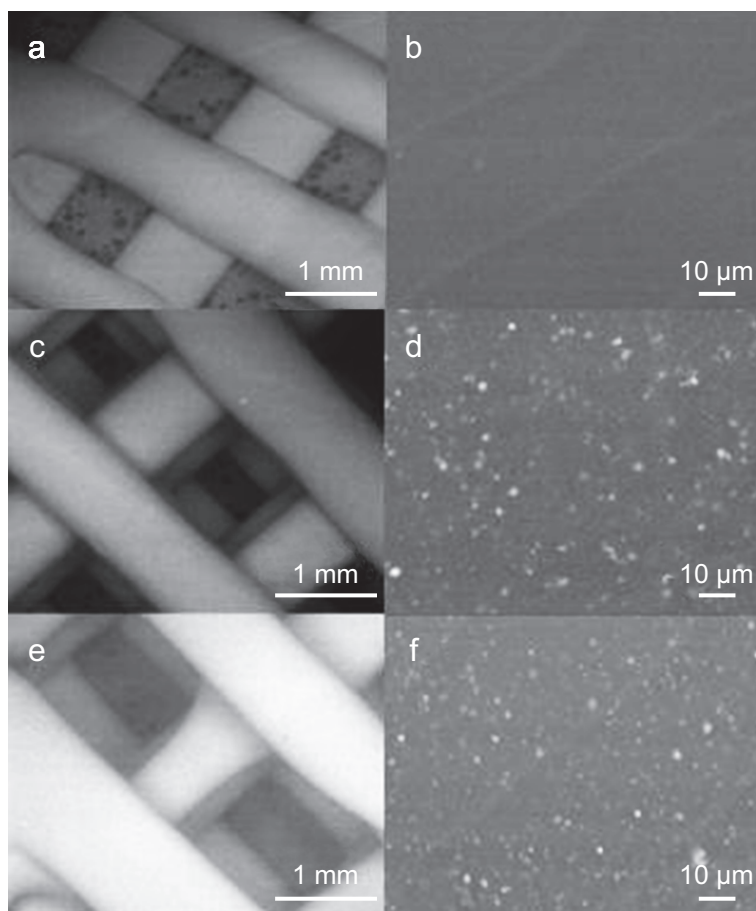
The morphological analysis of the filament and the surface of the scaffold was done by an SEM after the 3D printing. SEM of the PLA (a-b), PLA/nHA-A1 (c-d), and PLA/ nHA-A2 (e-f) samples are shown in Figure 3. The filament of the PLA, PLA/nHA- A1 and PLA/ nHA-A2 scaffolds presented in Figure 3 (a,c,e) show the uniformity

of the filaments and the porosity. In Figure 3 (d,f), the presence of nHA dispersed evenly along the scaffold surface can be seen by the white points on the surface. With that, the efficiency of the casting method in the dispersion of the nanoparticles in the polymeric matrix grants homogeneity of nHA along the composite scaffold.

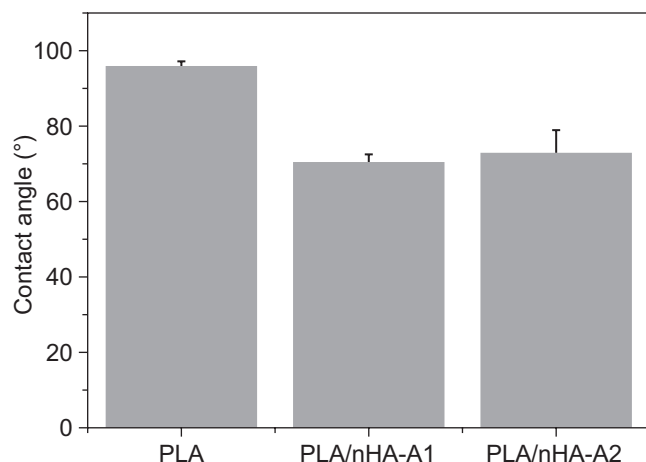
### Wettability Test

Figure 4 presents the evaluation of the contact angle of the PLA, PLA/nHA-A1 e PLA/nHA-A2, showing that the PLA had a contact angle of  $95.5^\circ \pm 1.12^\circ$ , which means that the material has a hydrophobic behavior. The nanocomposites PLA/nHA-A1 and PLA/ nHA-A2 had respectively a contact angle of  $70.4^\circ \pm 1.92^\circ$  e  $72.7^\circ \pm 6.02^\circ$ , characterizing hydrophilic

**Figure 3.** SEM of scaffolds (a-b) PLA, (c-d) PLA/nHA-A1, and (e-f) PLA/nHA-A2.



**Figure 4.** The average contact angle of PLA, PLA/nHA.1, and PLA/nHA.2 scaffolds.



behavior [7,8]. The composites had hydrophilic behavior is caused by the presence of nHA.

#### In vitro Scaffold Degradation Test

The scaffolds were submerged in PBS for 91 days to evaluate the degradation rate (Figure

5). All of the samples had mass loss, but PLA obtained the lowest mass loss percentage in relation to the composite scaffolds, justified by their hydrophobic behavior. The composite obtained the biggest degradation rate because of its hydrophilic behavior, which is provided by the insertion of nHA, corroborating with the studies of Rodovalho and colleagues [5]. In this study, PLA/nHA-A1 obtained a degradation rate similar to PLA/nHA-A2, showing that the different nHA particle sizes did not impact the degradation rate of the composites.

#### Cytotoxicity

The results of cellular viability test of the PLA, PLA/nHA-A1 e PLA/nHA-A2 are showed in Figure 6. The viability of scaffold was superior than 90 %, which states that the material didn't have significant toxicity to the cells. The values of cellular viability aren't 100 % viables because the scaffold occupied a space in the surface of the plate and interferes with the cell carpet.

**Figure 5.** Percentage of mass loss for the PLA, PLA/nHA-1, and PLA/nHA-2 scaffolds during the 91-day degradation period.

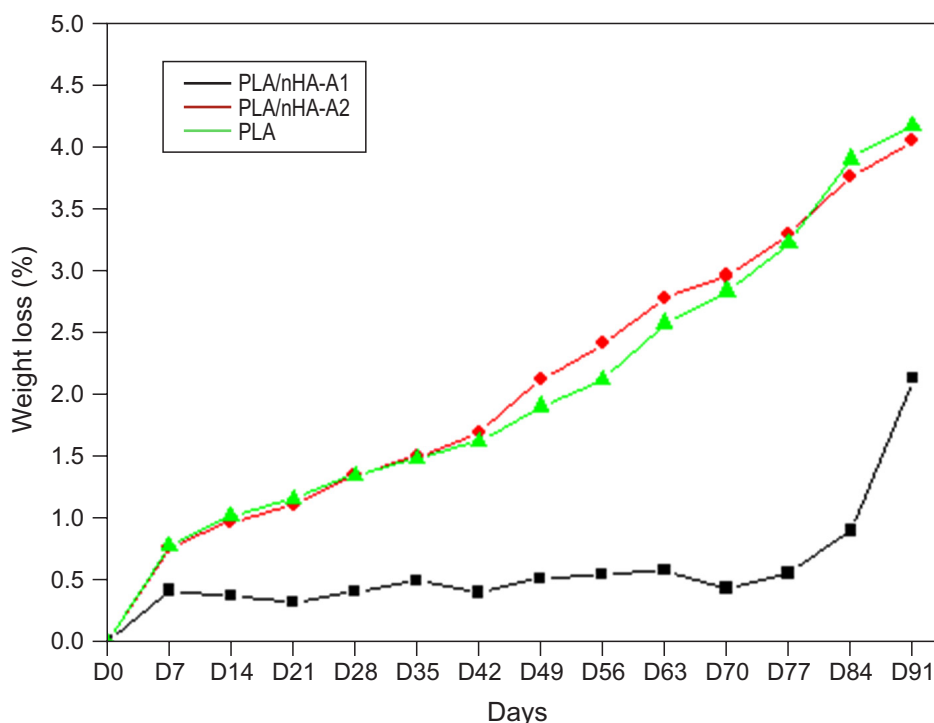
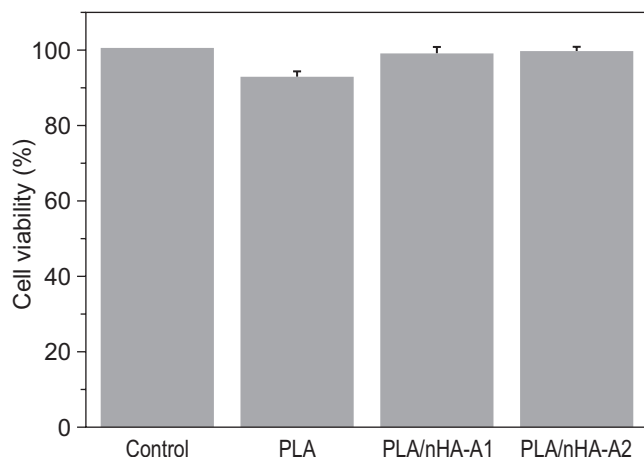


**Figure 6.** Percentage of cell viability of PLA, PLA/nHA-1, and PLA/nHA-2 scaffolds.



## Conclusion

This study had the objective of evaluating the influence of nanoparticles of hydroxyapatite with a concentration of 3 % wt. in the PLA/nHA composite. The wettability test showed that the insertion of nHA in the polymeric matrix with a concentration of 3 % wt. or above provided a hydrophilic behavior to the composite, seeing that the PLA has a hydrophobic behavior. The degradation of the composite scaffolds obtained a bigger loss of mass in relation to the PLA, and this is because of the hydrophilic behavior that the nHA provided to the composite, but the difference of nHA nanoparticles, in this concentration, didn't impact the results. However, the compounds developed showed satisfactory results for future applications in tissue engineering.

## Acknowledgments

The authors are grateful to SENAI CIMATEC University Center, Coordination for the Improvement

of Higher Education Personnel (CAPES), Research Support Foundation of Bahia State (FAPESB), Research and Innovation Foundation of Santa Catarina State (FAPESC) for their support in the development of this study.

## References

1. Chen X et al. 3D printed porous PLA/nHA composite scaffolds with enhanced osteogenesis and osteoconductivity *in vivo* for bone regeneration. *Biomedical Materials (Bristol)* 2019;14(6).
2. Prashak C et al. Mechanical reliability and *in vitro* bioactivity of 3D-printed porous polylactic acid-hydroxyapatite scaffold. *Journal of Materials Engineering and Performance* 2021;30(7):4946–4956.
3. Oladapo BI et al. 3D printing and morphological characterisation of polymeric composite scaffolds. *Engineering Structures* 2020;216.
4. Modolon HB et al. Nanostructured biological hydroxyapatite from Tilapia bone: A pathway to control crystallite size and crystallinity. *Ceramics International* 2021;47(19):27685–27693.
5. Rodovalho A et al. Influence of size and crystallinity of nanohydroxyapatite (nHA) particles on the properties of Polylactic Acid/nHA nanocomposite scaffolds produced by 3D printing. *Journal of Materials Research and Technology* 2024;30:3101–3111.
6. Smieszek A et al. New approach to modification of poly (L-lactic acid) with nano-hydroxyapatite improving functionality of human adipose-derived stromal cells (hASCs) through increased viability and enhanced mitochondrial activity. *Materials Science and Engineering C* 2019;98:213–226.
7. Pandey A, Singh G, Singh S, Jha K, Prakash C. 3D printed biodegradable functional temperature-stimuli shape memory polymer for customized scaffoldings. *Journal of the Mechanical Behavior of Biomedical Materials* 2020;108.
8. Perumal G. et al. Synthesis of magnesium phosphate nanoflakes and its PCL composite electrospun nanofiber scaffolds for bone tissue regeneration. *Materials Science and Engineering C* 2020;109.



## Development Process of a Medicinal Cannabidiol Dosing Pen

José Santos Damasceno<sup>1\*</sup>, Gabriel Barreto Teles Fonseca<sup>1</sup>

<sup>1</sup>SENAI CIMATEC University; Salvador, Bahia, Brazil

**Inhalation devices that allow controlled administration of active ingredients are undergoing constant technological evolution. In Brazil, there is a demand for devices that meet the requirements of this treatment modality, as it enables more precise application and improved dose management. The present study describes the development process employed in the medicinal cannabidiol dosing pen, an inhalation device designed for medical treatments with vaporized cannabidiol. Its functionality, based on controlled and standardized doses prescribed by medical professionals, offers the potential for remote treatment of individuals affected by conditions such as Alzheimer's and Parkinson's disease, among others. The method includes a prior art analysis focusing on inhalation-based devices and outlines a prototype development workflow through partial deliverables assigned by the project.**

**Keywords:** Medicinal Cannabidiol. Inhalation Device. Medical-Electronic Inhalation Device. Dosing Pen.

Inhalation devices are widely utilized in medical practice due to their effectiveness in drug delivery. This approach demonstrates that inhaling vaporized medication offers greater patient treatment efficiency than other administration methods. According to Upadhyay and colleagues [1], oral application, compared to inhalation, is slower and less predictable in absorption, with peak concentration typically occurring between one to three hours. In contrast, the inhalation method allows drugs to penetrate directly into the systemic circulation through the nasal mucosa, which is thin and highly vascularized, resulting in faster access to the brain and a quicker onset of therapeutic effects [1].

Among the medications suited for this method is CBD (cannabidiol), a compound derived from cannabis. Based on various scientific studies, CBD is used in the treatment of anxiety, spasms, acute/severe pain, and seizures, offering a potential alternative to opioid use. Currently, the sale of cannabis-based products in Brazil requires approval and authorization from ANVISA,

as outlined in Resolution RDC 327/2019. Considering this context, the technical team developed an electronic system that employs an electrical resistance mechanism to vaporize an active substance (CBD). The goal was to create a prototype that integrates medical functionality, ensures standardized dose administration, and allows for physician control and prescription.

The development process adhered to standards such as ABNT NBR ISO 60601-1:2010 (including Amendment 1:2016) and its collateral standards (Parts 2:2017, 6:2011, 8:2010, 9:2010, and 11:2021), as well as ABNT NBR ISO 80601-2-74:2020. In this light, this article's primary objective is to describe this device's development stages. The project framework aligns with a Technology Readiness Level (TRL) ranging between 2 and 5, focusing on presenting a functional prototype based on a concept tailored to meet project needs.

### Materials and Methods

The project involved the development of an electronic device for the controlled administration of medicinal CBD doses via oral inhalation.

The process was divided into four main stages:

**a) Informational Stage** – This stage includes a detailed analysis, disassembly, and functional understanding of similar devices, market and

Received on 15 September 2024; revised 12 December 2024.  
Address for correspondence: José Santos Damasceno.  
Av. Orlando Gomes, 1845, Piatã, Salvador, Bahia, Brazil.  
Zipcode: 41650-010 E-mail: jose.damasceno@ba.estudante.senai.br.

J Bioeng. Tech. Health 2024;7(4):333-336  
© 2024 by SENAI CIMATEC. All rights reserved.



management evaluations, and identification of applicable standards and patents.

- b) **Conceptual Stage** – This phase focuses on defining the functional characteristics of the device and designing the prototype.
- c) **Preliminary Stage** – During this phase, prototypes were tested, and simulations were conducted to evaluate their performance.
- d) **Prototyping Stage** – This stage refined the final structure, conducted dose control testing and adjustments, and conducted post-processing for final finishes.

To manage the project effectively, SENAI CIMATEC utilized tools and resources provided by its organizational framework. These included the DIP&T (Department of Innovation and Technology Projects), the TRL classification (based on ISO/FDIS 16290—Space Systems: Definition of Technology Readiness Levels (TRLs) and their criteria for assessment), and product life cycle analysis.

The multidisciplinary technical team consisted of experts in biomedical equipment, embedded electronics, creative industries, and energy efficiency. The project office managed activities and progress throughout the project, providing crucial support in coordination and oversight.

## Results and Discussion

The medicinal CBD dosage pen was developed based on market technologies, technical usability

concepts, and normative principles. The device is designed in two separable parts: an upper and a lower section connected via a SNAP-type fitting. Additionally, it features USB-C charging, an air duct to facilitate vapor flow, and a system of contact pins enabling electronic communication between the two sections.

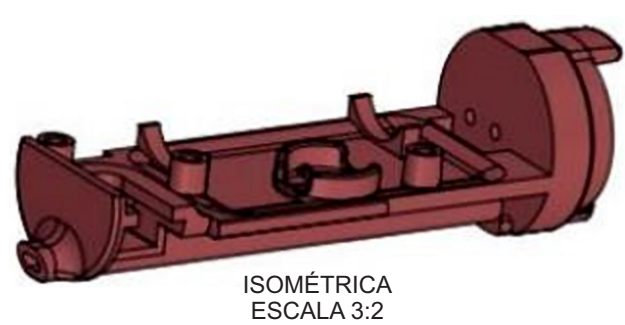
The upper section generally houses the storage compartment for vaporizing the substance in contact with an electric coil. The lower section contains the electronic structure, including the microcontroller, charging circuits, and activation mechanisms. Visually, the device's external structure showcases a cylindrical design with an ergonomically flattened mouthpiece at the upper tip (Figure 1). Internally, a magazine component is introduced (Figure 2), which houses and secures most electronic components, including the contact pins, coil, reservoir, and others.

Regarding the pen's logical functioning, it was established that when the user inhales, the heating coil is activated, initiating the process of timed dose control and triggering visual/sensory indicators on the device (such as signals for activation, inhalation, and charging). Thus, when an electrical current passes through the coil, it heats up, vaporizing the CBD fluid, which is then directed to the outlet via the air duct. This approach ensures an efficient, safe, and controlled user experience during the dosage pen's operation. As part of the project's development stages, tests were conducted to validate the

**Figure 1.** Medicinal CBD dosage pen.



Figure 2. Magazine.

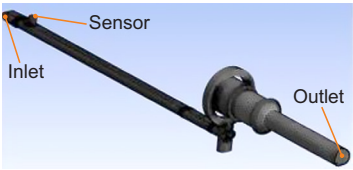
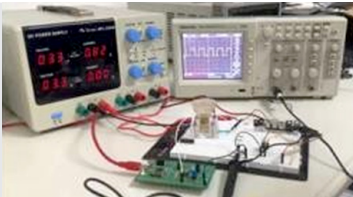




device's functionality (Table 1).

Comprehensive Results Analysis

Table 2 illustrates the data obtained from the vaporization validation in an experimental format. Using a closed-cycle process applied to each power level, the procedure involved charging the battery, activating the system for 4 seconds, performing 10 vaporization cycles, and measuring the mass thrice. For instance, for a dose of  $2.15 \pm 0.004$  mg, there were 10 vaporization cycles, resulting in an individual

Table 1. Tests conducted during the project.

Test Description	Project Stage	Associated Figure	Results
<b>Simulation of airflow through the air duct:</b> Understanding the minimum/maximum airflow required for device activation for different target audiences.	Preliminary Stage		Consolidation of the fluid-dynamic circuit; minimum inhalation established for the entire process.
<b>Validation of the heating system in the laboratory:</b> Assessing the impact of power variation, required heating current, and other factors.	Prototyping Stage		Identification of activation/heating current.
<b>Prototype validation:</b> Usability analysis.	Prototyping Stage		Validation of mouthpiece contact, assembly/disassembly of upper and lower parts, and connections.
<b>Validation of dose quantity and vaporized amount in the laboratory at power levels of 80%, 90%, and 99%:</b> Using an air propeller, the device was tested at three electrical power levels.	Prototyping Stage		Consolidation of vaporization for one dose of the substance.

**Table 2.** Relationship between dose and supplied power.

Duty/ Power	Dose (mg)	Battery Voltage Drop
80%	2.1mg $\pm$ 0.0004mg	0.218V
90%	4.48 $\pm$ 0.085mg	0.130V
99%	5.86mg $\pm$ 0.037mg	0.165V

dose of  $0.215 \pm 0.004$  mg. A similar analysis was conducted for the remaining power levels.

Due to the project's scope limitations, it was not possible to present the collected data with greater precision, as this aspect was not included in the initial activity execution plan. In all tests conducted, the cannabidiol used was medicinal oil provided by the client. The cannabidiol was solid at room temperature and became oily when exposed to elevated temperatures.

In a comparative analysis with similar devices (PAX ERA, DOSISTY BATTERY, MEDIPEN, POD SYSTEM ZERO CARE RENOVA EDITION, and others), the device features a partitioned structure in two parts, visual/sensory signaling, battery control, temperature control, a magazine, the use of commercial components for heating, a reservoir for CBD, logical system control through a microcontroller, configuration based on the patient's needs, and operation according to medical prescriptions. The system was designed to be functional for the medical field, incorporating all applicable features for this context.

## Conclusion

In summary, this article describes the development of the Cannabidiol Dosage Pen. The final results of the prototype, the designed concept, the applied operating principle, and other aspects are presented. The technical team faced difficulties regarding the availability of parts within the country and using embedded technologies in devices with this dimensional format. Under the management of the company CBDMed Brasil, the following steps include improving the device and conducting a clinical study to compartmentalize the device's actions in a practical context with patients and, ultimately, its commercialization in the national market. The main conflicting factor for this is certification by ANVISA, which, according to its regulations, prohibits products inspired by electronic cigarettes.

## References

1. Upadhyay G, Patel P, Fihurka O et al. Measurement of  $\Delta^9$ THC and metabolites in the brain and peripheral tissues after intranasal instillation of a nanoformulation. *Journal of Cannabis Research*. Available at: <<https://jcannabisresearch.biomedcentral.com/articles/10.1186/s42238-022-00171-8>>.
2. Agência nacional de Vigilância Sanitária - ANVISA. Anvisa aprova novo produto medicinal à base de Cannabis. Available at: <<https://www.gov.br/anvisa/pt-br/assuntos/noticias-anvisa/2022/anvisa-aprova-novo-produto-de-cannabis-a-ser-fabricado-no-brasil#:~:text=A%20Ag%C3%A2ncia%20Nacional%20de%20Vigil%C3%A2ncia,a%20ser%20fabricado%20no%20Brasil.>>>.

## Development of a Sunscreen Formulation Enriched with *Camellia sinensis* Extract in the Treatment of Melasma

Amanda Cerqueira Ribeiro Santos<sup>1\*</sup>, Esther Gabrielle Ribeiro Nascimento<sup>1</sup>, Isis Santos Silva<sup>1</sup>, Júlia Alves Gribel de Oliveira<sup>1</sup>, Rainy Teixeira Gonzaga<sup>1</sup>, Tatiana Oliveira do Vale<sup>1</sup>, Érica Patrícia Lima Pereira<sup>1</sup>

<sup>1</sup>SENAI CIMATEC University; Salvador, Bahia, Brazil

This study evaluated the antioxidant potential of *Camellia sinensis* by quantifying its bioactive compounds, which contribute to the treatment of melasma. Consequently, developing a sunscreen formulation enriched with *Camellia sinensis* extract was proposed. The findings were derived from physicochemical and microbiological analyses supported by bibliographic references. By determining the phenolic compound content in four different concentrations of *Camellia sinensis* extract, the highest percentages of gallic acid were identified in two concentrations. These results highlight the extract's antioxidant and photoprotective properties against free radicals and its promising potential to inhibit the activity of the tyrosinase enzyme.

**Keywords:** Melasma. *Camellia sinensis*. Phytotherapy. Antioxidant. Photoprotection.

Following the increasing incidence of skin diseases, such as melasma, caused by prolonged exposure to the sun, this study explored the possibility of developing a sustainable herbal sunscreen enriched with *Camellia sinensis* (green tea) extract to aid in the prevention and treatment of these conditions.

In recent years, research on the use of phytotherapy, particularly in dermatological cosmetics, has grown significantly. This expansion reflects the increasing exploration of the active compounds in plants. According to the World Health Organization (WHO), medicinal plants are defined as those that exert therapeutic effects, promoting balance within the body. Accordingly, natural properties with functions equal to or superior to existing dermatological products are being sought to minimize the long-term use of synthetic chemicals on the skin.

As sustainability becomes a crucial factor in corporate strategies, innovation is no longer limited to new technologies but also includes aligning economic, social, and environmental values.

Companies recognized as innovative prioritize these values, creating products that resonate with their audience. In this context, the cosmetics market has embraced using raw materials derived from plants, fruits, and seeds. These "bio-cosmetics" are gaining popularity for combining environmental sustainability with human health benefits (Gallina, 2021).

The rise of phytocosmetics in the global market is driven by increasing demand for natural products, reflecting a shift towards conscious consumption and sustainable practices. The demographic attracted to these products, often called "green consumers," opt for natural and organic alternatives over synthetic formulations. These choices are justified by their perceived safety and minimal environmental impact (Lyrio et al., 2011). Moreover, such products adhere to environmental conservation and sustainability (Borges et al., 2013).

This study analyzed the photoprotective potential of *Camellia sinensis* when used in sunscreens to assist in treating melasma. Research shows that the antioxidant properties of flavonoids and polyphenols in *Camellia sinensis* extract are effective in treating dark spots and combating aging, cardiovascular diseases, and cancer. The extract's ability to inhibit leukocyte infiltration into the skin minimizes damage caused by solar radiation. By significantly reducing the activity of the enzyme tyrosinase—a key factor in melanin production—

Received on 14 September 2024; revised 28 November 2024.  
Address for correspondence: Amanda Cerqueira Ribeiro Santos. SENAI CIMATEC University Center. Av. Orlando Gomes, 1845 - Piatã, Salvador, Bahia, Brazil. E-mail: amanda.ribeiro6@ba.estudante.senai.br.

J Bioeng. Tech. Health 2024;7(4):337-341  
© 2024 by SENAI CIMATEC. All rights reserved.

*Camellia sinensis* offers a promising solution for mitigating dark spots caused by sun exposure. The medicinal plant and phytotherapeutic industry represents a valuable economic and health innovation avenue. Products derived from phytotherapeutic compounds have demonstrated significant market potential compared to those based on synthetic chemicals.

Additional aspects considered during this research include the extract's anti-inflammatory properties. As stated by the Eucerin website (2024), the protective layer of the skin is slightly acidic, with an optimal pH range between 4.7 and 5.75.

The study also assessed the extract's organoleptic and antimicrobial properties, ensuring compliance with Anvisa's standards for stability and formulation acceptance. For instance, increased particle mobility during stability testing revealed potential formulation instabilities, necessitating adjustments in its organoleptic composition.

Key questions addressed in this study include:

- How can green tea be utilized as a skin-whitening agent?
- How can the antioxidant potential of *Camellia sinensis* extract be quantified through its

bioactive compounds?

- What are the physicochemical properties of the formulation?
- What are the benefits of a sunscreen enriched with phytocosmetics?

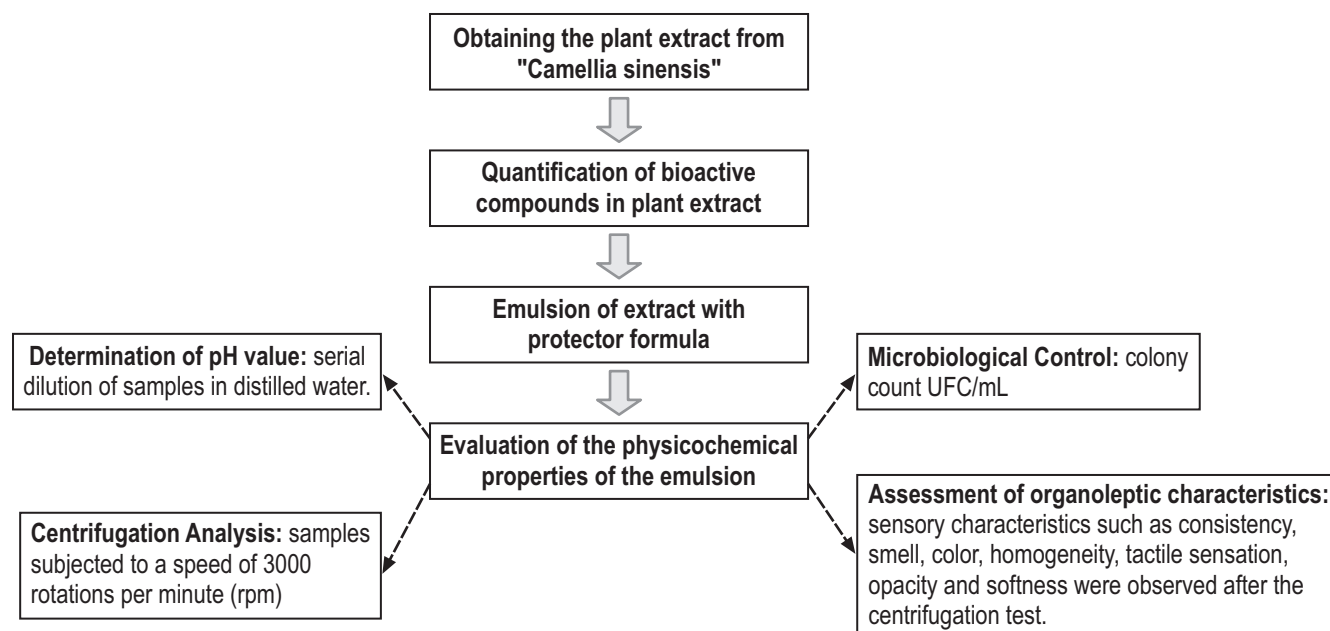
This article aims to evaluate the antioxidant potential of *Camellia sinensis* extract, focusing on its flavonoid and polyphenol content and their ability to mitigate UV-induced skin damage. Additionally, the study explores its potential for reducing skin inflammation and lightening hyperpigmentation.

The development of this product emphasizes sustainability by replacing environmentally harmful compounds with plant-based alternatives, aligning with the growing demand for eco-friendly and herbal solutions in the cosmetics market.

## Materials and Methods

This study adopted an exploratory approach, integrating both qualitative and quantitative methods. The research encompassed bibliographic, documentary, and experimental procedures. A detailed experimental plan was developed to meet the proposed objectives (Figure 1).

**Figure 1.** Flowchart describing the experimental steps to be performed.





### Conditioning and Preparation of *Camellia sinensis* Leaf Samples

The *Camellia sinensis* leaves were received and stored in the Biotechnology Laboratory at SENAI Cimatec (Salvador-BA). The leaves were washed in a 1% hypochlorite solution and then dried in an oven at 40°C for 72 hours. After drying, the leaves were crushed in a blender and macerated for 48 hours using PA ethanol (absolute ethyl alcohol, C<sub>2</sub>H<sub>6</sub>O) to obtain the extract.

### Obtaining the Plant Extract

The extract was filtered and processed using a rotary evaporator and a magnetic stirrer to evaporate the ethanol. Subsequently, the final yield of the extract was analyzed to assess the economic potential of *Camellia sinensis*.

### Quantification of Bioactive

#### *Compounds in the Plant Extract*

The bioactive compounds in the extract were quantified in duplicate using the spectrophotometric method with the Folin-Ciocalteu reagent, a mixture of phosphomolybdate and phosphotungstate, which is used to determine phenolic and polyphenolic antioxidants. Following the quantification, two emulsions were prepared by weighing the sunscreen base into two Falcon tubes and adding *Camellia sinensis* extract at 2% and 10% concentrations.

### Evaluation of Physicochemical Properties of the Plant Extract and Emulsion (Sunscreen Base + Plant Extract)

The emulsions and the pure sunscreen base underwent centrifugation analysis to evaluate the formulations' stability, following the methodology described by Matias and Intiane in their study on "Evaluation of the Physicochemical Stability of Compounded Sunscreens."

An organoleptic evaluation was conducted,

assessing sensory attributes such as consistency, odor, color, homogeneity, tactile sensation, opacity, and softness (ANVISA, 2004). The pH value of the 2% emulsion was measured to verify compatibility between the formulation's pH and the skin's natural pH. Finally, microbiological control tests were performed to assess colony-forming unit (CFU/mL) counts, ensuring compliance with Good Manufacturing Practices (GMP) as outlined by Anvisa's regulations.

## **Results and Discussion**

### Obtaining the Plant Extract and Calculating the Yield

The yield calculation for the extract was performed by dividing the final volume of the extract (10 mL) by the initial mass of *Camellia sinensis* leaves (300 g) and multiplying the result by 100. This resulted in a yield of approximately 3.33% after three days, considered satisfactory.

$$\frac{10}{300} \times 100 = 0.333... \times 100 = 3.33\%$$

### Quantification of Bioactive Compounds in the Extract

Schmitz and colleagues, in their study "Green tea and its actions as a chemoprotector," highlighted flavonoids and catechins as the primary therapeutic chemical components in *Camellia sinensis*. These compounds are potent antioxidants that inhibit skin tumor formation caused by chemical carcinogens or UVB radiation.

Using the Folin-Ciocalteu spectrophotometric method, the bioactive compounds in the extract were quantified, confirming the presence of gallic acid, a phenolic acid. When evaluating concentrations of 100 µL, 10 µL, 1 µL, and 0.1 µL of the extract, the highest gallic acid percentages were observed in the 100 µL and 10 µL concentrations (13.17% and 11.02%, respectively) (Table 1).

These findings indicate a high concentration of phenolic compounds, even at minimal volumes.



**Table 1.** Concentrations of gallic acid equivalent (GAE) in *Camellia sinensis* extract.

Concentration (μL)	% GA
0.1	7.57
1	9.12
10	11.02
100	13.17

These results underscore the antioxidant activity of the *Camellia sinensis* extract, demonstrating its photoprotective potential against free radicals and its ability to inhibit tyrosinase, an enzyme linked to melanin production.

#### Evaluation of the Emulsion's Organoleptic Characteristics

According to Matias, Bianchetti, and Rigo (2016), quality control of compounded formulations is essential for verifying stability, safety, and efficacy. The organoleptic characteristics of the emulsions were analyzed after centrifugation, focusing on attributes such as color, softness, homogeneity, tactile sensation, opacity, consistency, and odor.

Three samples were evaluated:

- Sample 1: Sunscreen base without extract.
- Sample 2: 10% emulsion containing *Camellia sinensis* extract.
- Sample 3: 2% emulsion containing *Camellia sinensis* extract.

Under artificial white light, the emulsions displayed uniform color, ideal consistency, and high homogeneity. Their tactile sensation, opacity, and overall sensory attributes were deemed excellent, confirming the formulations' suitability for use and stability.

#### Centrifugation Analysis

The centrifugation analysis further validated the stability of the formulations. The results confirmed

the emulsions' uniformity, optimal consistency, and superior homogeneity, ensuring high-quality formulations that meet the desired standards for topical application.

#### Determination of pH Value

Matias (2016) emphasized that skin pH, typically between 5.5 and 6.5, contributes to bactericidal and fungicidal protection. The pH values of the 2% emulsion were within this range, maintaining compatibility with skin alkalinity. The 10<sup>-1</sup> dilution of the more concentrated 10% emulsion also demonstrated suitability for topical application. All formulations exhibited average pH values of 5.3, confirming their compatibility with the epidermis.

#### Microbiological Control Test

João Artur Grandim, in his "Microbiology Guide," emphasized the importance of controlling microbiological contamination in cosmetic production. Uncontrolled microbial growth can render products unsellable. Cosmetic formulations, especially those containing organic substances, water, and mineral salts, are prone to microbial growth.

Microbiological testing showed growth on all plates, but colony counts were within acceptable limits. The 10<sup>-3</sup> dilution plate showed only one colony, and the highest observed growth across dilutions (10<sup>-1</sup>, 10<sup>-2</sup>, and 10<sup>-3</sup>) was below Anvisa's threshold of 10<sup>2</sup> CFU/mL for Type 1 products and 5 × 10<sup>-3</sup> CFU/mL for Type 2 products.

The results confirmed that the formulations complied with Anvisa's microbiological quality standards, ensuring safety and suitability for consumer use.

#### **Conclusion**

The rising incidence of melasma and the demand for novel photoprotective active ingredients that are safe for the skin highlights the importance of introducing innovative herbal products to the market. These

products provide consumers with practical options for mitigating the harmful effects of solar radiation. Developing a sunscreen formulation enriched with *Camellia sinensis* extract offers a promising approach to addressing this need, as plant-based inputs with photoprotective properties are more accessible, cost-effective, and environmentally sustainable to produce. The findings of this study confirm the photoprotective potential of *Camellia sinensis* extract in sunscreen formulation. With a concentration of 13.17% gallic acid—a polyphenol known for its potent antioxidant properties—in just 100 microliters of extract, the results underscore the significant efficacy of this natural ingredient. These results suggest that larger volume measurements could yield even more favorable outcomes, enhancing its applicability in sunscreen products.

In conclusion, the investigation into the photoprotective properties of *Camellia sinensis* extract opens a promising pathway for developing sunscreen formulations that also aid in melasma treatment. The antioxidant-rich properties of this plant extract contribute to its whitening and photoprotective capabilities, expanding the range of cosmetics available to consumers. Moreover, its plant-based and sustainable nature aligns with global efforts to promote environmentally friendly products, enhancing its appeal in the cosmetics industry.

## References

1. Borges RCG, Garvil MP, Rosa GAA. Production of phytocosmetics and sustainable cultivation of biodiversity in Brazil. e-RAC 2013;3(1). Available at: <https://pt.slideshare.net/jackelineconsecar/produo-de-fitocosmticos-e-cultivo-sustent-vel-da-biodiversidade-no-brasil>.
2. Araújo AIF et al. Plants native to Brazil used in phytocosmetics. Available at: [https://pt.scribd.com/document/84711614/plantas-nativas-do-brasil-empregadas-em-f itocosmetica](https://pt.scribd.com/document/84711614/plantas-nativas-do-brasil-empregadas-em-f-itocosmetica). Accessed on: 3 May. 2024.
3. Brazil. Ministry of Health. National Health Surveillance Agency (Anvisa). Cosmetic product stability guide. 1st ed. v. 1, 52 p. Brasília, 2004. Available at: <https://www.gov.br/anvisa/pt-br/centraisdeconteudo/publicacoes/cosmeticos/manuais-e-guias/guia-de-estabilidade-de-cosmeticos.pdf/view>.
4. Matias I. Assessment of the physicochemical stability of manipulated sunscreens. Completion work for Course II, of the Pharmacy course at Centro Universitário Univates. 2016. Available at: <https://www.univates.br/bdu/bitstreams/7a874bac-0725-432a-95e8-4793ff7a44e8/download>.
5. Gradim JA, Aangels M. Microbiology Guide: microbiological control in the personal hygiene, perfumery and cosmetics industry. Brasília: Brazilian Association of the Personal Hygiene, Perfumery and Cosmetics Industry, 2015. Available at: <https://superaparque.com.br/upload/20160516-100554-GuiaMicrobiologia.pdf>.
6. Gallina RP. Antioxidant phytocosmetics: use of phytoactives as a resource for anti-aging treatment. Centro Universitário Internacional UNINTER, 2021. Available at: <https://www.revistasuninter.com/revistasauade/index.php/revista-praticas-interativas/article/view/1245>.
7. Pinto AC et al. Biodiesel: an overview. Journal of the Brazilian Chemical Society 2005;16(6B):1313-1330.
8. Silva IG. Pena de morte para o nascituro. O Estado de S. Paulo, São Paulo, 19 set. 1998. Available at: [http://www.providafamilia.org/pena\\_morte\\_nascituro.htm](http://www.providafamilia.org/pena_morte_nascituro.htm).

## Influence of the Defects in a Graphene Oxide on the Reduction via Ascorbic Acid for Structuring Aerogels

Camila Miranda Fonseca Duarte<sup>1,2\*</sup>, Eliel Gomes da Silva Neto<sup>3</sup>, Iara de Fatima Gimenez<sup>2</sup>

<sup>1</sup>SENAI CIMATEC University; Salvador, Bahia; <sup>2</sup>Federal University of Sergipe; Aracaju, Sergipe; <sup>3</sup>Federal University of Bahia; Salvador, Bahia, Brazil

**Studies of graphene oxide (GO) have reached new structural possibilities by controlled reducing reactions using ascorbic acid. With the ability of selective reduction, this acid induces the tailoring effect of the sheets, causing a porous lattice. The present study proposes an investigation onto the quality of graphene oxide produced using Hummers' method to understand the reduction mechanism of ascorbic acid better. X-ray diffractometry, Fourier transform infrared spectroscopy with attenuated total reflectance and Raman Spectroscopy analyses were performed. The sample presented a typical crystalline structure of GOs, with appreciable degrees of oxidation and moderate density of defects—promising characteristics in forming the porous network of aerogels.**

**Keywords:** Graphene Oxide. Hummers' Method. Ascorbic Acid. Graphene Oxide Reduction. Lattice Defects.

The need for more practical alternatives to obtain graphene allowed the discovery of derivatives with notable applicability, such as graphene oxide (GO). This material, the oxidized, non-stoichiometric version of graphene, is commonly produced by the chemical exfoliation reaction of graphite [1]. In this reaction, oxygenated functions (hydroxyls, epoxy, carboxyls, and carbonyls) react with the graphene sheets, expanding the lamellae of the graphite structure. Subsequently, effective exfoliation takes place through sonication in suspension, yielding sheets of different sizes, stacking (mono, bi, and a few layers), and degrees of oxidation [2,3]. This material can also be reduced, removing these oxygenated functions from its sheets, achieving appreciable purities, and restoring the properties of graphene.

Hydrazine has established itself as the most effective reducing agent among the reduction alternatives. However, the toxicity of its reaction products and environmental damage have demanded new, safer, and more eco-friendly alternatives [4,5]. Thus, ascorbic acid emerges as a suitable

alternative to meet both requirements, ensuring high efficiency in reducing the oxidized sheets with practically non-toxic by-products. As an additional benefit, it also produces reduced graphene with a larger specific surface area, compared to hydrazine, by acting indirectly as a separator between the sheets, forming a porous network and producing hydrogels [6,7].

Nevertheless, reduction and oxidation are critical processes for the structure of the resulting graphene sheets. Both excess oxidation and oxidative precursors can cause defects in the graphene network that directly affect the subsequent reduction activity. This occurs since, under more aggressive oxidations, the continuity of the graphene network is affected, increasing the number of defects, which, for the most part, are considered edge zones [8,9].

In the case of ascorbic acid, its primary reduction target is the oxygenated functional groups in the basal plane (hydroxyls and epoxy groups). At the same time, the edge species (carboxyls and carbonyls) are less influenced. Additionally, edge species will interact with each other through hydrogen bonds [7,8], causing a tailoring effect between the sheets and promoting a hierarchical porosity structure [6].

The possibility of obtaining these porous structures, known as graphene aerogels, from a simple methodology based on the environmentally friendly reduction of GO draws attention due to

Received on 18 September 2024; revised 28 November 2024.  
Address for correspondence: Camila Miranda Fonseca Duarte. Rua Luís Eduardo Magalhães, 192, Itapua. Zipcode: 41630-700. Salvador, Bahia, Brazil. E-mail: camila.duarte@fieb.org.br.

J Bioeng. Tech. Health 2024;7(4):342-347  
© 2024 by SENAI CIMATEC. All rights reserved.

the numerous possible applications. However, understanding the structure of the graphene oxide precursor and how it will influence the reduction mechanism of ascorbic acid is essential to achieving stable aerogel structures [10]. Therefore, the present work sought to evaluate the quality of graphene oxide produced by the Hummers method, relating its defects and network to the reducing action of ascorbic acid to form aerogels.

## Materials and Methods

The method adopted for synthesizing graphene oxide was based on the work of Yoo M and Park H [11], which uses the Hummers method. Initially, 5 g of graphite was added to a beaker containing 115 mL of  $\text{H}_2\text{SO}_4$  in an ice bath (approx. 6 °C) and stirred for one hour. Then, 15 g of  $\text{KMnO}_4$  was slowly added to the system, controlling the temperature, kept under stirring at 40 °C for 3 hours. Finally, 230 mL of distilled water was carefully added to the system to dilute it, avoiding the sudden rise of the temperature so as not to exceed 90 °C, for 30 min under continuous stirring, then further 115 mL of  $\text{H}_2\text{O}_{\text{dest}}$  to cool the solution to room temperature. Upon reaching 35 °C, 15 mL of  $\text{H}_2\text{O}_2$  was added to the system under continuous stirring for another 15 min to stop the reaction.

Finally, the stirring stopped, and the solution was allowed to settle overnight. The supernatant was removed, and the decanted cake was washed in 500 mL HCl 10%, under agitation for 1 h, and then allowed to settle. This process was repeated twice, and the decanted product was vacuum filtered in a Buchner funnel with a glass fiber filter. The cake obtained was dried under mild conditions (40 °C) overnight, resulting in a monolith, which was stored in a container isolated from light and named GO.

The material obtained was subjected to X-ray diffractometry (XRD) performed on a Shimadzu XDR-6000 diffractometer, with  $\text{CuK}\alpha$  radiation, 40 kV, 30 mA, graphite monochromator, in a scanning range of 5° to 80° with a step of 2 °/min. The RAMAN spectrum was obtained using a

JASCO 5200 instrument with a laser width of 532 nm and 0.3 mW of power. The Fourier transform infrared spectroscopy with Attenuated Total Reflectance (FTIR-ATR) was performed using a Thermo Scientific Nicolet iS10 spectrometer at room temperature in the 500-4000  $\text{cm}^{-1}$  range. Micrographs were also obtained using a Jeol JEM1400 plus Transmission Electron Microscope (TEM) operating under a voltage of 120 kV.

## Results and Discussion

The diffractogram obtained in the GO sample (Figure 1) presents two prominent peaks at 10.38° and 42.32°, characteristic of the graphene oxide structure, according to the literature [4,12,13]. It is well known that the central peak of graphite occurs at  $2\theta \approx 26.4^\circ$ , referring to the {002} plane, having an interplanar distance of 3.375 Å [12]. After being subjected to the oxidative process, the graphite lamellae are expanded by the intercalated oxygenated species, causing an increase in the d- d-spacing of the structure. This effect features by the appearance of the peak at 10.38°, which, by Bragg's Law, reflects an interplanar distance of  $\sim 8.5$  Å and denotes the interlayer expansion of the {001} plane, confirming the efficiency of the oxidative process in the intercalation of graphite [14,15]. The second peak, located at  $2\theta = 42.32^\circ$ , refers to the {101} plane of the  $\text{sp}^2$  graphitic lattice, present mainly in graphene oxides whose precursor is synthetic graphite [12], as this present methodology. It is worth mentioning that the width of the observed peaks is due to the high distribution of the sheet sizes, which can be interpreted as a reflection of the randomness of the crystallite sizes, also characteristic of the GO samples.

When analyzing the spectra obtained by FTIR-ATR (Figure 2), it is possible to notice an abundance of oxygenated functions present in the GO sample; for instance, OH, C=O, and C-O-C, reinforcing the hypothesis that the oxidation of the graphite sheets was effective, in agreement with the peak shift seen in the XRD results. The broad zone between

**Figure 1.** A diffractogram of the sample was obtained using Hummers' method.

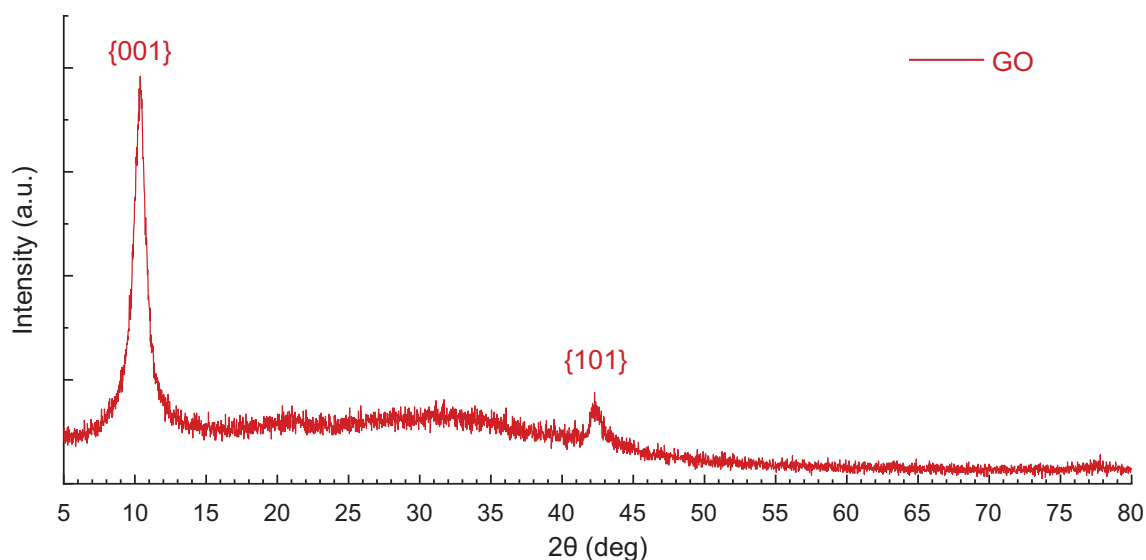
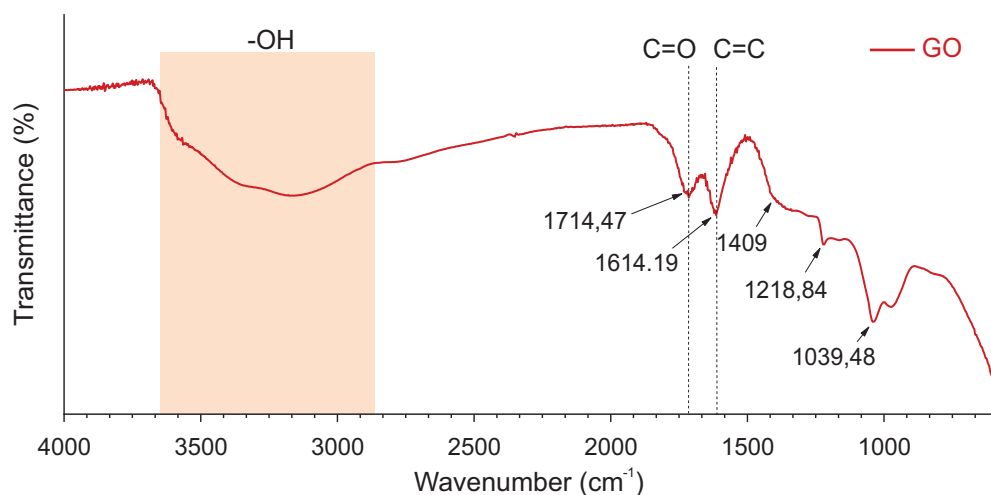


**Figure 2.** FTIR-ATR spectrum of graphene oxide sample obtained via Hummers.



3600 and 2900 cm<sup>-1</sup>, highlighted in red in Figure 2, frequently seen in graphene oxides, refers to the presence of hydroxyl groups, usually linked to the network in the basal plane [3,16] or even associated with carboxylic groups. In addition, the two leading characteristic bands of GO were also identified, in 1714 and 1614 cm<sup>-1</sup>, consistent with those found in the literature [7,16], endorsing the understanding that the sample is a graphene oxide, attesting to the effectiveness of the synthesis. Carboxylic acid (shoulder ~1400 cm<sup>-1</sup>) and epoxy (1218.84 and

1039.48 cm<sup>-1</sup>) structures were also identified in the spectrum [13].

When observing the Raman spectrum of the GO sample obtained (Figure 3), the presence of two peaks, characteristic of graphene oxide [17,18], centered at 1346 and 1601 cm<sup>-1</sup>, referring to the D and G bands, respectively, is noted. The D band reflects the degree of disorder linked to the defects present in the lattice. This band does not appear in perfect graphene and is, therefore, related to a mechanism where the presence of defects activates



phonons outside the center of the Brillouin zone in a double resonance process; the G band, on the other hand, refers to the vibration of the  $sp^2$  bonds of the basal plane, being usually observed in perfect graphene spectra. However, changes in its position and width can be associated with the sheets' oxidation level. In the presence of

defects, a band called D' near the G band region is responsible for some of the broadening and displacement effects (Figure 4) [17–19]. In the high-energy region of the spectrum, above  $2500\text{ cm}^{-1}$ , second-order 2D, D+D', and 2D' bands of low intensity were identified, which is expected in graphene.

**Figure 3.** RAMAN spectrum of graphene oxide sample produced by Hummers.

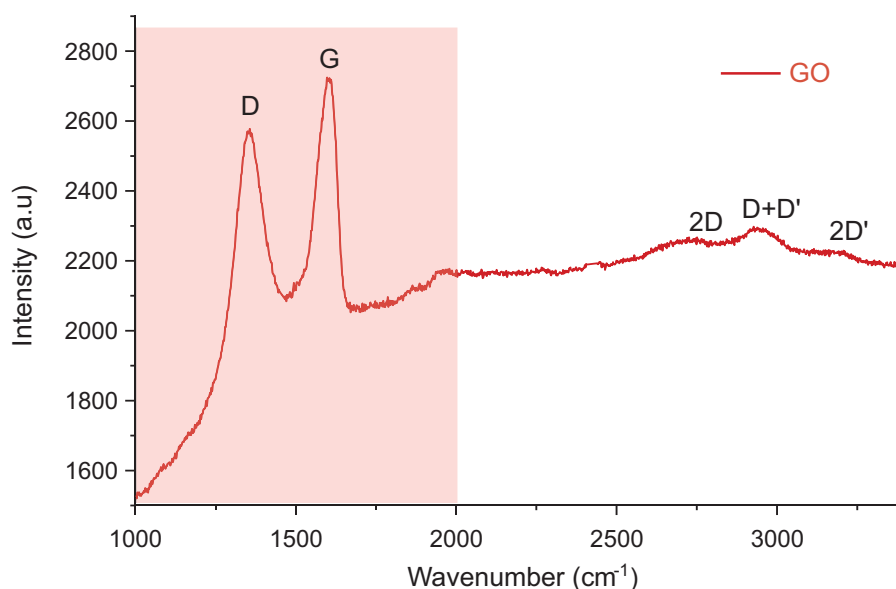
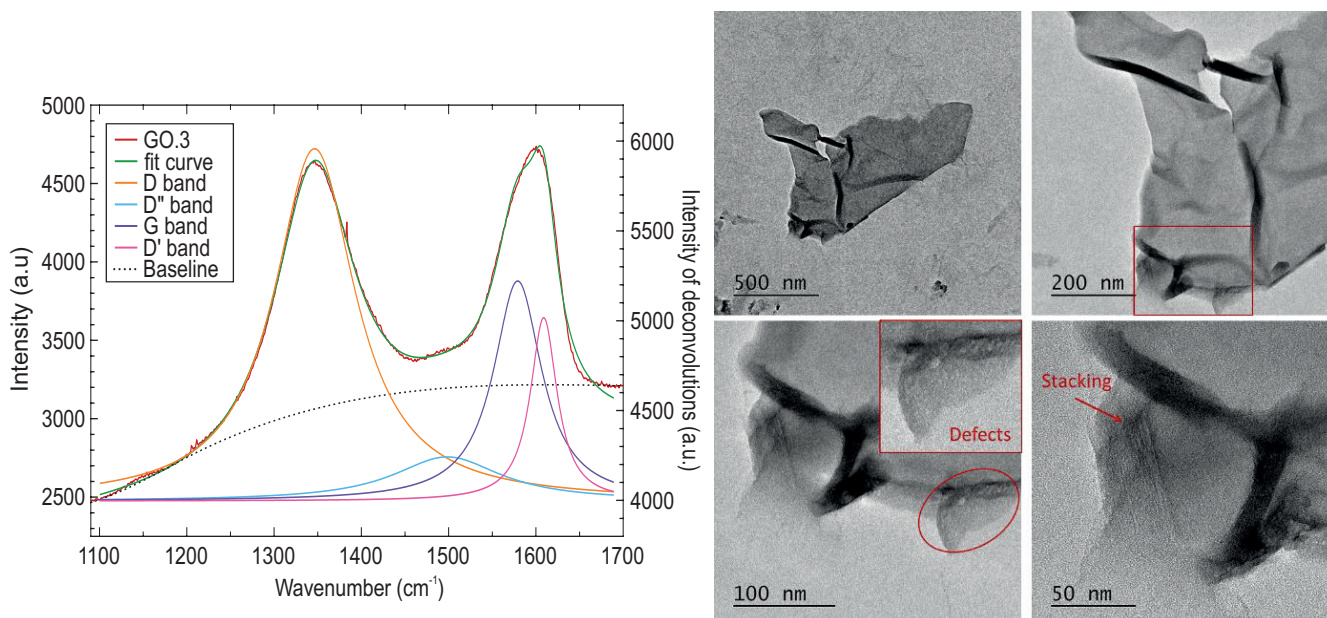


**Figure 4.** Deconvolution of the RAMAN spectrum in the D and G band region (on left) and micrographs obtained via TEM of the sample after exfoliation (on right).





Derivatives with a certain degree of defects, such as the synthesized sample, occur because the relationship between the intensities of the 2D and DD+D bands reflects the C sp<sup>2</sup> density of the GO sheets [18].

To better understand the structure of the synthesized GO and evaluate the quality of its sheets, the deconvolution of the Raman spectrum was performed using Lorentzian functions (Figure 4) [19]. The presence of the D", D, G, and D' bands was identified, with their peaks located at 1498.37 cm<sup>-1</sup>, 1346.40 cm<sup>-1</sup>, 1579.11 cm<sup>-1</sup>, and 1608.97 cm<sup>-1</sup>, respectively.

From the curve fit data, the degree of disorder of the sample was calculated using the ratio of the area under the curve of the D and G bands (AD/AG) since they represent the probability of phonon scattering. In the sample, this ratio is 2.69, which characterizes the synthesized graphene oxide with a low to moderate degree of disorder [18,19]. Furthermore, according to Lopez-Díaz D. and colleagues [18], in values of AD/AG 3.5, it is possible to identify the type of defect with the highest incidence in the material by evaluating the ratio AD'/AD, which in the analyzed sample presented a value of 0.17, indicating the coexistence of vacancy defects (0.14) and crystallite edges (0.29), with a predominance of vacancies [18]. The presence of the D' and D" bands, with noticeable intensities, further supports the understanding of the significant presence of defects since the first indicates the presence of impurities in the graphene network, which can be associated with the oxygenated functions present in the sheets. The second reflects the degree of amorphicity of the sample, which in turn is also influenced by the small crystallite sizes [18,19]. TEM images in Figure 4 (on the right) show a structure of the GO sample after exfoliation, where smooth edge zones can be noted, characteristic of armchair configurations [20], in addition to perforations in the sheets resulting from the oxidative process and zones indicative of sheet stacking. Using Raman spectroscopy, we can also estimate the average crystallite size through Equation 1 [13]

### Equation 1.

$$L_a = \frac{2,4E^{-10} \times (\lambda_{laser})^4}{(A_{D'}/A_G)}$$

Considering the laser wavelength ( $\lambda_{laser}$ ) of 532 nm and applying the values from the curves, an average crystallite size of 7.1 nm was found. This size can be interpreted as the distance between the defects in the graphene sheet; the smaller this size, the greater the density of defects in our sample [17,18].

The characteristics obtained were evaluated according to the ascorbic acid reduction mechanism, aiming to preliminarily predict how the material will behave to form the porous network of the reduced graphene oxide aerogel. Therefore, when analyzing the average crystallite size with the identified oxygenated species, the synthesized GO presents a high edge zone where -COOH and C=O species are predominant. On the other hand, the literature indicates that the reducing action of ascorbic acid is concurrent with the formation of the porous network and has selectivity for the epoxy and -OH groups located in the basal plane, while those at the edges are less influenced, enabling an interaction of the sheets by hydrogen bonds, which induces the formation of hydrogel agglomerates [6–8].

Still, another critical point to be observed in structuring a stable porous network is the overlapping of the sheets forming the walls. In the reduction process via ascorbic acid, the parallel stacking of the sheets is influenced by their size. This is because the presence of the edge functions causes steric effects, generating a random interaction between the edges and basal planes of the sheets smaller than 10 nm, while in dimensions greater than 80 nm, the basal functions prevent the effective stacking connection between layers, which can result in low structural stability of the aerogel [10]. Still, other synthesis parameters also directly interfere with quality, such as pH, agitation, and temperature reduction, and must be considered to obtain structures per the desired objective.

## Conclusion

It is concluded that the GO obtained has a moderate defect degree, most of which are vacancies, as indicated in the FTIR. Raman spectroscopy measurements revealed that the average crystallite diameter was approximately 7.1 nm. The small size represents a reasonable but not very intense defect density, which is interesting since starting from an exfoliated and less damaged GO is an advantage, which means that the oxygenated edge species will also be predominant in the sample, as identified by the bands corresponding to the -COOH and C=O structures in the FTIR-ATR spectrum. These characteristics are promising for forming a porous network in this material, which is spontaneous and structured since the starting GO has sufficient edge functions for the tailoring effect of the sheets, which are responsible for generating the aerogel structure. Other parameters such as sheet size, degree of reduction, and ordered stacking are effects of complementary synthesis methods that are being studied by the team for future work.

## Acknowledgments

The authors thank the institutions SENAI CIMATEC and Federal University of Bahia for their contribution to the infrastructure needed to carry out the experiments and characterizations presented in this work.

## References

1. Coros M, Pogăcean F, Măgeruşan L et al. A brief overview on synthesis and applications of graphene and graphene-based nanomaterials. *Front Mater Sci* 2019;23–32.
2. Chen X, Qu Z, Liu Z et al. Mechanism of oxidization of graphite to graphene oxide by the Hummers method. *ACS Omega* 2022;7:23503–23510.
3. Hou Y, Lv S, Liu L et al. High-quality preparation of graphene oxide via the Hummers' method: Understanding the roles of the intercalator, oxidant, and graphite particle size. *Ceram Int* 2020;46:2392–2402.
4. Bychko I, Abakumov A, Didenko O et al. Differences in the structure and functionalities of graphene oxide and reduced graphene oxide obtained from graphite with various degrees of graphitization. *Journal of Physics and Chemistry of Solids* 2022;164.
5. Stobinski L, Lesiak B, Malolepszy A et al. Graphene oxide and reduced graphene oxide studied by the XRD, TEM and electron spectroscopy methods. *J Electron Spectros Relat Phenomena* 2014;195:145–154.
6. Ortiz-Anaya I, Nishina Y. Unveiling the reduction process of graphene oxide by ascorbic acid: Grafting and reduction sequences for high surface area graphene materials. *Chempluschem* 2023;88.
7. Palomba M, Carotenuto G, Longo A. A brief review: The Use of L-ascorbic acid as a green reducing agent of graphene oxide. *Materials* 2022;15.
8. de Silva KKH, Huang HH, Yoshimura M. Progress of reduction of graphene oxide by ascorbic acid. *Appl Surf Sci* 2018;447:338–346.
9. Li M, Deng T, Zheng B et al. Effect of defects on the mechanical and thermal properties of graphene. *Nanomaterials* 2019;9.
10. Lee SP, Ali GAM, Hegazy HH et al. Optimizing reduced graphene oxide aerogel for a supercapacitor. *Energy and Fuels* 2021;35:4559–4569.
11. Yoo MJ, Park HB. Effect of hydrogen peroxide on properties of graphene oxide in Hummers method. *Carbon N Y* 2019;141:515–522.
12. Kim JH, Shim GH, Vo TTN et al. Building with graphene oxide: effect of graphite nature and oxidation methods on the graphene assembly. *RSC Adv* 2021;11:3645–3654.
13. Hou Y, Lv S, Liu L et al. High-quality preparation of graphene oxide via the Hummers' method: Understanding the roles of the intercalator, oxidant, and graphite particle size. *Ceram Int* 2020;46:2392–2402.
14. Iakunkov A, Talyzin A V. Swelling properties of graphite oxides and graphene oxide multilayered materials. *Nanoscale* 2020;12:21060–21093.
15. Yu W, Sisi L, Haiyan Y et al. Progress in the functional modification of graphene/graphene oxide: A review. *RSC Adv. Royal Society of Chemistry* 2020;15328–15345.
16. Hiosseini MA, Malekie S, Ebrahimi N. The analysis of linear dose-responses in gamma-irradiated graphene oxide: Can FTIR analysis be considered a novel approach to examining the linear dose-responses in carbon nanostructures? *Radiation Physics and Chemistry* 2020;176.
17. Anusuya T, Pathak DK, Kumar R et al. Deconvolution and quantification of defect types from the first order Raman spectra of graphene oxide derivatives. *FlatChem* 2022;35.
18. López-Díaz D, Delgado-Notario JA, Clericó V et al. Towards understanding the Raman spectrum of graphene oxide: The effect of the chemical composition. *Coatings* 2020;10.
19. Lee AY, Yang K, Anh ND et al. Raman study of D' band in graphene oxide and its correlation with reduction. *Appl Surf Sci* 2021;536.
20. Lee XJ et al. Review on graphene and its derivatives: Synthesis methods and potential industrial implementation. *J Taiwan Inst Chem Eng* 2019;98:163–180.

## Evaluating the Influence of Processing Conditions on Colloidal Stability and Particle Size in Fibrillated Nanocellulose

Marina Andrade<sup>1\*</sup>, Ana Paula Gonçalves<sup>1</sup>, Lucas Horiuchi<sup>1</sup>, Vinícius Oliveira<sup>1</sup>, Rodrigo Polkowski<sup>1</sup>

<sup>1</sup>TRL9 LAB Testing and Technical Analysis; Salvador, Bahia, Brazil

**Cellulose nanofibers (CNF) are nanostructures derived from cellulose's crystalline and amorphous regions through mechanical, chemical-mechanical, or enzymatic processes. Due to their high aspect ratio, extensive surface area, remarkable modulus of elasticity, and superior mechanical strength, CNFs have emerged as promising reinforcement materials in composite applications. Key properties such as colloidal stability, assessed via zeta potential, and nanofibril particle size provide critical insights into the dispersion and interaction of these fibers within a polymer matrix. These parameters are essential for optimizing composite performance and ensuring uniform fiber distribution. This study aimed to evaluate the influence of different preparation conditions on the zeta potential and particle size of CNFs, providing a better understanding of how processing parameters affect their characteristics. Keywords: Cellulose Nanofiber. Zeta Potential. Particle Size. Composites.**

Cellulose is the most abundant biopolymer on Earth, predominantly sourced from lignocellulosic materials such as agro-industrial waste [1]. Brazil is strategically positioned in this field due to its rich diversity of lignocellulosic resources and status as one of the world's largest agricultural producers. This ensures a significant contribution to the global availability of lignocellulosic biomass [2].

Among the many applications of cellulose, the production of nanostructures, such as cellulose nanofibers (CNFs), stands out. CNFs are nanostructures characterized by crystalline and amorphous domains obtained through mechanical, chemical-mechanical, or enzymatic processing methods [3]. These nanofibers exhibit exceptional properties, including a high aspect ratio, extensive surface area, high crystallinity, and a superior modulus of elasticity. Moreover, their ability to form interconnected networks enhances their mechanical properties, such as tensile strength, making them ideal as reinforcing materials in composites [4,5].

For CNFs to function effectively as reinforcement materials, they must maintain

stability and avoid agglomeration, as aggregation negatively impacts the composite's mechanical performance. Analyzing the zeta potential is one of the most reliable methods to evaluate this stability. This parameter provides insight into the electrical charge on the surface of suspended particles, which is crucial for determining the stability of colloidal dispersions. A high zeta potential (positive or negative) indicates strong electrostatic repulsion between particles, preventing aggregation and ensuring a stable suspension. Conversely, a low zeta potential suggests a tendency for particle aggregation, which can compromise the material's dispersion and, consequently, its mechanical and barrier properties [6].

Particle size analysis is another critical aspect of characterizing CNFs, as it directly influences their surface area, mechanical strength, and interaction with other composite components. Accurate particle size control ensures optimal nanofiber dispersion within matrices and tailors the material's performance in specific applications such as films, coatings, or biocomposites. This analysis allows researchers to assess the fibrillation process's efficiency, detect agglomerates, and make necessary adjustments to achieve desired material characteristics.

The duration of defibrillation significantly impacts the width and length of nanofibrils. Extended defibrillation times result in smaller

Received on 20 September 2024; revised 17 November 2024.  
Address for correspondence: Marina Reis de Andrade. Rua Mundo, 121, Edf. Tecnovia Sala 409c 4º Andar, Trobogy. Zipcode: 41.745-715. Salvador, Bahia, Brazil. E-mail: marina.andrade@trl9.tech.

J Bioeng. Tech. Health 2024;7(4):348-351  
© 2024 by SENAI CIMATEC. All rights reserved.

fibril dimensions, which are crucial for enhancing specific properties. For example, De Carvalho and colleagues (2019) [7] demonstrated that longer fibrillation times improve the mechanical properties of nanopapers by reducing fibril size. Similarly, Eriksen and colleagues (2008) [8] explored the production of microfibrillated cellulose (MFC) and found that prolonged processing times decreased fibril diameter, thereby enhancing the strength of MFC-reinforced paper. This study aims to evaluate the influence of different preparation conditions on cellulose nanofibers' zeta potential and particle size. These findings will contribute to developing CNFs as effective reinforcing materials for various applications.

## Materials and Methods

### Obtaining Cellulose Nanofibrils

The detailed procedure for obtaining cellulose nanofibrils (CNFs), including the specific agricultural residue source, is currently under patent filing by TRL9 and cannot be disclosed in this work. However, the CNFs were produced through a mechanical defibrillation process using Ultra-Turrax equipment. The process parameters—homogenization speed and residence time—were varied, resulting in four distinct samples.

### Zeta Potential and Particle Size Analysis

#### *Zeta Potential Analysis*

The zeta potential of the samples was analyzed using a Malvern Zetasizer Nano ZS. A 1 mL aliquot of the filtered CNF suspension was loaded into a DST1070 cuvette and placed into the equipment for measurement. For each sample, three measurement rounds were performed. The results were processed using the Zetasizer software, and the output data (intensity and power) were exported to Excel for compilation. The compiled data were further analyzed in Origin 2023b software, where the "Average Multiples

Curves" function generated a single averaged graph for each sample's three readings.

#### *Particle Size Analysis*

Particle size measurements were performed on the same equipment (Malvern Zetasizer Nano ZS) and followed the same three-round measurement protocol. The main differences were the type of analysis and the cuvette configuration, which were adjusted in the equipment's software for particle size evaluation.

## Results and Discussion

### Zeta Potential and Colloidal Stability

Zeta potential plays a pivotal role in characterizing cellulose nanofibrils (CNFs), influencing the colloidal stability of suspensions and the material's overall quality. During the production of CNFs, zeta potential monitoring is essential to optimize conditions such as pH or the addition of stabilizing agents, ensuring fibrils remain well-dispersed and prevent agglomeration. Table 2 summarizes each sample's zeta potential and particle size (Z-Ave) values. Values exceeding  $\pm 30$  mV generally indicate high colloidal stability due to strong electrostatic repulsion between particles. None of the samples achieved this threshold, suggesting moderate to low stability.

### Influence of Processing Conditions on Zeta Potential

The samples were differentiated based on homogenization speed and residence time. The following trends were observed:

#### *Effect of Residence Time*

Comparing A1 to A2 and A3 to A4, increased residence time reduced zeta potential. This indicates a greater tendency for particles to

agglomerate over time, potentially due to thermal agitation and heating during prolonged processing.

### *Effect of Homogenization Speed*

A rise in homogenization speed (from 14,000 to 18,000 rpm) also reduced zeta potential. Increased speed intensifies thermal agitation and ion mobility in the surrounding medium, altering the electrical double layer and promoting agglomeration.

As particles' kinetic energy increases with temperature, ion redistribution in the electrical double layer diminishes the magnitude of the zeta potential, reducing suspension stability. CNFs with high zeta potential values are crucial for homogeneous composite production and maintaining mechanical and barrier properties [9,10].

Chemical surface modifications of CNFs may help improve their zeta potential, enhance stability, and ensure better interaction with polymer matrices [11].

### Particle Size Analysis

Particle size is critical in determining the dispersion quality and mechanical properties of CNF-based composites. The results indicate the following:

### *Effect of Speed on Particle Size*

Comparing A1 to A3 and A2 to A4, higher homogenization speeds significantly reduced particle size due to the intensified shear forces breaking down the fibers.

### *Effect of Time on Particle Size*

Prolonged defibrillation time also reduced particle size, as observed when comparing A1 to A2 and A3 to A4.

Increased residence time enhances fiber fragmentation, promoting the production of smaller nanofibrils.

**Table 1.** Sample preparation conditions (speed and time).

Sample	Homogenization Speed (rpm)	Homogenization Residence Time (min)
A1	14,000	10'
A2	14,000	20'
A3	18,000	10'
A4	18,000	20'

**Table 2.** Zeta potential values and particle size distribution of the samples.

Sample	Homogenization Condition (rpm)/(min)	Zeta Potential (mV)	Z-Ave (d.nm)
A1	14,000 / 10'	-15.7	957.6
A2	14,000 / 20'	-10.8	499.4
A3	18,000 / 10'	-15.4	438.3
A4	18,000 / 20'	-2.94	338.6



These findings align with previous studies demonstrating that longer defibrillation times result in reduced fibril dimensions, crucial for applications requiring high mechanical strength and uniformity [12,13].

### Key Observations

- Increasing homogenization speed and time during mechanical defibrillation reduces particle size but adversely affects zeta potential.
- Achieving optimal CNF stability and particle size balance may require chemical stabilization techniques or controlled processing parameters to minimize heat generation
- This analysis underscores the importance of carefully optimizing defibrillation conditions to produce CNFs with desirable characteristics for industrial and biomedical applications.

### **Conclusion**

This study demonstrated that increasing mechanical defibrillation time and speed during Ultra-turrax processing effectively reduces cellulose nanofibril (CNF) particle size. The observed dimension reduction can be attributed to intensified shear forces and fiber fragmentation under prolonged and higher-speed defibrillation conditions.

Zeta potential was identified as a crucial parameter for assessing the colloidal stability of CNFs, which directly impacts their dispersion within polymer matrices and the resulting composite properties. A1 and A3 exhibited comparable zeta potential values among the samples, indicating moderate stability. However, these values can be further improved through surface modifications of the nanofibrils, which will be a key focus in future work. Optimizing zeta potential and particle size will pave the way for developing sustainable composites with enhanced mechanical and functional properties.

### **Acknowledgments**

The authors express their gratitude to TRL9 LAB Company and the Brazilian Research Agency CNPq for their technical and financial support, which was instrumental in completing this study.

### **References**

1. Magalhães S et al. Eco-friendly methods for extraction and modification of cellulose: An overview. *Polymers* 2023;15(14):3138-3163.
2. Pereira ALS et al. Bionanocompósitos preparados por incorporação de nanocristais de celulose em polímeros biodegradáveis por meio de evaporação de solvente, automontagem ou eletrofiliação. *Química Nova* 2014;37(7):1209-1219.
3. Abdul Khalil HPS et al. Production and modification of nanofibrillated cellulose using various mechanical processes: A review. *Carbohydrate Polymers* 2014;99:649-665.
4. Janoobi M et al. Producing low-cost cellulose nanofiber from sludge as new source of raw Materials. *Industrial Crops and Products* 2012;40:232-238.
5. Nissila T et al. Ice-templated cellulose nanofiber filaments as a reinforcement material in Epoxy. *Composites. Nanomaterials* 2021;11(2):490-504.
6. Pompeu LD et al. Evaluation of stability of aqueous dispersions using zeta potential data. *Disciplinarum Scientia* 2018;19(3):381-388.
7. de Carvalho DM et al. Impact of the chemical composition of cellulosic materials on the nanofibrillation process and nanopaper properties. *Industrial Crops and Products* 2019;127:203-211.
8. Eriksen Ø et al. The use of microfibrillated cellulose produced from kraft pulp as strength enhancer in TMP paper. *Nordic Pulp & Paper Research Journal* 2008;23(3):299-304.
9. Venditti R. *Encyclopedia of Microfluidics and Nanofluidics*, Springer link. 2014:1-10.
10. Siro I et al. Microfibrillated cellulose and new nanocomposite materials: A review. *Cellulose* 2010;17(3):459-494.
11. Sharma PR et al. Functionalized celluloses and their nanoparticles: Morphology, thermal and sorption properties. *Carbohydrate Polymers* 2014;109:135-142.
12. Carter N et al. Production and characterization of cellulose nanofiber slurries and sheets for biomedical applications. *Frontiers in Nanotechnology* 2021;3:1-21.
13. Tan Y et al. From cellulose to cellulose nanofibrils—A comprehensive review of the preparation and modification of cellulose nanofibrils. *Materials* 2020;13(22):5062-5094.

## Hybrid Polyamide Membranes Obtained by the Immersion Precipitation Method

Joanne Graziela Andrade Mendes<sup>1\*</sup>, Damares Oliveira de Jesus Ferreira<sup>1</sup>, Airan Magalhães Moura<sup>1</sup>, Carlos Antônio Pereira de Lima<sup>2</sup>, Arthur de Sousa Ferreira<sup>2</sup>, Keila Machado de Medeiros<sup>1</sup>

<sup>1</sup>Center for Science and Technology in Energy and Sustainability, Federal University of Recôncavo of Bahia; Feira de Santana, Bahia; <sup>2</sup>Department of Sanitary and Environmental Engineering, State University of Paraíba; Campina Grande, Paraíba, Brazil

**This research explores replacing petrochemical derivatives with renewable resources, focusing on developing natural fiber composites. Hybrid membranes composed of polyamide 6 and sodium hydroxide-treated sisal fiber were fabricated using immersion precipitation. The membranes were analyzed for water absorption, porosity, permeability fluxes, and yield. Results indicate that the fiber content influences porosity and pore radius. Pure membranes and those containing 1% fiber exhibited higher porosity than those with 3% and 0.33% fiber. All membranes demonstrated high dye removal efficiency, achieving yields above 95%. The study concludes that incorporating sisal fiber enhances the membrane properties, making them highly effective for textile dye separation and microfiltration applications.**

**Keywords:** Membrane. Sisal Fiber. Polyamide 6. Immersion Precipitation. Dye Removal.

The exploration of renewable resources as alternatives to petrochemical derivatives has garnered significant attention due to their environmental benefits. Among these alternatives, composites reinforced with natural fibers have demonstrated outstanding potential for various applications [1].

Natural fibers exhibit mechanical properties that enhance the characteristics of polymer matrices, making them a viable choice for reinforcement [2]. Commonly used natural fibers include sisal, coconut, bamboo, and banana. In Brazil, fibers such as jute, banana, piassava, sugarcane, coconut, sisal, and cotton dominate the market, accounting for 93% of national production [3]. Sisal fiber, in particular, offers advantages such as low cost, biodegradability, and non-toxicity [4]. However, the size and processing of these fibers significantly influence the resulting composites' properties by affecting dispersion and membrane morphology.

Sisal fiber is notable for its mechanical strength, although it is hydrophilic compared to other natural fibers. When incorporating hydrophilic fibers into hydrophobic polymers, surface treatments are often required to enhance interfacial adhesion and improve mechanical performance—key factors for producing high-quality composites [5]. Chemical and physical surface treatments can enhance the interaction between sisal fiber and polymer matrices, improving the mechanical properties of reinforced membranes. These properties are influenced by fiber/matrix adhesion, the volume fraction of fibers, and their dispersion within the matrix [6].

Membrane separation processes (MSPs) have diverse applications in the medical, biological, and pharmaceutical fields, as well as in the chemical and food industries [3]. The phase inversion method is desirable due to its simplicity, cost-effectiveness, and efficiency in preparing symmetric and asymmetric microporous membranes [2]. Polyamides, known for their excellent abrasion resistance and thermal stability, are commonly used with natural fibers like sisal to produce polymer composites with enhanced properties.

This study aims to develop hybrid membranes of polyamide 6 and sodium hydroxide-treated sisal fiber fabricated using immersion precipitation.

Received on 15 September 2024; revised 22 November 2024.  
Address for correspondence: Joanne Graziela Andrade Mendes. Av. Centenário, 697 - Sim, Feira de Santana - BA, Brazil, Zipcode: 44042-280. E-mail: mendesanne736@gmail.com.

J Bioeng. Tech. Health 2024;7(4):352-357  
© 2024 by SENAI CIMATEC. All rights reserved.

## Materials and Methods

### Preparation of Treated Sisal Fiber

Sisal fiber was used in three proportions—0.33%, 1.0%, and 3.0%—to prepare hybrid membranes. The fibers underwent a surface treatment involving immersion in a 3.0% sodium hydroxide solution for 1 hour. Following the treatment, the fibers were thoroughly rinsed in distilled water baths until a neutral pH was achieved. The neutralized fibers were then dried in an oven at 80°C for 24 hours to remove residual moisture.

### Membrane Fabrication

Polyamide 6 (PA6), coded as Technyl® C216, with an average molar mass of 10,500 g/mol and intrinsic viscosity (IV) of 134 mL/g, supplied by Rhodia/SP, served as the polymer matrix. PA6 pellets and hybrid mixtures containing 0.33%, 1.0%, and 3.0% (by weight) of treated sisal fiber were dissolved in hydrochloric acid to prepare the membranes. The solutions underwent homogenization for 4 hours at room temperature to ensure uniform dispersion of the fibers.

### Membrane Characterization Water Absorption Capacity

Water absorption capacity was evaluated by immersing the membranes at 24°C for 48 hours. The test was conducted in triplicate for accuracy.

### Porosity

Membrane porosity was determined by immersing the membranes in water for 48 hours. Measurements included the initial membrane mass, the amount of water absorbed, the volume of the membranes, and the density of water.

### Pore Radius

The mean pore radius of the membranes was calculated using the Guerout-Efford-Ferry equation,

which correlates porosity and other physical parameters.

### Permeability Flux

Continuous flow experiments were performed using a perpendicular filtration cell under a constant pressure of 1.0 bar. To measure permeability, filtrate samples were collected at 1-minute intervals for a total duration of 60 minutes.

### Textile Dye Removal Efficiency

The membranes' capacity to remove textile dyes was evaluated using ultraviolet-visible spectroscopy. These analyses were conducted at the Materials Characterization Laboratory of the Center for Science and Technology in Energy and Sustainability, Federal University of Recôncavo of Bahia.

## Results and Discussion

### Water Absorption and Porosity

Figure 1 (a) illustrates the water absorption, and Figure 1 (b) shows the porosity of the pure PA6 membranes and hybrids with 0.33%, 1%, and 3% sisal fiber.

The retention capacity of a membrane is influenced by its porosity, which can either expand or improve permeability. Figure 1 shows that, in general, water absorption decreases with increasing fiber content. In the porosity analysis, a membrane obtained by immersion precipitation is mainly influenced by phase separation, responsible for membrane formation and pore distribution. Figure 1(b) shows that the pure PA6 membrane and the PA6 membrane with 1% sisal fiber present greater porosity than those containing 3% and 0.33% fiber, following the exact water absorption behavior. Adding 1% fiber promoted the best water absorption and porosity results. However, a high concentration of fibers, as in the membranes with 3% sisal, led to agglomeration and reduced porosity. This behavior

can be explained by the surface treatment performed on the fiber, which aims to improve the filler/matrix interface. Applying aqueous sodium hydroxide ( $\text{NaOH(aq)}$ ) on the sisal fiber causes the ionization of the hydroxyl group into an alkoxide. With the reduction of the hydrophilic OH groups, the surface roughness of the fiber increases, exposing more reactive sites and improving adhesion to the matrix, which significantly favors the mechanical behavior of the composite [7].

### Average Pore Radius

Figure 2 shows the average pore radius of the pure PA6 membrane and its hybrids, which contain

0.33%, 1%, and 3% sisal fiber. The pores of the membranes are microscopic channels that allow the passage of substances and are essential in filtration and separation processes.

In the case of the PA6 membranes analyzed, the average pore radius of the pure and 0.33% sisal fiber membranes is smaller than that of the membranes containing 1% and 3% fiber. This behavior can be explained by the influence of the fiber concentration on pore formation, with a gradual increase in the average pore radius as a function of the increase in the percentage of fibers added to the polymer matrix.

When the fiber concentration is high, as in the case of the membranes with 3% fiber, pore dilation may

**Figure 1.** a) Water absorption and b) Porosity of pure PA6 membranes and hybrids with 0.33%, 1%, and 3% sisal fiber.

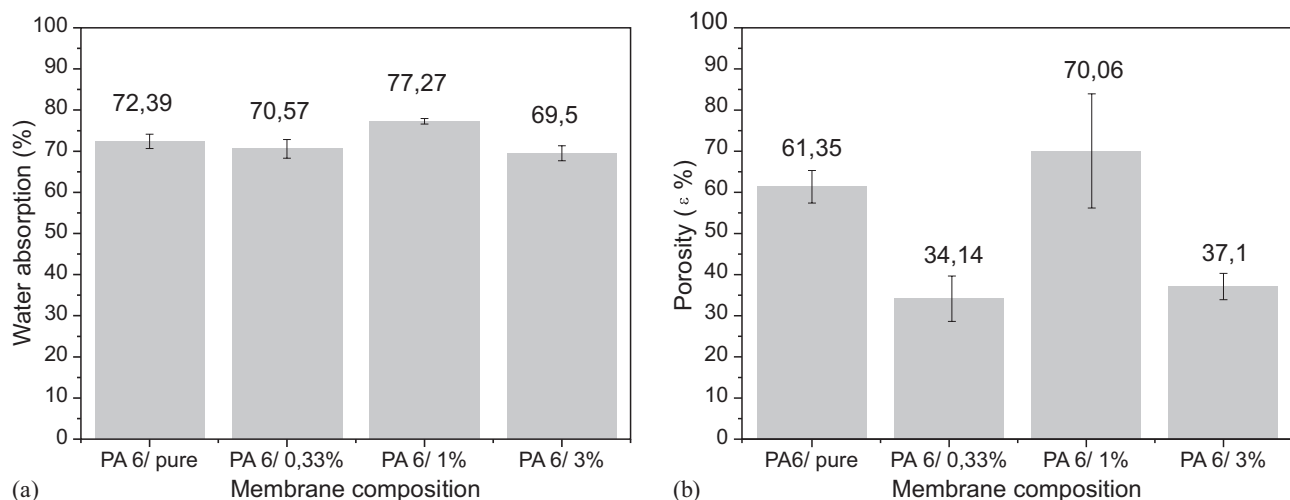
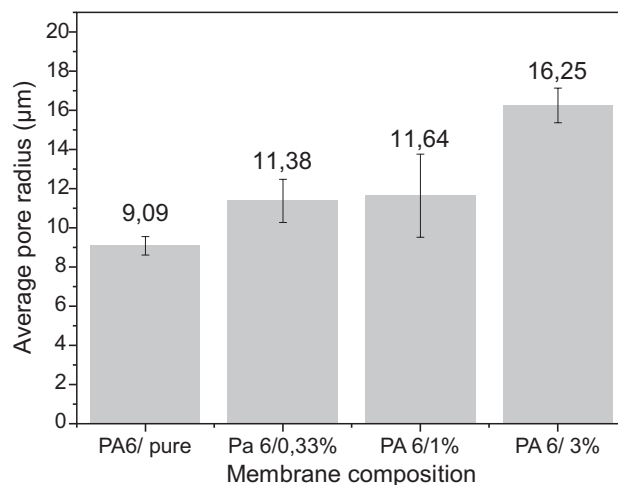


**Figure 2.** The average radius of the pure and hybrid PA6 membranes with 0.33, 1, and 3% sisal fiber.



occur, resulting in an increase in the average radius. On the other hand, a very low fiber concentration (0.33%) may also lead to pore dilation, possibly due to changes in the flow and temperature of the water during the membrane formation process. Therefore, the amount of fibers incorporated and the process conditions, such as the water temperature, affect the average pore radius.

### Flow Measurements

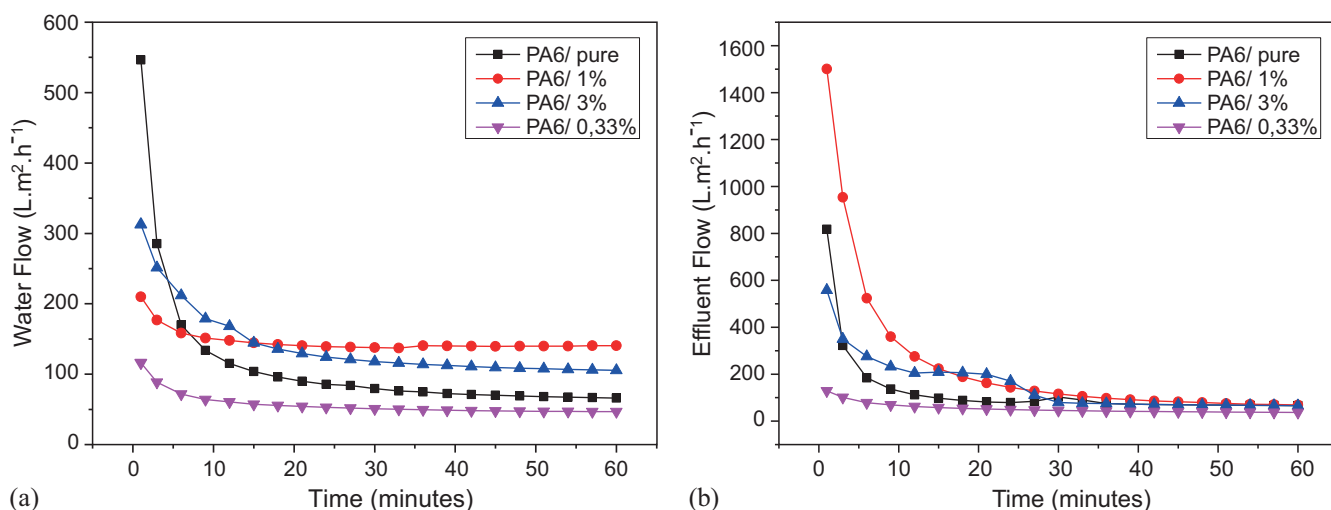
The curves presented in Figure 3 illustrate the flux measurements performed, providing a visual representation of the permeability characteristics of the membranes. Initially, a decrease in flux was observed in Figure (a), followed by a stabilization approximately 20 minutes after the start of the measurement. This stabilization can be attributed to a mechanical compaction process induced by the applied pressure or to the eventual swelling of the membranes since exposure to water tends to gradually reduce the size of the pores, directly influencing their permeability. The membrane with 0.33% sisal fiber presented the lowest flux, while the membrane with 1% fiber presented a slightly

higher flux than the other membranes. This suggests that the fiber concentration influences the pore dilation.

Figure (b), with the addition of the dye, shows that, during the measurements, an initial decrease in flux occurred, followed by stabilization after approximately 25 minutes. The membrane containing 1% sisal fibers presented the highest initial flux, which subsequently stabilized. The membrane with 0.34% sisal fibers presented the lowest flux throughout the measurement period. These observations indicate that the amount of sisal fibers significantly affects the flux behavior and stabilization of the membranes. In general, we can observe that the permeate fluxes of both water and effluent occurred a gradual increase in fluxes with the increase in the concentration of sisal fiber added to the polymer matrix, following a behavior

Similar to that obtained for the average pore radius. In addition, it is possible to observe an increase in the values of the permeate fluxes with the effluents, probably due to the increase in the temperature of the effluents over time, which has dilated the pores of the membranes without compromising the separation performance of the membranes.

**Figure 3.** a) Water permeate flux of pure PA6 membranes and their hybrids with 0.33, 1, and 3% sisal fiber at 1.0 bar pressure. b) Permeate effluent flow with the addition of dye from pure PA6 membranes and their hybrids with 0.33, 1, and 3% sisal fiber at a pressure of 1.0 bar.





## Membranes Yield

Dyes are highly pigmented organic compounds impart color to materials by selectively absorbing light [8]. By analyzing the concentration of the diluted dye in the effluent, we can determine the specific wavelength associated with the dye. In addition, this method allows us to evaluate the amount of dye remaining in the effluent after treatment. The visible light absorption range for dyes ranges from 428 to 512 nm. Using spectrophotometry, we identified the absorption peak of the dye and constructed an absorbance curve, as illustrated in Figure 4 (a), for concentrations of 50 mg.L<sup>-1</sup>, 100 mg.L<sup>-1</sup>, 200 mg.L<sup>-1</sup>, 300 mg.L<sup>-1</sup>, 400 mg.L<sup>-1</sup>, and 500 mg.L<sup>-1</sup>.

Using the calibration curve for dye absorbance at varying concentrations from 50 50 mg.L<sup>-1</sup> to

500 50 mg.L<sup>-1</sup>, we derived a linear fit equation ( $y = 0.00129x + 0.01965$ , where  $y$  represents the dye concentration based on absorbance) with a coefficient of determination ( $R^2$ ) of 0.99774, as depicted in Figure 4(b). This result indicates that the absorbance for the dye at each concentration follows a linear relationship. With the calibration curve established, we can now determine the dye concentration in the permeate by correlating the wavelength with the absorbance reading.

Subsequently, we evaluated the membrane efficiency (%) (Table 1). All membranes tested in the dye separation process in water at a concentration of 500 mg.L<sup>-1</sup> exhibited a significant dye reduction in the permeate, reaching efficiencies higher than 95%.

**Figure 4.** a) Absorption spectra of red dye at concentrations of 50 mg.L<sup>-1</sup>, 100 mg.L<sup>-1</sup>, 200 mg.L<sup>-1</sup>, 300 mg.L<sup>-1</sup>, 400 mg.L<sup>-1</sup>, and 500 mg.L<sup>-1</sup>. b) Dye absorbance calibration curve.

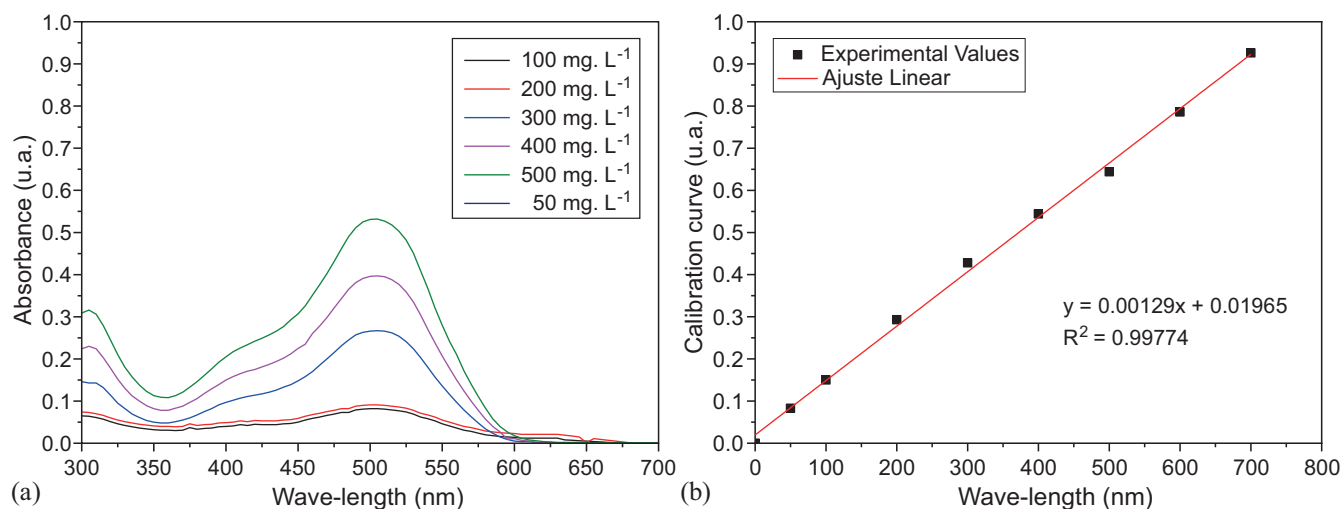


**Table 1.** The concentration of non-permeated dye at 500 mg.L<sup>-1</sup> and yield.

Membrane Composition	Absorbance (ua)	Concentration (mg/L <sup>-1</sup> )	Yield (%)
PA6/Pure	0.161	8.28	98.34
PA6/0.33%	0.421	21.55	95.69
PA6/1%	0.019	1.04	99.79
PA6/3%	0.359	18.38	96.32

## Conclusion

Hybrid membranes of polyamide 6 (PA6) reinforced with sisal fibers were successfully developed using immersion-precipitation. The study demonstrated that the fiber content significantly influences the porosity and retention capacity of the membranes. Specifically, water absorption decreased with higher fiber concentrations, indicating a strong correlation between fiber content and porosity.

The addition of sisal fibers enhanced the mean pore radius, improving the membranes' permeability characteristics. Flux measurements confirmed hybrid membranes exhibited superior permeate flux compared to pure PA6 membranes. Moreover, all membranes achieved a high dye separation efficiency, with yields exceeding 95%, confirming their potential application in microfiltration systems and the treatment of textile effluents.

This research highlights the viability of using renewable resources, such as sisal fibers, to improve polymer membrane performance, offering a sustainable alternative for advanced separation processes.

## Acknowledgments

The authors gratefully acknowledge the Conselho Nacional de Desenvolvimento Científico e Tecnológico (CNPq), the Advanced Water Treatment Research Group, and the Center for Science and Technology in Energy and Sustainability at the Federal University of Recôncavo da Bahia for their sponsorship and invaluable support throughout this study.

## References

1. Kleba I, Zabold J. Poliuretano com fibras naturais ganha espaço na indústria automotiva, *Plástico Industrial* 2004;11:88-99.
2. Pothan LA, Thomas S. Polarity parameters and dynamic mechanical behavior of chemically modified banana fiber reinforced polyester composites. *Composites Science and Technology* 2003;63:1231-1240. DOI: [https://doi.org/10.1016/S0266-3538\(03\)00092-7](https://doi.org/10.1016/S0266-3538(03)00092-7).
3. Satyanarayana KG, Guimarães JL, Wypych F. Studies on lignocellulosic fibers of Brazil. Part I: Source, production, morphology, properties and applications. *Composites Part A: Applied Science and Manufacturing* 2007;38(7):1694-1709. DOI: <https://doi.org/10.1016/j.compositesa.2007.02.006>.
4. Kuruvilla J, Tolêdo Filho RD, Beena J, Sabu T, Carvalho LH. A review on sisal fiber reinforced polymer composites. *Revista Brasileira de Engenharia Agrícola e Ambiental*, Campina Grande 1999;3(3):367-379.
5. Srisuwan S, Prasertsopha N, Suppakarn N, Chumsamrong P. The effects of alkalized and silanized woven sisal fibers on mechanical properties of natural rubber modified epoxy resin. *Energy Procedia* 2014;56:641-648. DOI: <https://doi.org/10.1016/j.egypro.2014.07.127>.
6. Spadetti C, Silva Filho EA, Sena GL, Melo CVP. Thermal and mechanical properties of post-consumer polypropylene composites reinforced with cellulose fibers. *Polímeros: Ciência e Tecnologia* 2020;30(3):e2320, 2020. DOI: <https://doi.org/10.1590/0104-1428.2320>.
7. Fiore V, Scalici T, Nicoletti F, Vitale G, Prestipino M, Valenza A. A new eco-friendly chemical treatment of natural fibres: Effect of sodium bicarbonate on properties of sisal fibre and its epoxy composites. *Composites Part B: Engineering* 2016;85:150-160. DOI: <https://doi.org/10.1016/j.compositesb.2015.09.028>.
8. Índice de Cores O Índice de Cores™. Society of Dyers and Colorists and American Association of Textile Chemists and Colorists. Available at: <https://colour-index.com/definitions-of-a-dye-and-a-pigment>. Accessed on: June 9, 2024.

## Ecotoxicity Study Using Dibenzothiophene and Mercury Chloride in "Brine Shrimp"

Melise Lemos Nascimento<sup>1,2\*</sup>, Madson Moreira Nascimento<sup>2,3</sup>, Gisele Olímpio da Rocha<sup>1,2</sup>,  
Jailson Bittencourt de Andrade<sup>2,3</sup>

<sup>1</sup>Interdisciplinary Center of Energy and Environment (CIEnAm), Federal University of Bahia (UFBA),

<sup>2</sup>National Institute of Science and Technology in Energy and Environment (INCT), Federal University of Bahia (UFBA);

<sup>3</sup>SENAI-CIMATEC University; Salvador, Bahia, Brazil

**This study investigated the ecotoxicity of Dibenzothiophene (DBT) and mercuric chloride (HgCl<sub>2</sub>) using *Artemia franciscana* (brine shrimp) as a model organism. Acute toxicity tests were conducted to individually determine the LC<sub>50</sub> values for DBT and HgCl<sub>2</sub> at concentrations of 1, 2, 4, 8, and 10 mg L<sup>-1</sup>. Results from the probit model revealed that the LC<sub>50</sub> of HgCl<sub>2</sub> was 33.11 mg L<sup>-1</sup>, which is approximately ten times higher than that of DBT (3.89 mg L<sup>-1</sup>), indicating that DBT is significantly more toxic. When combined, these contaminants exhibited a pronounced lethal synergy, resulting in total mortality of *Artemia franciscana* at all tested concentrations. These findings underscore the critical need to understand the synergistic effects of environmental contaminants and call for further research into the chronic toxicity and long-term sublethal impacts of polycyclic aromatic sulfur heterocycles (PASHs) on marine ecosystems.**

**Keywords:** Ecotoxicological Test. Brine Shrimp. Dibenzothiophene. Mercuric Chloride. Synergistic Contamination.

The species *Artemia franciscana*, commonly known as brine shrimp (BS), is a saltwater microcrustacean with five life stages, of which the nauplii stage is the most frequently used in ecotoxicity tests [1,2]. These tests provide valuable insights into the toxic effects of contaminants on aquatic biota in marine environments [3]. Consequently, *Artemia franciscana* is widely used as a model organism *in vivo* ecotoxicity studies, mainly through median lethal dose (LD<sub>50</sub>) or lethal concentration (LC<sub>50</sub>) assessments, which measure mortality when the species is exposed to substances such as heavy metals (e.g., cadmium, copper, zinc, and nickel) [4] or organic compounds (e.g., methylparaben, dicamba herbicide, and polypropylene microplastics) [5-7]. Beyond ecotoxicological studies, BS has been employed in reproductive toxicity evaluations, mutagenicity assessments (e.g., the Ames test), and chronic toxicity studies [8,9], highlighting its extensive

and diverse applications in high-impact research. Ecotoxicity tests traditionally focus on isolated contaminants, such as nanomaterials, microplastics, cosmetics, pharmaceuticals, and pesticides [11-5]. However, contemporary environmental contamination often involves multiple pollutants, necessitating revised testing methodologies to assess the effects of combined contaminants [16,17]. Recent studies, such as those by Albarano and colleagues (2023) [18], have explored the interactions of polycyclic aromatic hydrocarbons (PAHs) mixtures on BS, revealing gene expression changes in both nauplii and adult stages. These findings emphasize the ecological importance of studying mutual contamination and its potential impacts on biological processes in marine invertebrates.

In 2019, a significant oil spill on the Brazilian coast released a mixture of contaminants, including polycyclic aromatic sulfur heterocycles (PASHs), into marine ecosystems [19]. PASHs, such as mercaptans, thiophenes, benzothiophenes, and dibenzothiophenes (DBTs), are natural constituents of crude oil [20] and are gaining attention due to their carcinogenic and mutagenic properties and widespread presence in depositional environments [21]. Recent studies have identified DBT derivatives,

Received on 28 September 2024; August 19 November 2024.

Address for correspondence: Melise Lemos Nascimento. Avenida Milton Santos, s/n, Campus Ondina, Salvador, Bahia, Brazil. Zipcode: 40170-115. E-mail: melise.lemos@gmail.com.

J Bioeng. Tech. Health 2024;7(4):358-362

© 2024 by SENAI CIMATEC. All rights reserved.

such as 2,3-dimethyl benzothiophene (2,3-DMBT), 4-methyl benzothiophene (4-MBT), and 4,6-methyl dibenzothiophene (4,6-MDBT) [22], in marine organisms like ascidians, which were contaminated by maritime transport activities [22]. Similar findings were observed in *Lepas anatifera*, raising concerns about potential risks to marine organisms and their predators [23]. Concurrently, toxic metals like mercury have been documented in polychaetes from regions such as Todos os Santos Bay, Brazil [24]. Despite these findings, the specific effects of PASHs and their interaction with heavy metals on marine biota remain poorly understood.

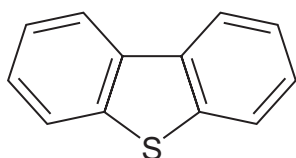
This study evaluates the toxicity of DBT and mercuric chloride ( $\text{HgCl}_2$ ) on *Artemia franciscana* through *in vivo* ecotoxicity tests, considering both individual and combined exposure scenarios. The co-contamination test (DBT +  $\text{HgCl}_2$ ) was designed to investigate potential synergistic effects, providing a deeper understanding of the ecological risks posed by the interaction of organic and metallic contaminants in marine environments.

## Materials and Methods

### Hatching of Nauplii

Newly hatched nauplii of *Artemia franciscana* were obtained from commercially dried cysts (Yepist, Bahia, Brazil). Approximately 100 mg of cysts were hatched in artificial seawater ( $37 \text{ g L}^{-1}$ ) at  $28^\circ\text{C}$  under continuous illumination and aeration conditions. After 24 hours, the newly hatched nauplii and unhatched cysts were separated from their shells using a phototaxis-based method. The hatched nauplii were immediately transferred with a Pasteur pipette to tubes containing artificial seawater and maintained at  $25 \pm 1^\circ\text{C}$  until use in toxicity tests.

**Figure 1.** Dibenzothiophene compound.



### Acute Toxicity of DBT, $\text{HgCl}_2$ , and DBT + $\text{HgCl}_2$

A 24-hour acute toxicity test was conducted to determine the  $\text{LC}_{50}$  values for:

- Dibenzothiophene (DBT) in ethanolic solution,
- Mercuric chloride ( $\text{HgCl}_2$ ) in aqueous solution, and
- Combined exposure to DBT +  $\text{HgCl}_2$ .

The  $\text{LC}_{50}$  value represents the concentration of a substance that causes mortality in 50% of the test population after a specified exposure period. The concentrations tested for each toxicant were 1, 2, 4, 8, and  $10 \text{ mg L}^{-1}$ . The control group consisted of artificial seawater with ethanol (the solvent used for DBT). All tests were performed in triplicate, each replicate containing 10 *Artemia nauplii*, resulting in 30 nauplii per concentration and control group (Table 1).

After 24 hours of exposure, mortality was assessed. Dead nauplii were identified as those exhibiting no movement for 10 seconds under continuous observation.

### Statistical Analysis

The  $\text{LC}_{50}$  values were calculated using the probit model in Microsoft Excel. Mortality data were plotted on a  $\log_{10}$  concentration scale against the percentage of mortality to determine the relationship between concentration and toxicity. Graphs of mortality data were generated using GraphPad Prism 5D.

## Results and Discussion

$\text{LC}_{50}$  values represent the concentration of a substance that causes mortality in 50% of a population and provide a measure of the substance's toxicity. The results for  $\text{LC}_{50}$  showed that the control group containing ethanol did not result in any mortality among the nauplii, confirming ethanol's low toxicity as a solvent. In the tests with DBT, the  $\text{LC}_{50}$  was  $3.89 \text{ mg L}^{-1}$ , indicating significant toxicity (Figure 2). Comparatively,  $\text{HgCl}_2$  showed a higher  $\text{LC}_{50}$  value of

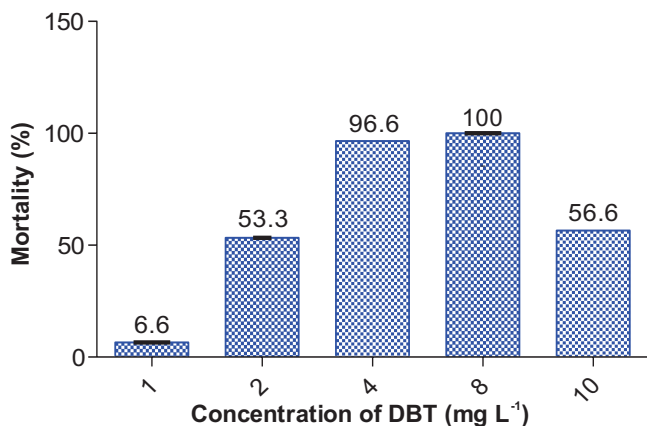
**Table 1.** Experimental design.

Toxicity Tests	Composition solution	Replicates	Concentrations	Total BS naupliis
Control Group	Artificial seawater + Ethanol	3	-	30
DBT	DBT + Water + Ethanol	15	1, 2, 4, 8, 10 mg L <sup>-1</sup>	150
HgCl <sub>2</sub>	HgCl <sub>2</sub> + Water	15	1, 2, 4, 8, 10 mg L <sup>-1</sup>	150
DBT + HgCl <sub>2</sub>	HgCl <sub>2</sub> + DBT Water + Ethanol	15	1, 2, 4, 8, 10 mg L <sup>-1</sup>	150

33.11 mg L<sup>-1</sup> (Figure 3), suggesting lower immediate toxicity within the 24-hour exposure period (Table 2). However, mercury's known bioaccumulative properties could explain the reduced short-term mortality, as its effects may intensify over time. When DBT and HgCl<sub>2</sub> were combined, total mortality was observed at all concentrations tested, including the lowest (1 mg L<sup>-1</sup>) (Figure 4). This highlights a lethal synergistic interaction between the two contaminants, where their combined toxicity far exceeded their individual effects.

## Results and Discussion

The solubility of DBT (1.47 mg L<sup>-1</sup>) is significantly lower than that of HgCl<sub>2</sub> (73.30 mg L<sup>-1</sup>). An ethanolic solution was used to improve DBT's solubility in water. Despite this, the common ion effect in artificial seawater likely reduced the solubility of both compounds due to the presence of Na<sup>+</sup> and Cl<sup>-</sup> ions, which may have influenced mortality rates.

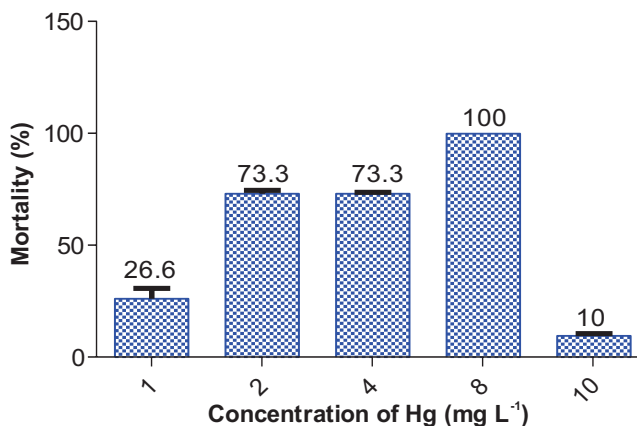
**Figure 2** Mortality of BS in DBT.

Mortality increased gradually with DBT concentrations up to 8 mg L<sup>-1</sup> but decreased at 10 mg L<sup>-1</sup>, potentially due to precipitation of DBT as solubility limits were reached. HgCl<sub>2</sub> demonstrated higher mortality rates than DBT at equivalent concentrations, reflecting the greater sensitivity of *A. franciscana* to HgCl<sub>2</sub>.

The co-contamination tests with DBT and HgCl<sub>2</sub> revealed a synergistic effect, resulting in 100% mortality across all concentrations. This highlights the importance of studying combined pollutant effects, as they can magnify toxicity and pose significant ecological risks.

## Conclusion

Marine environments are increasingly exposed to contamination from diverse sources, such as industrial discharge, agricultural runoff, and household waste. This study's acute toxicity tests demonstrated that HgCl<sub>2</sub> is significantly more toxic than DBT, with

**Figure 3.** Mortality of BS in HgCl<sub>2</sub>.



**Table 2.** Mortality and LC<sub>50</sub>.

Toxicity Tests	Concentrations (mg L <sup>-1</sup> )	Mortality (%)	LC <sub>50</sub>	Solubility
Control Group	0	0	---	---
DBT	1	6.6	3.89	1.47 mg L <sup>-1</sup>
	2	53.3		
	4	96.6		
	8	100		
	10	56.6		
HgCl <sub>2</sub>	1	26.6	33.11	73.302 mg L <sup>-1</sup>
	2	73.3		
	4	73.3		
	8	100		
	10	10		
DBT + HgCl <sub>2</sub>	1	100	---	---
	2	100		
	4	100		
	8	100		
	10	100		

Source: SciFindern (CAS Chemical Abstracts Service).

an LC<sub>50</sub> value approximately ten times higher. Furthermore, when combined, these contaminants exhibited a lethal synergistic effect, causing total mortality at all tested concentrations. These findings underscore the critical need to investigate the combined effects of environmental

contaminants. Future research should focus on chronic toxicity and sublethal effects to understand the long-term implications of exposure to PASHs and other pollutants in marine ecosystems.

**Acknowledgments**

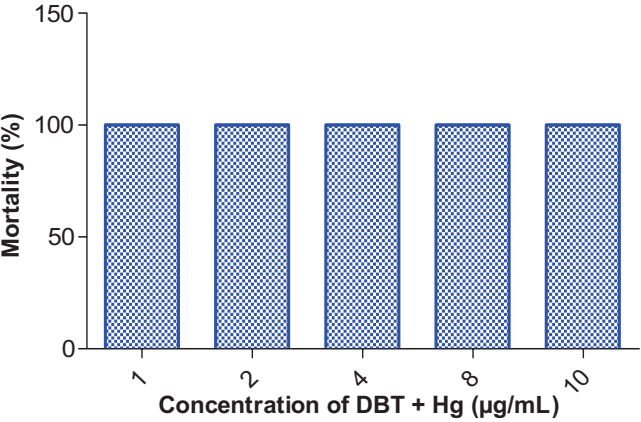
This study was supported by the Brazilian Coordenação de Aperfeiçoamento de Pessoal de Nível Superior (CAPES).

**References**

1. Nunes BS, Carvalho FD, Guilhermino LM, Stappen GV. Use of the genus *Artemia* in ecotoxicity testing. *Environmental Pollution* 2006;144(2):453-462.

2. Jeyavani J, Sibiya A, Bhavaniramya S, Mahboob S, Al-Ghanim KA, Nisa Z, Riaz Mn, Nicoletti M, Govindarajan M, Vaseeharan B. Toxicity evaluation of polypropylene microplastic on marine microcrustacean *Artemia salina*: An analysis of implications and vulnerability, *Chemosphere* 2022;296:1-9.

**Figure 4.** Mortality of BS in DBT + HgCl<sub>2</sub>.



3. Pinto R, Zanete J. Integrative ecotoxicity evaluation of Cd, Cu, Zn and Ni in aquatic animals reveals high tolerance of *Artemia franciscana*, *Chemosphere* 2023;341:1-9.
4. Silva-Neto HA, Zucolotto V, D'Alessandro EB, Tavares MGO, Filho NRA, Coltro WKT, Grosseli GM, Fadini PS, Urban RC. Preliminary assessment of toxicity of aerosol samples from central-west Brazil using *Artemia* spp. bioassays. *Chemosphere* 2023;336:1-7.
5. Comeche A, Martin-Villamil M, Picó Y, Varó I. Effect of methylparaben in *Artemia franciscana*, *Comparative Biochemistry and Physiology Part C. Toxicology & Pharmacology*. 2017;199:98-105.
6. Homoa J, Stachowiak W, Olejniczak A, Chrzanowski L, Niemczak M. Ecotoxicity studies reveal that organic cations in dicamba-derived ionic liquids can pose a greater environmental risk than the herbicide itself. *Science of The Total Environment* 2024;922:1-13.
7. Tayemeh MB, Abei H, Golokhvast HA, Joo HS, Pikila K, Johari SA, Mansouri B. Individual and binary exposure to nanoscales of silver, titanium dioxide, and silicon dioxide alters viability, growth, and reproductive system: Hidden indices to re-establish *Artemia* as a toxicological model in saline waters, *Environmental Pollution* 2023;331:1-12.
8. Medina JJM, Naso LG, Perez AL, Rizzi A, Ferrer EG, Williams AM. Antioxidant and anticancer effects and bioavailability studies of the flavonoid baicalin and its oxidovanadium (IV) complex. *Journal of Inorganic Biochemistry* 2017;166:150-161.
9. Albarano L, Ruocco N, Lofrano G, Guida M, Librato G. Genotoxicity in *Artemia* spp.: An old model with new sensitive endpoints. *Aquatic Toxicology* 2022;252:1-12.
10. Lu J, Zhu X, Tian S, LV X, Chen Z, Jiang Y, Liao X, Cai Z, Chen B. Graphene oxide in the marine environment: Toxicity to *Artemia salina* with and without the presence of Phe and Cd<sup>2+</sup>, *Chemosphere* 2018;211:390-396.
11. Das Paramanik D, Lei S, Kay P, Goycoolea FM. Investigating on the toxicity and bio-magnification potential of synthetic glitters on *Artemia salina*. *Marine Pollution Bulletin* 2023;190:1-10.
12. Saha G, Chandrasekaran N. A combined toxicological impact on *Artemia salina* caused by the presence of dust particles, microplastics from cosmetics, and paracetamol, *Environmental Pollution* 2024;348:1-8.
13. Pontes-Neto JG, Lyra MAM, Soares MFLR, Chaves LL, Soares-Sobrinho JL. Intercalation of olanzapine into CaAl and NiAl layered double hydroxides for dissolution rate improvement: Synthesis, characterization and *in vitro* toxicity, *Journal of Drug Delivery Science and Technology* 2019;52:986-996.
14. Rocha MJ, Rocha E. Pesticides in a temperate coastal lagoon in southwest Europe (Ria de Aveiro, Portugal) – Risk assessment and acute assays with *Artemia* and *Daphnia*. *Emerging Contaminants* 2024;10(2):1-17.
15. Cong Y, Wang Y, Zhang M, Jin F, Mu J, Li Z, Wang J. Lethal behavioral, growth and developmental toxicities of alkyl-PAHs and non-alkyl PAHs to early-life stage of brine shrimp, *Artemia parthenogenetica*, *Ecotoxicology and Environmental Safety* 2021;220:1-12.
16. Suzuki H, Makino W, Takahashi S, Urabe J. Assessment of toxic effects of imidacloprid on freshwater zooplankton: An experimental test for 27 species. *Science of the Total Environment* 2024;927:1-8.
17. Albarano L, de Rosa I, Sanraniello I, Montouri M, Serafini S, Toscanesi M, Trifuoggi M, Lofrano G, Guida UM, Libralato G. Synergistic, antagonistic, and additive effects of naphthalene, phenanthrene, fluoranthene and benzo(k)fluoranthene on *Artemia franciscana* nauplii and adult. *Environmental Pollution* 2023;335:1-7.
18. Prasantongkolmol T, Thongkorn H, Sunipasa A, Do HA, Saeung C, Jongpatiwut S. Analysis of sulfur compounds for crude oil fingerprinting using gas chromatography with sulfur chemiluminescence detector. *Marine Pollution Bulletin* 2023;186:1-10.
19. Zacharias DC, Crespo NM, da Silva NP, da Rocha RP, Gama CM, Silva RSB, Harari J. Oil reaching the coast: Is Brazil on the route of international oceanic dumping? *Marine Pollution Bulletin* 2023;196.
20. Ghosh P, Mukherji S. Fate, detection technologies and toxicity of heterocyclic PAHs in the aquatic and soil environments, *Science of The Total Environment* 2023;892:1-20.
21. Sampaio FXA, Nascimento MM, de Oliveira VA, Martinez ST, de Andrade JB, Machado ME. Determination of polycyclic aromatic sulfur heterocycles in ascidians (*Phallusia nigra*) using a green procedure, *Microchemical Journal* 2023;186:1-7.
22. Mello LC, Nascimento AP, Lopes BD, Lima ADF, Bezerra LEA, Mendes LF, Bastos LM, Nossol ABS, Martins MM, Martins LL, Cavalcante RM. Tarballs on the Brazilian coast in late 2022 sustain *Lepas anatifera* Linnaeus, 1758 (Crustacea: Cirripedia): Occurrence and risk of petroleum hydrocarbon ingestion, *Science of The Total Environment* 2023;896:1-8.
23. Sola MCR, de Jesus RM, Nascimento MM, da Rocha GO, de Andrade JB. Occurrence of mercury in polychaete species (Annelida) and their associated sediments from an important Southern Atlantic Ocean Bay. *Science of the Total Environment* 2022;851:1-9.
24. dos Santos HD, de Oliveira FF, de Olivera RA. Influence of solubility of ethanol extracts in *Artemia salina* tests. *Rev Virtual Quim* 2017;9:1535-1545.

## Rare Earth Elements in Bahia, Brazil: Potential for Global Production

Alexandre Pereira Wentz<sup>1\*</sup>, Maria das Graças Andrade Korn<sup>2,3</sup>, Jeancarlo Pereira dos Anjos<sup>4</sup>, Fabiano Ferreira de Medeiros<sup>1</sup>, Paulo Henrique Marques Modesto<sup>1</sup>, Fabrício Dias Rodrigues<sup>1</sup>, Sara Silva Alves<sup>1</sup>, Alexandre Porto<sup>1</sup>, Caio Silva Assis Felix<sup>2,3</sup>, Eduarda de Lima Guimarães<sup>3</sup>, Lilian Lefon Nani Guarieiro<sup>1,2</sup>

<sup>1</sup>SENAI CIMATEC University; <sup>2</sup>National Institute of Science and Technology in Energy and Environment - INCT, Federal University of Bahia; <sup>3</sup>Institute of Chemistry, Federal University of Bahia; Salvador, Bahia; <sup>4</sup>Center of Natural and Human Sciences, Federal University of ABC; Santo André, Minas Gerais, Brazil

Rare earth elements (REE) are critical for modern technologies, especially in driving the global energy transition. Brazil, with substantial investments in the state of Bahia, has emerged as a key player in the global REE reserves. This study evaluates the presence of REE in sediments collected from Novo Horizonte, Bahia, to explore their potential for future exploitation. Sediment samples were processed using the USEPA3051A digestion method, followed by centrifugation and analysis via inductively coupled plasma optical emission spectrometry (ICP OES). The analysis revealed significant concentrations of REE, particularly cerium, neodymium, and yttrium. These results highlight Bahia's strategic importance in contributing to global REE production and supporting a sustainable, technology-driven economy.

**Keywords:** Rare Earth Elements (REE). Sustainability. Energy Transition.

Rare earth elements (REE) are vital components in many advanced technologies, particularly those driving the transition to renewable energy. According to the International Energy Agency, the demand for REE is projected to increase three to seven times by 2040 [1].

REEs are indispensable in applications such as catalysts, alloys, polishing compounds, phosphors, nuclear reactors, permanent magnets, key components of wind turbines, and electric vehicle motors. Growing demand for these technologies has elevated the importance of elements such as Praseodymium (Pr), Neodymium (Nd), Terbium (Tb), and Dysprosium (Dy) [2]. To meet the requirements of the 2016 Paris Agreement, REE demand would need to quadruple, emphasizing the urgency of exploring new ore deposits [3]. Despite their name, REEs are not exceptionally rare; some are more abundant in the earth's crust than copper (Cu) [4]. These elements occur in two main deposit types:

- Primary deposits are formed through magmatic-hydrothermal processes.
- Secondary deposits result from weathering and sedimentary processes.

Commonly exploited minerals include monazite and bastnaesite while emerging sources such as eudialyte and steenstrupine are investigated in regions like Greenland and Sweden [5].

REE can be obtained through three primary methods:

- Primary extraction: Mining directly from ore deposits.
- Recovery from secondary sources: Recycling from end-of-life electronics.
- Extraction from unconventional sources: Utilizing industrial waste, including coal ash and mine tailings [1].

### Global Production and Supply Chain

China dominates global production, accounting for ~70% of rare earth oxide (REO) production, followed by the United States (14%) and Australia (4%) [6]. Beyond production, China leads in processing, handling approximately 85% of the global market, followed by Malaysia and

Received on 21 September 2024; revised 2 December 2024.  
Address for correspondence: Alexandre Pereira Wentz.  
ACentro de Ciências Naturais e Humanas – CCNH,  
Universidade Federal do ABC. Zipcode: 09280-560, Santo  
André, SP, Brazil. E-mail: wentzap@hotmail.com.

J Bioeng. Tech. Health 2024;7(4):363-368  
© 2024 by SENAI CIMATEC. All rights reserved.

Estonia. In 2020 China consumed 150,000 tons of REOs, leading global demand, followed by Japan, the United States, and the European Union [7].

In 2023, the United States imported \$190 million worth of REE compounds and metals, a 7% decline from \$208 million in 2022 [6]. As clean energy technologies and decarbonization initiatives expand, the demand for REE is expected to grow significantly [8]. This increase has driven the development of new exploration and processing projects worldwide to ensure a stable supply chain for these critical elements [9].

### Brazil's Role in REE Reserves

Brazil holds approximately 15% of the world's REE reserves, ranking as the third-largest reserve globally with 21 million tons [6,10-12]. Notable reserves are distributed across regions such as:

- Araxá, Poços de Caldas, and Tapira (Minas Gerais).
- Jacupiranga (São Paulo).
- Catalão and Itapirapuã (Goiás).
- Pitinga Mine (Amazonas).
- Minaçu and Montividiu do Norte (Goiás) [12].

Other regions, including São Gonçalo do Sapucaí (Minas Gerais) and São Francisco de Itabapoana (Rio de Janeiro), also contain smaller REE deposits. Protected areas, such as Morro dos Seis Lagos (Amazonas) and Serra do Repartimento (Roraima), hold significant potential, but legal restrictions have hindered exploration [12].

Substantial investments have recently been directed towards Bahia, especially in the regions of Jequié [13-16] and Novo Horizonte, where promising REE deposits have been identified [17].

This study aims to analyze and characterize the presence of REE in sediment samples collected from Bahia, Brazil. Using inductively coupled plasma optical emission spectrometry (ICP OES), the research assesses their potential for economic exploitation and examines their geological distribution.

## **Materials and Methods**

The research comprised three main stages: (i) soil sample collection, (ii) sample preparation, and (iii) sample characterization using ICP OES (Inductively Coupled Plasma Optical Emission Spectrometer). The iCAP PRO XP model from Thermo Fisher Scientific (Waltham, Massachusetts, USA) was utilized.

### Soil Sample Collection

Soil samples were collected from the Novo Horizonte region in Bahia. Due to confidentiality constraints, the precise coordinates of the sampling locations are not disclosed. The sample collection followed the ABNT NBR 6457 standard [18], involving the removal of representative soil portions via scraping or excavation, which resulted in altered natural compactness and consistency.

Ten sediment samples, each weighing approximately 3 kg, were collected. These samples were packed in heavy-duty plastic bags and labeled with external and internal identifiers. The internal labels were enclosed in a protective plastic envelope and included details such as the collection location, date, and depth.

### Sample Preparation

Sample digestion was performed using a microwave digestion system (Ethos A, Milestone, Italy) based on the USEPA3051A method [19]. Approximately 0.5 g of dried soil was weighed, and 9 mL of HNO<sub>3</sub> (69% v/v) and 3 mL of HCl (37% v/v) were added. The digestion protocol involved heating the mixture for 5.5 minutes to 175°C, maintaining this temperature for an additional 4.5 minutes. After cooling to room temperature, the digested sample was transferred to a 50 mL Falcon tube, diluted with ultra-pure water to a final volume of 40 mL, and centrifuged for 10 minutes at 4000 RPM. Blanks and a certified reference material (Buffalo River Sediment, NIST 8704) underwent identical procedures to ensure analytical accuracy.

### Sample Characterization

Samples were analyzed using an ICP OES equipped with the following features:

- Concentric nebulizer connected to a cyclonic chamber.
- Vertical torch.
- Echelle polychromator.

Charge injection device (CID) matrix detector. The operating parameters for the ICP OES included:

- Radiofrequency power: 1.25 kW.
- Plasma gas flow: 12.5 L/min.
- Auxiliary gas flow: 0.50 L/min.
- Carrier gas flow: 0.50 L/min.
- Exposure duration: 20 seconds.
- Viewing orientation: Axial.

The following elements and their spectral lines (in nm) were analyzed:

- Atomic emission lines (I): As I (189.042), Si I (288.158).
- Ionic emission lines (II): Ba II (455.403), Cd II (214.438), Ce II (404.076), Co II (228.616), Cr II (283.563), Dy II (353.170), Er II (337.271), Eu II (412.970), Gd II (342.247), La II (412.323), Lu II (261.542), Mn II (257.610), Nd II (401.225), Ni II (231.604), Pb II (220.353), Pr II (422.535), Sc II (361.384), Sm II (360.949), Sr II (407.771), Tb II (350.917), Th II (283.231), Ti II (334.941), Tm II (342.508), V II (292.402), Y II (371.030), Yb II (369.419), Zr II (339.198).

The high-purity argon gas (99.999%) supplied by White Martins (São Paulo, SP, Brazil) was used during the analysis. Calibration curves for the ICP OES were constructed using 1000 mg/L CPA CHEM multi-element standards containing 17 rare earth elements from Aluretec®.

### Detection Limits (LOD) and Quantification Limits (LOQ)

The background equivalent concentration (BEC) and signal-to-background ratio (SBR) were

employed to calculate the limits of detection and quantification. The BEC was calculated using:

$$BEC = C_{\text{standard}} SBR, \text{ where } SBR = \frac{I_{\text{standard}} - I_{\text{blank}}}{I_{\text{blank}}}$$

$$\text{BEC} = \frac{C_{\text{standard}}}{SBR} = \frac{C_{\text{standard}}}{\frac{I_{\text{standard}} - I_{\text{blank}}}{I_{\text{blank}}}} = \frac{C_{\text{standard}} I_{\text{blank}}}{I_{\text{standard}} - I_{\text{blank}}}$$

Here,  $C_{\text{standard}}$  is the reference element concentration, and  $I_{\text{standard}}$  and  $I_{\text{blank}}$  are the emission intensities of the standard and blank solutions, respectively.

The LOD and LOQ were calculated as follows:

$$LOD = 3 \times RSD_{\text{blank}} \times BEC, LOQ = 10 \times RSD_{\text{blank}} \times BEC$$

$$\text{where } RSD_{\text{blank}} = \frac{\text{standard deviation of blank}}{\text{blank emission intensity}}$$

## **Results and Discussion**

The results of the characterization of soil samples from the Novo Horizonte-BA region are expressed in  $\mu\text{g g}^{-1}$  and summarized in Table 1. The accuracy of the experimental data was assessed and confirmed by analysis of the certified reference material Buffalo River Sediment - NIST 8704. The results obtained were consistent with the certified values at a 95% confidence level, attesting to the reliability and suitability of the methodology for determining rare earth elements (REE).

### Quantification and Comparison with Clarke Values

The study quantified 29 elements across 10 sediment samples. Each sample was analyzed in triplicate, with each element's mean and standard deviation calculated and presented. The concentrations of REEs found in the samples were compared with Clarke values, representing the average abundance of these elements in the earth's



**Table 1.** Quantification of 29 elements in 10 samples with mean and standard deviation.

Analyte	LOD ( $\mu\text{g g}^{-1}$ )	LOQ ( $\mu\text{g g}^{-1}$ )	Certified Value (NIST 8704) ( $\mu\text{g g}^{-1}$ )*	Value Found (NIST 8704) ( $\mu\text{g g}^{-1}$ )	Contents Found in the Samples ( $\mu\text{g g}^{-1}$ )	Abundance in Clarke's Table (ppm)
As	0.11	0.36	-	-	12.44 $\pm$ 1.51	1.8
Cd	0.01	0.05	2.94 $\pm$ 0.29	2.85 $\pm$ 0.08	0.18 $\pm$ 0.025	0.1
Ce	0.11	0.36	66.5 $\pm$ 2.0	56.7 $\pm$ 3.94	103.1 $\pm$ 6.89	60
Co	0.34	1.14	13.57 $\pm$ 0.43	16.8 $\pm$ 1.26	87.11 $\pm$ 5.96	25
Cr	0.31	1.02	121.9 $\pm$ 3.8	114.7 $\pm$ 7.79	13.3 $\pm$ 1.48	100
Dy	0.05	0.15	-	-	6.53 $\pm$ 0.39	3.5
Er	0.06	0.20	-	-	104.2 $\pm$ 17.2	2.3
Eu	0.03	0.11	1.31 $\pm$ 0.04	1.11 $\pm$ 0.05	1.31 $\pm$ 1.51	1.0
Gd	0.07	0.22	-	-	11.52 $\pm$ 0.90	4.0
La	0.05	0.15	-	-	62.99 $\pm$ 5.14	30
Lu	0.03	0.10	-	-	0.68 $\pm$ 0.05	0.5
Mn	0.09	0.29	544 $\pm$ 21	520 $\pm$ 2.10	34.6 $\pm$ 5.59	950
Nd	0.15	0.48	-	-	65.38 $\pm$ 4.96	33
Ni	0.06	0.19	42.9 $\pm$ 3.7	40.6 $\pm$ 2.17	0.42 $\pm$ 0.1	---
Pb	0.34	1.12	150 $\pm$ 17	139 $\pm$ 0.74	4.27 $\pm$ 0.3	14
Pr	0.15	0.50	-	-	16.77 $\pm$ 80.2	9.1
Si	0.11	0.35	-	-	108.1 $\pm$ 13.2	---
Sm	0.15	0.51	-	-	6.73 $\pm$ 0.5	6.0
Sr	0.04	0.13	-	-	4.95 $\pm$ 2.84	375
Tb	0.17	0.55	-	-	1.6 $\pm$ 0.13	0.9
Ti	0.08	0.25	-	-	145.7 $\pm$ 25.8	---
Tm	0.09	0.29	-	-	1.20 $\pm$ 0.19	0.3
V	0.04	0.12	94.6 $\pm$ 4.0	96.9 $\pm$ 3.76	4.13 $\pm$ 0.28	70
Y	0.03	0.08	-	-	29.98 $\pm$ 2.21	33
Yb	0.03	0.10	-	-	1.72 $\pm$ 0.16	2.8
Zr	0.09	0.31	-	-	36.76 $\pm$ 2.75	165

crust. Clarke values are important in economic geology to identify anomalous concentrations and guide resource exploitation strategies [20, 21].

- Cerium (Ce): 70.95  $\mu\text{g/g}$
- Neodymium (Nd): 25.50  $\mu\text{g/g}$
- Erbium (Er): 104.2  $\mu\text{g/g}$

### Significant REE Findings

The analysis revealed substantial concentrations of key rare earth elements, including:

These concentrations suggest a slight enrichment in REEs, which aligns with the region's geological characteristics. The lithology, dominated by peralkaline rocks saturated in silica,

is naturally enriched in REEs [22]. Additionally, the high concentrations may partially result from anthropogenic sources.

### Applications and Industrial Relevance

The significant presence of cerium, neodymium, and yttrium is particularly notable due to their critical roles in modern industries, including:

- Permanent magnets for renewable energy technologies, such as wind turbines and electric vehicle motors.
- Catalysts used in industrial processes.
- Phosphors for energy-efficient lighting and displays.

These findings underscore the potential of the Novo Horizonte region as a strategic resource for rare earth elements, essential for advancing clean energy and high-tech applications.

### Environmental and Economic Implications

REEs in sediment samples offer valuable insights for environmental monitoring and sustainable resource management. Future exploration and exploitation strategies must consider balancing economic development with environmental preservation.

### Method Validation

The methodology employed, including microwave digestion and ICP OES analysis, demonstrated robustness and reliability. The alignment of results with the certified reference material (NIST 8704) further confirms the accuracy of the analytical approach. This validation ensures confidence in the findings and supports the method's applicability for future studies.

### **Conclusion**

The analysis of sediment samples from the Novo Horizonte region in Bahia revealed significant

concentrations of rare earth elements (REE), underscoring the importance of these deposits for future exploration in Brazil. The methodology employed, including microwave digestion and ICP OES analysis, proved effective and reliable for precisely determining these elements. The results contribute to a deeper understanding of the distribution of REE resources in the region, providing valuable insights for geological studies and resource management.

Given the growing global demand for clean technologies and renewable energy solutions, the data presented in this study point to a promising scenario for the sustainable development of REE reserves in Bahia. These resources are critical for various industrial applications, including electric vehicles, wind turbines, and other technologies driving the global energy transition. The findings highlight the potential of the Novo Horizonte region as a strategic source of REEs and contribute to efforts to ensure a balanced and sustainable approach to mineral extraction in the face of increasing environmental and economic challenges.

In conclusion, significant REE concentrations in Bahia present both an opportunity and a responsibility for sustainable exploitation, positioning Brazil as an important player in the global transition to clean energy and technological advancement.

### **Acknowledgments**

Conselho Nacional de Desenvolvimento Científico e Tecnológico – CNPQ. Chamada CNPq/MCTI/FNDCT N° 16/2022 – Aplicações de PD&I em Prospecção e Exploração de Recursos Minerais e de Petróleo & Gás Natural – Processo 405664/2022-2.

### **References**

1. Fatunde M. The race to produce rare earth materials, MIT Technology Review. 2024. Available from: <https://www.technologyreview.com/2024/01/05/1084791/rare-earth-materials-clean-energy/>
2. Xenia KA. The role of critical world energy outlook special report minerals in clean energy transitions. 2021.

- Available from: <https://www.iea.org/reports/the-role-of-critical-minerals-in-clean-energy-transitions>
- 3 MCTIC, Acordo Paris 2016. Available at: [https://www.gov.br/mcti/pt-br/acompanhe-o-mcti/sirene/publicacoes/acordo-de-paris-e-ndc/arquivos/pdf/acordo\\_paris.pdf](https://www.gov.br/mcti/pt-br/acompanhe-o-mcti/sirene/publicacoes/acordo-de-paris-e-ndc/arquivos/pdf/acordo_paris.pdf) 2017.
  4. Haxel GB, Hedrick JB, Orris GJ. Rare earth elements-critical resources for high technology. Supporting Sound management of our mineral resources. 2005.
  5. Kato Y, Fujinaga K, Nakamura K, Takaya Y, Kitamura K, Ohta J, et al. Deep-sea mud in the Pacific Ocean as a potential resource for rare-earth elements. *Nature Geoscience* 2011;4(8):535–9, 2011. Available at: <https://www.nature.com/articles/ngeo1185>.
  6. U.S. Geological Survey. Mineral Commodity Summaries 2024. 2024; Available at: <https://pubs.usgs.gov/publication/mcs2024>.
  7. U.S. Geological Survey. Mineral commodity summaries 2023. 2023. Available from: <https://pubs.usgs.gov/publication/mcs2023>.
  8. IEA (International Energy Agency). International Energy Agency. The Role of Critical Minerals in Clean Energy Transitions – Analysis - IEA. Available from: <https://www.iea.org/reports/the-role-of-critical-minerals-in-clean-energy-transitions>.
  9. Liu SL, Fan HR, Liu X, Meng J, Butcher AR, Yann L et al. Global rare earth elements projects: New developments and supply chains. *Ore Geol Rev* 2023;157:105428.
  10. REIA (The global rare earth industry association). Rare Earth – REIA Available at: <https://global-reia.org/rare-earth>.
  11. Pope N, Smith P. Brazil's critical and strategic minerals in a changing world. 2023; Available at: <https://igarape.org.br/wp-content/uploads/2023/10/Critical-and-Strategic-Minerals.pdf>.
  12. Silva GF. An overview of Critical and Strategic Minerals of Brazil. Serviço Geológico do Brasil. Available at: [https://www.sgb.gov.br/pdac/media/critical\\_and\\_strategic\\_minerals.pdf](https://www.sgb.gov.br/pdac/media/critical_and_strategic_minerals.pdf).
  13. Terras Raras. Brazilian Rare Earths assina com governo da Bahia para projeto de R\$ 3,5 bilhões. Brasil Mineral. Available at: <https://www.brasilmineral.com.br/noticias/brazilian-rare-earths-assina-com-governo-da-bahia-para-projeto-de-r-35-bilhoes>.
  14. Bahia pode se tornar polo produtor de Terras Raras, minerais usados em alta tecnologia no mundo, essenciais para fabricação de eletrônicos, turbinas eólicas e carros elétricos - Minera Brasil. Available from: <https://minerabrasil.com.br/bahia-pode-se-tornar-polo-produtor-de-terras-raras-minerais-usados-em-alta-tecnologia-no-mundo-essenciais-para-fabricacao-de-eletronicos-turbinas-eolicas-e-carros-eletricos/2024/04/02>.
  15. Terras raras. Australian Mines identifica novo alvo promissor no Projeto Jequié, na Bahia. Brasil Mineral. Available at: <https://www.brasilmineral.com.br/noticias/australian-mines-identifica-novo-alvo-promissor-no-projeto-jeque-na-bahia>.
  16. Ourprojects - Brazilian Rare Earths. Available at: [https://brazilianrareearths.com/?page\\_id=72](https://brazilianrareearths.com/?page_id=72).
  17. Arcanjo DJ. Caracterização dos minerais de terras raras de Novo Horizonte, Bahia. Universidade Federal de Ouro Preto Escola de Minas Departamento de Geologia Monografia no 305; 2018. Available at: [https://www.monografias.ufop.br/bitstream/35400000/1544/6/MONOGRFIA\\_Caracteriza%C3%A7%C3%A3oMineraisTerras.pdf](https://www.monografias.ufop.br/bitstream/35400000/1544/6/MONOGRFIA_Caracteriza%C3%A7%C3%A3oMineraisTerras.pdf).
  18. NBR-9604.
  19. U.S. EPA Method 3051A: Microwave Assisted Acid Digestion of Sediments, Sludges, and Oils - US EPA. Available from: <https://www.epa.gov/esam/us-epa-method-3051a-microwave-assisted-acid-digestion-sediments-sludges-and-oils>.
  20. Teixeira W et al. Decifrando a Terra, 2.ed., CIA Editora Nacional, 2007.
  21. Taylor SR, McLennan SM. The continental crust: Its composition and evolution: An examination of the geochemical record preserved in sedimentary rocks. Blackwell Science, Oxford, 1985:312.
  22. Chamouradian AR, Wall F. Rare earth elements: Minerals, mines, magnets (and more). *Elements* 2012;8(5):333–340. doi: 10.2113/gselements.8.5.333.

## Application of a Preprocessing Pipeline to VIS-NIR Data for Predicting Soil Nutrient Concentration Values

Eduardo Menezes de Souza Amarante<sup>1\*</sup>, Julian Santana Liang<sup>1</sup>, Carlos Alberto Campos da Purificação<sup>1</sup>, Rômulo Alexandrino Silva<sup>1</sup>

<sup>1</sup>Department of Software, SENAI CIMATEC University; Salvador, Bahia, Brazil

**This paper compares the impact of each preprocessing step in predicting soil nutrient concentration values using the partial least squares technique (PLS). The preprocessing pipeline comprises log transformation of the output variable, determination of the optimal number of components, and feature engineering. An increase in the coefficient of determination ( $R^2$ ) and an improvement in model stability were observed.**

**Keywords:** VIS-NIR Data. Preprocessing Pipeline. Soil Nutrient. Partial Least Square Regression.

Standard procedures for measuring soil properties are time-consuming, complex, and expensive. Therefore, an analytical technique that is fast, precise, and affordable is necessary to determine soil fertility levels.

The conventional spectroscopic modeling procedure requires the pretreatment of soil samples, such as drying and sieving, before scanning with a spectrophotometer [1]. Near-infrared spectroscopy (NIR) has been widely used to meet these needs. In addition, it can analyze many constituents simultaneously, making it a viable alternative to conventional laboratory analyses for assessing and monitoring soil quality [2-5].

He and colleagues [6] predicted levels of nitrogen (N), phosphorus (P), potassium (K), soil organic matter (OM), and pH content from NIR spectroscopy data. Wetterlind and colleagues [7] determined the soil texture, SOM, total N, pH and plant-available P, K and Mg from visible and near infrared reflection. Jin and colleagues [8] tested twenty-nine preprocessing combination techniques with VIS-NIR data of yellow loam samples to find the best combination for predicting potassium levels.

This research aimed to determine whether the chained processing techniques improve the performance of the partial least squares regression model. The models were evaluated using the coefficient of determination ( $R^2$ ) and root mean squared error (RMSE).

### Materials and Methods

#### Materials

In total, 420 soil samples were collected from five soil classes at two depths: 0- 20 cm and 20-40 cm, with 210 samples for each depth. The collected samples were dried at room temperature for seven to fifteen days. Before absorbance measurement, the soil samples were ground and sieved using a 2 mm mesh size to remove the particle effect size on reflectance spectra.

The spectrometer used was a FieldSpec 3, with a spectral range between 350 and 2500 nm, a resolution of 8 nm, and a precision of +/- 1 nm. A Spectralon ceramic plate was used to calibrate the device before each measurement. Each soil sample was measured 30 times, and the mean spectrum for each sample was calculated. The mean reflectance values were converted into absorbance measures using the formula  $\log(1/R)$ , where R represents the reflectance. The concentration values of boron were extracted using Mehlich-1 extraction, measured in  $\text{mg}/\text{dm}^3$ .

Received on 28 September 2024; revised 18 November 2024.  
Address for correspondence: Eduardo Menezes de Souza Amarante. Av. Orlando Gomes, 1845, Piatã. Zipcode: 41650-010. Salvador, Bahia, Brazil. E-mail: eduardo.amarante@fbter.org.br.

J Bioeng. Tech. Health 2024;7(4):369-374  
© 2024 by SENAI CIMATEC. All rights reserved.

### Exploratory Data Analysis

Initially, we conducted an exploratory data analysis on the entire dataset to identify patterns in the input and output variables. Figure 1 shows the distribution of nutrients with the outliers highlighted.

We performed a descriptive statistic of the nutrient values to obtain more precise information about the dataset. Table 1 shows the number of samples, minimum and maximum values, mean, median, and standard deviation. The distribution curve is right-skewed, with values concentrated near zero. Therefore, we applied an asymmetrical correction with  $\log(1+x)$ . Figure 2 shows the distribution of B values before and after the correction.

Figure 3 illustrates the average absorbance signal across the entire spectrum. In this picture,

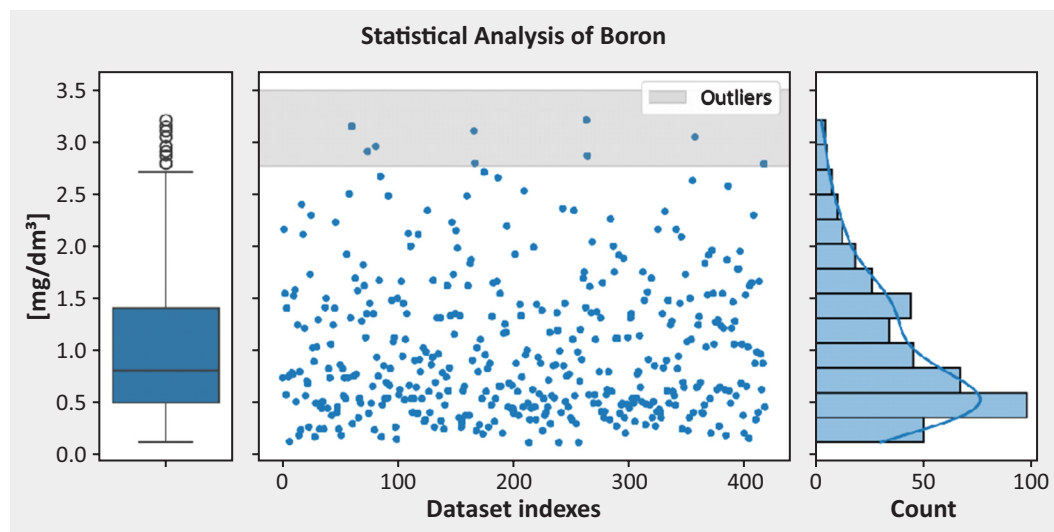
it is possible to identify the absorption region of mean peaks.

During the data exploration analysis for VIS-NIR data, we identified some records with a coefficient of absorption more significant than 1, which lacks physical meaning. A shift in absorbance values could correct them, but we kept them. We plotted the distribution curve from each input variable and realized that all of them are nearly bell-shaped, as shown in Figure 4. These outliers were kept, avoiding data shortage.

### Pipeline

Before applying the processing pipeline, we randomly separated eighty-four soil samples to constitute the testing dataset, ensuring they were excluded from all preprocessing steps. The remaining dataset was split into training and

**Figure 1.** Statistical analysis of boron nutrient.



On the left, the boxplot shows the outliers values with concentration values above 2.76875 mg/dm<sup>3</sup>. In the middle, the scatterplot illustrates how the concentration values are distributed according to the dataset indexes. On the right, we have the histogram of the concentration values.

**Table 1.** Stats of nutrient concentration values.

Count	Min	Max	Mean	Median	Standard Deviation
420	0.1100	3.2100	1.0014	0.8050	0.6697



**Figure 2.** Correctness of distribution with log transformation applied. The dotted and dashed lines represent the median and mean values of distribution, respectively.

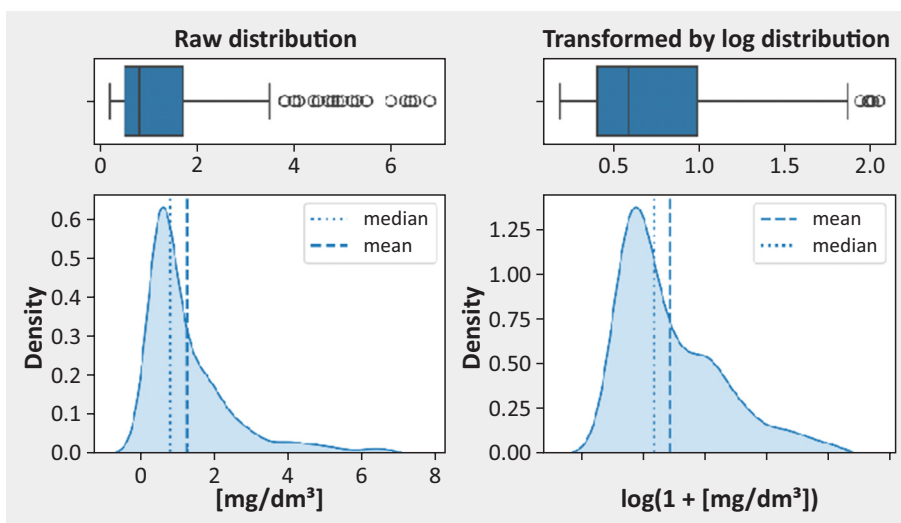


**Figure 3.** NIR spectrum mean.

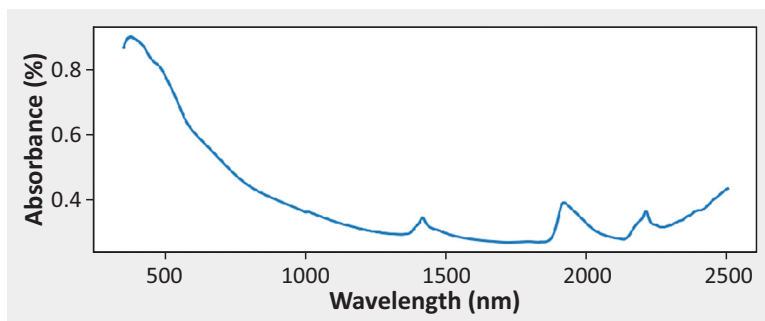
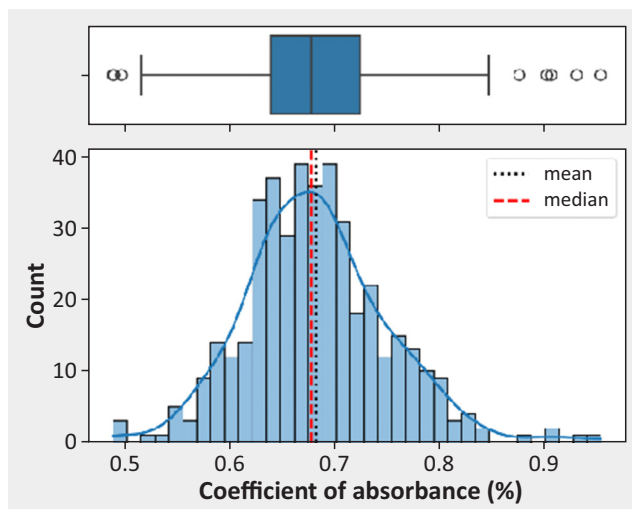


**Figure 4.** Distribution of absorption coefficients at 550 nm wavelength.



validation datasets, with 252 samples allocated for training, 84 for validation, and 84 for testing, respectively.

According to Figure 5, the pipeline starts with the baseline model, followed by applying three different preprocessing techniques. After each step, the coefficient of determination ( $R^2$ ) and the root mean square error (RMSE) were calculated on the validation dataset, allowing us to assess the impact of each preprocessing step on the model's performance. Each step following the log transformation in this pipeline can be seen as an additional preprocessing layer sequentially added as the pipeline progresses. As a result, four different models were produced and will be evaluated using the testing dataset. Table 2 outlines the processing layers at each step. K-fold cross-validation with ten folds was applied to determine the number of components optimally.

The PLS regressor used the resulting value to obtain the  $R^2$  and RMSE error. This value was then carried forward through the subsequent steps of the pipeline. The pipeline ends with a statistical feature engineering process applied to each row in the dataset, incorporating features such as Q3/Q1, Q3 x Q1, number of peaks, kurtosis, skew, Q1, mean, minimum, and maximum values. It's important to note that the outliers in the output variables, as shown in Figure 1, were not removed.

After each step, the models were evaluated using the validation dataset, allowing their results to be compared.

## Results and Discussion

Partial least squares regression analysis results for the dry soil samples for boron determination (Table 3). The  $R^2$  values in the validation dataset

**Figure 5:** Pipeline flows.

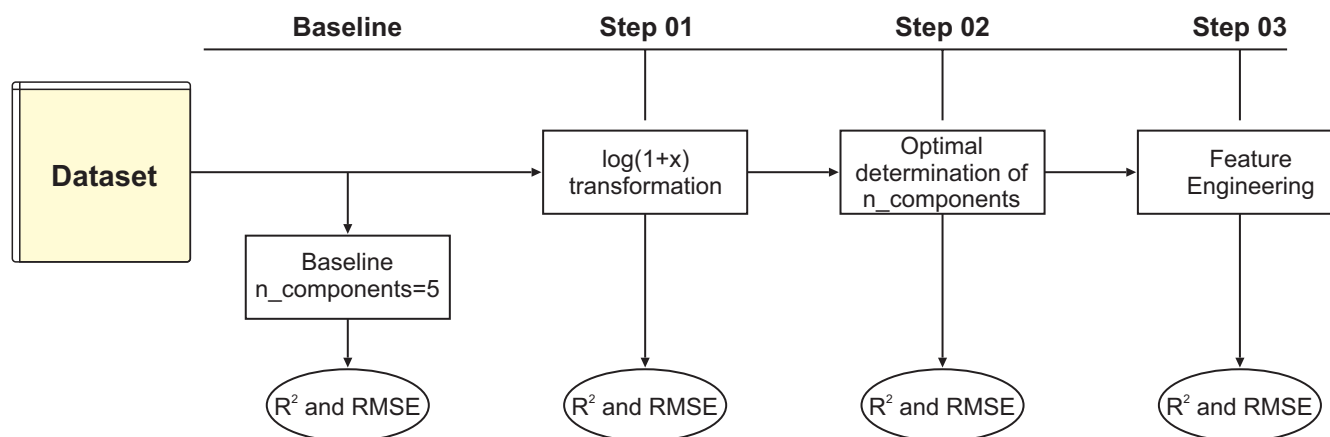


**Table 2.** Chained pipeline processing.

Steps	Processes		
	Log	N components optimization	Feature Engineering
Step 1	x		
Step 2	x	x	
Step 3	x	x	x

**Table 3.** Partial least squares result of the dry soil for validation and testing datasets.

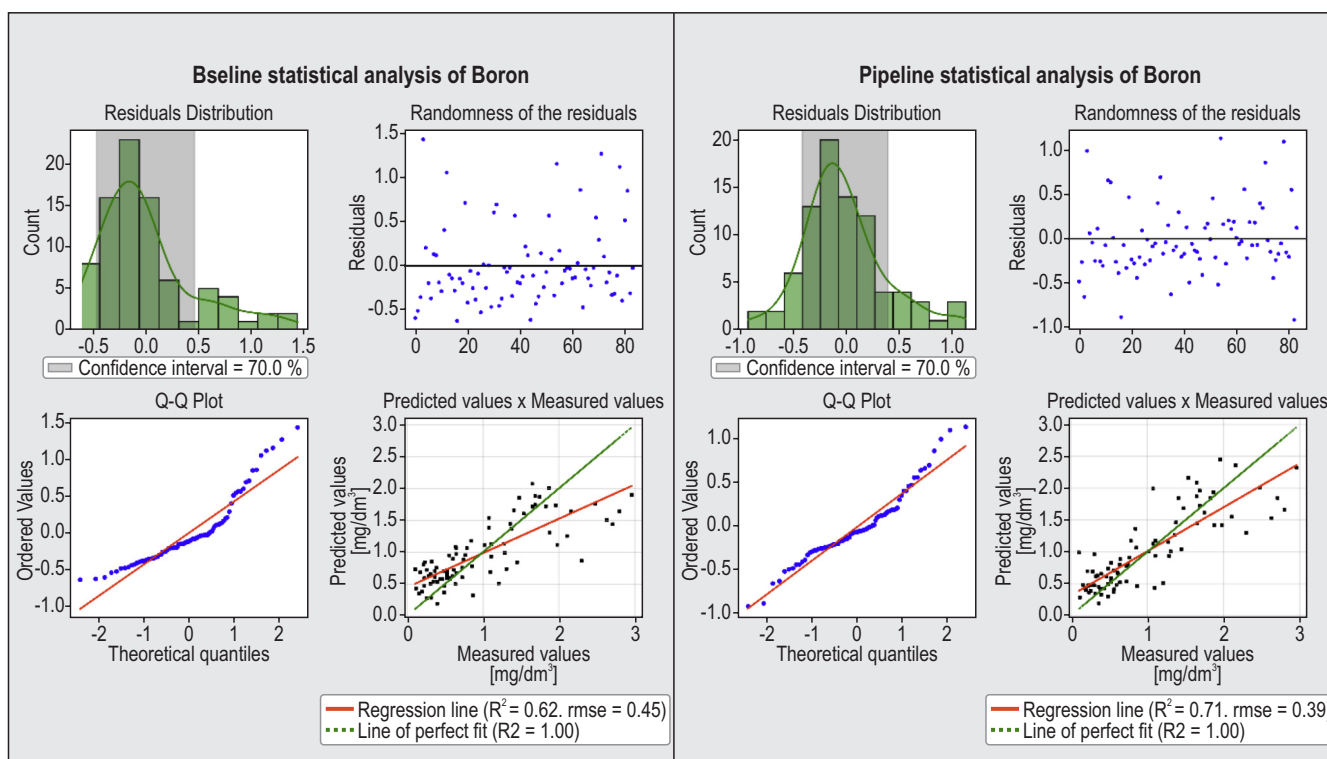
Steps	Validation		Test	
	R <sup>2</sup>	RMSE	R <sup>2</sup>	RMSE
Baseline	0.4937	0.4525	0.6150	0.4454
Step 1	0.5008	0.4493	0.6091	0.4489
Step 2	0.6304	0.3866	0.7175	0.3816
Step 3	0.6623	0.3696	0.7067	0.3884

for each step were 0.4937, 0.5008, 0.6304, and 0.6623, showing a relevant improvement. The models fitted with the entire dataset were tested on an unknown testing dataset. In the testing dataset, the coefficients of determination were 0.6150 for baseline, 0.6091 for step 01, 0.7175 for step 02, and 0.7067 for step 03, respectively. Figure 6 shows the statistical analysis of the baseline and step 03 regression residuals from the testing dataset. After passing through the

entire pipeline, the residuals produced follow a normal distribution.

### Conclusion

The preprocessing techniques applied in the dataset produced a relevant improvement in RMSE and R<sup>2</sup> metrics, starting with R<sup>2</sup> = 0.6150 and RMSE = 0.4454 mg/dm<sup>3</sup> for the baseline model and ending up with R<sup>2</sup> = 0.7067 and RMSE

**Figure 6.** Statistical analysis of residuals produced by the regression. On the left is the baseline model, and on the right, after passing through the pipeline.

equal to 0.3884 mg/dm<sup>3</sup>. The R<sup>2</sup> values obtained for the testing dataset were more significant than those for the validation dataset, but the RMSE error values were similar. The differences between R<sup>2</sup> and RMSE values obtained from validation and testing datasets can be explained by a shortage of data at certain concentration levels resulting from different data distributions on training, validation, and testing sets. The findings indicate that preprocessing techniques are crucial in producing a useful predictive model for soil nutrient concentration from spectral data. In addition, the amount of data is also a critical factor in the model's performance. The reduced dataset, particularly with limited representation at certain concentration levels, introduces variability in the model's ability to generalize across the full spectrum of data. With fewer data points, the model might be capturing noise or specific patterns in the validation set that do not generalize well to the testing set. This reinforces the need for a more prominent and representative dataset for future works.

### Acknowledgments

This research was executed in partnership between SENAI CIMATEC and ITECH startup. The authors would like to acknowledge the Brazilian Company for Industrial Research and Innovation (EMBRAPII) 's support and investments in RD&I.

### References

1. Maleki MR et al. Phosphorus sensing for fresh soils using visible and near infrared spectroscopy. *Biosystems Engineering* 2006;95(3):425-436. doi: 10.1016/j.biosystemseng.2006.07.015.
2. Xu S. et al. Comparison of multivariate methods for estimating selected soil properties from intact soil cores of paddy fields by Vis-NIR spectroscopy. *Geoderma* 2018;310:29-43.
3. Vasques GM, Grunwald S, Sickman JO. Comparison of multivariate methods for inferential modeling of soil carbon using visible/near-infrared spectra. *Geoderma*, 2008;146:14-25.
4. Vohland M, Besold J, Hill J, Fründ H. Comparing different multivariate calibration methods for the determination of soil organic carbon pools with visible to near infrared spectroscopy. *Geoderma* 2011;166:198-205.
5. Chang CW, Laird DA, Mausbach MJ, Hurburgh CR. Near infrared reflectance spectroscopy—principal components regression analysis of soil properties. *Soil Science Society of America Journal* 2001;65:480-490.
6. He Y, Huang M, García A, Hernández A, Song H. Prediction of soil macronutrients content using near-infrared spectroscopy. *Computers and Electronics in Agriculture* 2007;58:144-153.
7. Wetterlind J, Stenberg B, Söderström M. Increased sample point density in farm soil mapping by local calibration of visible and near infrared prediction models. *Geoderma* 2010;156:152-160. Available at: <http://www.elsevier.com/locate/geoderma>.
8. Jin X et al. Prediction of soil-available potassium content with visible near- infrared ray spectroscopy of different pretreatment transformations by the boosting algorithms. *Applied Sciences* 2020;10(4):1-15. Available at: <https://www.mdpi.com/2076-3417/10/4/1397>.

## An Adjusted Model of Proton Conductivity in Nafion® Membranes

Artur Santos Bispo<sup>1\*</sup>, Chrislaine do Bomfim Marinho<sup>1</sup>, Fernando Luiz Pellegrini Pessoa<sup>1</sup>, José Luis Gonçalves de Almeida<sup>1</sup>

<sup>1</sup>SENAI CIMATEC University; Salvador, Bahia, Brazil

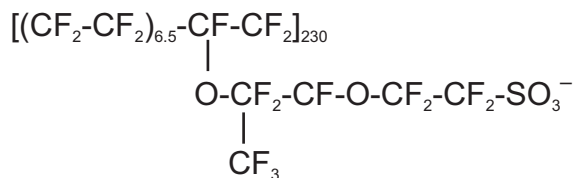
This developed and evaluated an adjusted model for proton conductivity in Proton Exchange Membrane (PEM) electrolyzer systems due to the increasing demand for alternative energy sources and the significance of green hydrogen (GH<sub>2</sub>). We performed a logarithmic regression based on experimental data on conductivity and membrane water content to achieve this goal. The main results indicate that the adjusted model shows better agreement with the logarithmic behavior of conductivity when compared to the typical model proposed in 1991. Furthermore, the calculated ohmic overpotential from the adjusted model demonstrated higher accuracy. Therefore, the adjusted model provides a more precise tool for sizing and optimizing (GH<sub>2</sub>) production systems using PEM technology.

**Keywords:** PEM Electrolysis. Proton Conductivity. Nafion. Mathematical Modeling.

With the increasing demand for alternative energy sources to mitigate environmental impacts, green hydrogen (GH<sub>2</sub>) emerges as a promising energy option. Among the technologies for producing GH<sub>2</sub>, Proton Exchange Membrane (PEM) electrolysis stands out, given its significant advantages in system design, H<sub>2</sub> production rate, purity, and energy efficiency [1].

One of the main differentiating factors of this technology lies in its proton exchange membrane. Composed of PFSA (perfluoro sulfonic acid ionomer, shown in Figure 1) - commercially known as Nafion®, this polymeric membrane acts as the electrolyte in the electrolytic system, meaning that it is responsible for facilitating the transfer of charge between the electrodes (H<sup>+</sup>) – from anode to cathode, in this case [2].

**Figure 1.** PFSA/Nafion® molecular structure.



Therefore, the membrane integrity, besides its protons selectivity and conductivity, are crucial factors in determining the useful life of the equipment, the H<sub>2</sub> production rate, and its purity level. Thus, the importance of developing mathematical models that describe proton behavior in ionomeric systems becomes evident [2]. Among the proton conductivity models available in the literature, the semi-empirical model developed by Springer and colleagues [3] is undoubtedly one of the most widely used (Equation 1). Several authors, such as Görgün [4], Awasthi and colleagues [5], and Kim and colleagues [6], used this model to define the ohmic overpotential of electrolyzers and PEM fuel cells.

According to Springer and colleagues [3], using the Arrhenius equation, this model was developed based on experimental proton conductivity data ( $\sigma_{H^+}$ , from 303 K to 353 K). The pre-exponential term ( $\sigma_{303K}$ ) is a function of the membrane water content ( $\lambda$ ), which defines the conductivity at a reference temperature of 303 K (Equation 2). The exponential term is a function of temperature,

### Equation 1.

$$\sigma_{H^+} = \sigma_{303K} * e^{[1268(\frac{1}{303} - \frac{1}{T})]}$$

### Equation 2.

$$\sigma_{K303} = (0.00514\lambda - 0.00326)$$

Received on 18 September 2024; revised 20 November 2024.  
Address for correspondence: Artur Santos Bispo. Avenida Orlando Gomes, 1845, Piatã. Salvador, Bahia, Brazil.  
Zipcode: 41650-010. E-mail: artur.bispo@outlook.com.br.

J Bioeng. Tech. Health 2024;7(4):375-379  
© 2024 by SENAI CIMATEC. All rights reserved.



allowing for the adjustment of conductivity values under different operational conditions.

However, despite yielding satisfactory results within moderate ranges of  $\lambda$  ( $< 18$ ), the model fails to accurately describe the conductivity behavior concerning membrane hydration, portraying it as a linearly increasing profile (first-degree function) due to the empirical pre-exponential term instead of logarithmic behavior shown by most of the experimental data in the literature. An alternative to this is presented in the model developed by Choi [2], which considers proton transport mechanisms in polymeric membranes (Surface, Grotthuss, and Vehicle). However, this phenomenological model exhibits high complexity in its equations and difficulty determining some parameters (not readily available in open literature). Figure 2 compares the aforementioned models and experimental data reproduced by Peckham and colleagues [7].

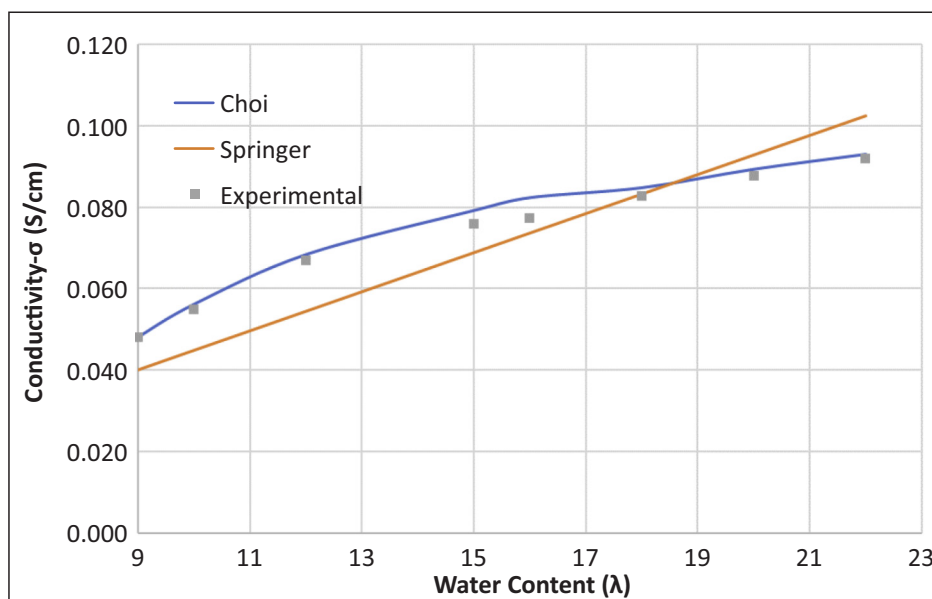
Therefore, this work aims to develop an adjustment to the mathematical model proposed by Springer and colleagues [3] to achieve a conductivity model that is both straightforward to use – with just one equation and two variables – and more accurate in describing the behavior concerning the hydration

of the polymeric membrane. Additionally, an analysis of ohmic overpotential ( $\eta_{ohm}$ ) calculation sensitivity concerning the typical and adjusted models will be carried out.

## Materials and Methods

As mentioned in the previous section, the main issue with the Semi-empirical model by Springer is its linear function behavior, which differs significantly from the logarithmic behavior observed in the experimental conductivity measurements. Furthermore, as seen earlier, the pre-exponential term of Equation 1 – obtained, according to the author, through regression based on experimental data – is responsible for this specific conductivity ( $\sigma_{H^+}$ ) profile as a function of membrane water content ( $\lambda$ ). Thus, a literature review was conducted using open-source platforms such as Google Scholar, Web of Science (Clarivate), SciELO, and CAPES, aiming to find experimental data to perform parameter estimation and model fitting. Data on  $\sigma_{H^+}$  and  $\lambda$  comparison – at 303.15 K – are found in Peckham and colleagues [7], Zawodzinski and colleagues [8], Sone and colleagues [9], and Zhang and Edwards [10] (Figure 3).

**Figure 2.** Comparison between Springer, Choi, and Experimental data.



A logarithmic regression was performed from the acquired experimental data to estimate a new pre-exponential term for the model. For this purpose, a generic logarithmic equation (Equation 3) was assigned.

### Equation 3.

$$\sigma_{303K} = a * \ln(\lambda) + b$$

Then, employing the least squares mathematical method, the values of 'a' and 'b' (slope and intercept coefficients, respectively) were estimated, resulting in Equation 4.

### Equation 4.

$$\sigma_{303K} = 0.0475 * \ln(\lambda) + 0.0571$$

Finally, the adjusted Springer model can be obtained by replacing the pre-exponential term in Equation 1 with Equation 4 (Equation 5).

### Equation 5.

$$\sigma_{H^+} = [0.0475 * \ln(\lambda) + 0.0571] * e^{\left[1268 \left(\frac{1}{303} - \frac{1}{T}\right)\right]}$$

Furthermore, comparative analyses were performed between the models (Springer and adjusted Springer) and the experimental data to evaluate the accuracy of each model and its

impacts on ohmic overpotential calculation for a cell working at 298.15 K, current density of 1.35 A/cm<sup>2</sup>, and membrane thickness of 0.033 cm. These analyses and the discussion regarding the results can be found in the following section.

## Results and Discussion

Figure 4 illustrates a graphical comparison between the results of the typical Springer model and the adjusted model proposed by this study. Despite the lower coefficient of determination ( $R^2 = 0.933$ ) when compared to the one proposed by Springer and colleagues [3] ( $R^2 = 0.954$ ), the adjusted Springer model provides better fitting results to the experimental data, following the logarithmic behavior of conductivity as membrane hydration intensifies. Other point to be noted is that the typical model exhibits a pronounced deviation from a specific range of membrane water content, indicating higher conductivity values than the actual ones. Indeed, this behavior can be detrimental to the sizing of electrolytic systems for green hydrogen production, as it would lead to fictitious higher values for GH<sub>2</sub> generation.

**Figure 3.** Experimental data by several authors.

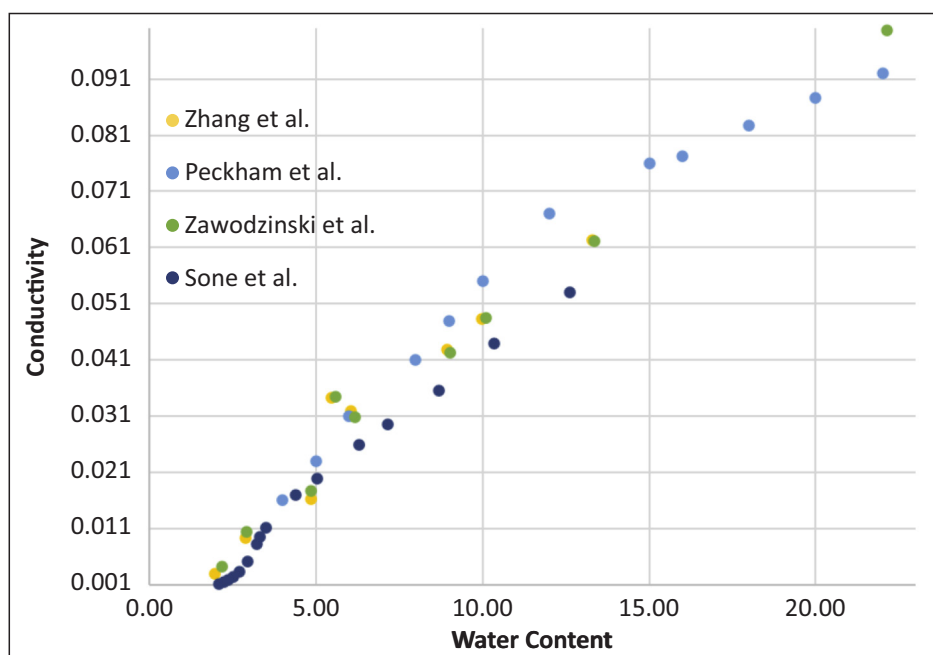
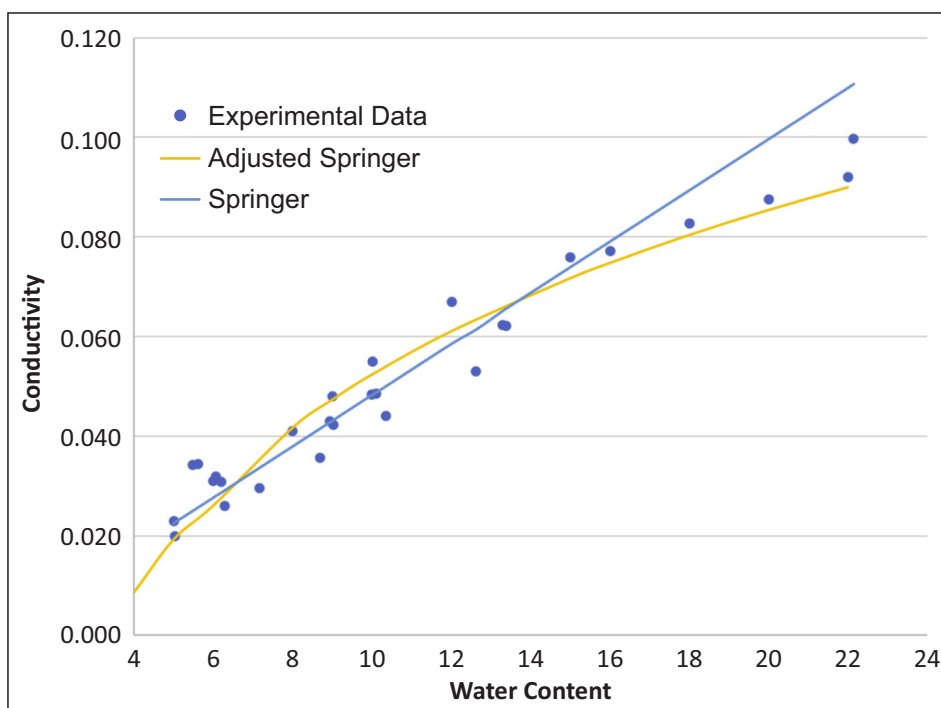


Figure 5 depicts the behavior of ohmic overpotential as a function of the water content provided by each model. As observed and consistent with the aforementioned, at higher values of membrane solvent loading, the typical Springer

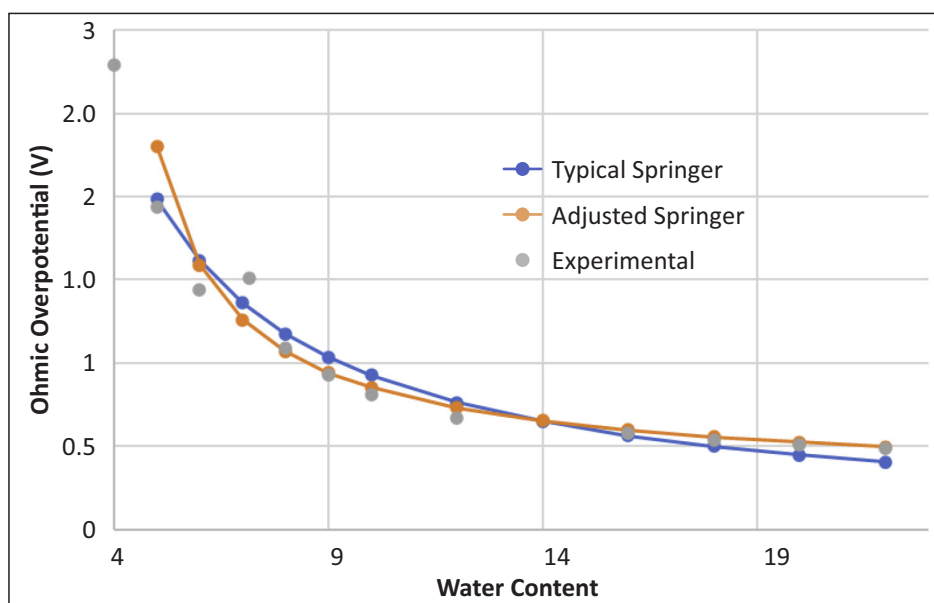
model describes a system with fewer ohmic losses – less resistant to proton transport.

Furthermore, concerning the prediction of  $\eta_{ohm}$ , the adjusted model showed superior performance, with a coefficient of determination  $R^2 = 0.99$ .

**Figure 4.** Comparison between Springer, Adjusted Springer, and Experimental data.



**Figure 5.** Ohmic overpotential comparison.



However, it is worth noting that, for practical purposes, the results provided by the typical model still exhibit high accuracy, with  $R^2 = 0.98$ .

## Conclusion

An adjusted model for proton conductivity in Proton Exchange Membrane (PEM) electrolyzer systems was developed and evaluated due to increasing demand for alternative energy sources and the significance of green hydrogen ( $\text{GH}_2$ ) in this context, Logarithmic regression was applied based on experimental data of conductivity and membrane water content, resulting in a model that better reflects the logarithmic behavior of conductivity compared to the typical model proposed by Springer and colleagues [3]. The results demonstrate that the adjusted model provides higher precision in estimating ohmic overpotential. This represents a significant advancement in understanding proton conductivity in PEM systems, enabling more efficient sizing and optimization of  $\text{GH}_2$  production systems. To drive the viability and widespread adoption of green hydrogen as a clean and renewable alternative for society's energy needs, further research on accurate models and a deeper understanding of ionomeric membrane properties is necessary. Thus, this study contributes to progress in this promising field, paving the way for a more sustainable and environmentally conscious future.

## References

1. Kumar SS, Himabindu V. Hydrogen production by PEM water electrolysis – A review. *Materials Science for Energy Technologies* 2019;2(3):442-454.
2. Choi P. Investigation of thermodynamic and transport properties of proton- exchange membranes in fuel cell applications. Worcester Polytechnic Institute. Doctor Degree Dissertation, 2004.
3. Springer TE, Zawodzins TA, Gottesfeld S. Polymer electrolyte fuel cell model. *Journal of the Electrochemical Society* 1991;138(8):2334.
4. GÖRGÜN H. Dynamic modelling of a proton exchange membrane (PEM) electrolyzer. *International journal of hydrogen energy*, v. 31, n. 1, p. 29-38, 2006.
5. Awasthi A, Scoyy K, Basu S. Dynamic modeling and simulation of a proton exchange membrane electrolyzer for hydrogen production. *International Journal of Hydrogen Energy* 2011;36(22):14779-14786.
6. Kim H, Park M, Lee KS. One-dimensional dynamic modeling of a high-pressure water electrolysis system for hydrogen production. *International Journal of Hydrogen Energy* 2013;38(6):2596-2609.
7. Peckham TJ, Schmeisser J, Holdcroft S. Relationships of acid and water content to proton transport in statistically sulfonated proton exchange membranes: Variation of water content via control of relative humidity. *The Journal of Physical Chemistry B* 2008;112(10):2848-2858.
8. Zawodzinski TA et al. Water uptake by and transport through Nafion® 117 membranes. *Journal of the Electrochemical Society* 1993;140(4):1041.
9. Sone Y, Ekdunge P, Simonsson D. Proton conductivity of Nafion 117 as measured by a four-electrode AC impedance method. *Journal of the Electrochemical Society* 1996;143(4):1254.
10. Zhang B, Edwards BR. Modelling proton conductivity in perfluorosulfonate acid membranes. *Journal of the Electrochemical Society* 2015;162(9):F1088.

## Anaerobic Digestion of *Agave sisalana*: Existing Data, Trends, and Potential Applications

Julio C.A. Toqueiro<sup>1\*</sup>, Otanéa B. Oliveira<sup>2,3</sup>, Oscar F.H. Adarme<sup>1,4</sup>, Gustavo Mockaitis<sup>3,4</sup>

<sup>1</sup>Interdisciplinary Research Group on Biotechnology Applied to the Agriculture and the Environment, School of Agricultural Engineering, University of Campinas; Campinas, São Paulo; <sup>2</sup>SENAI CIMATEC University; Salvador, Bahia;

<sup>3</sup>Interinstitutional Graduate Program in Bioenergy (USP/UNICAMP/UNESP); Campinas, São Paulo; <sup>4</sup>Arrakis Bioenergia; Camaçari, Bahia, Brazil

The increasing global demand for renewable energy is driving the search for clean and sustainable sources, such as biogas obtained from the anaerobic digestion of waste, emerging as a promising alternative. This article aims to present an overview of the studies already developed on the anaerobic digestion of *Agave* sp. with a focus on the sisalana variety and possible applications of the generated biogas. The anaerobic digestion process consists of four stages: hydrolysis, acidogenesis, acetogenesis, and methanogenesis, where microorganisms convert organic matter into biogas, mainly composed of methane and carbon dioxide. Studies show that pretreatments, such as aerobic and fungal treatments, and co-digestion with other residues can increase the efficiency of the process. Biogas from *Agave sisalana* has several applications, including power generation injection into gas pipelines. Despite challenges such as the need for investment in infrastructure and technology, the anaerobic digestion of *Agave sisalana* presents significant potential for renewable energy production in Brazil, especially considering the increasing demand for green energy.

**Keywords:** Sisal. Anaerobic Digestion. Biogas. Bioenergy.

The global demand for renewable energy is rapidly increasing due to concerns about climate change and the declining availability of fossil resources. Biogas, produced through the anaerobic digestion of organic waste, stands out as a clean and sustainable energy source. *Agave sisalana*, or sisal, is a succulent and fibrous plant with CAM (Crassulacean Acid Metabolism) metabolism cultivated primarily to produce natural fibers, generating a significant amount of waste during the defibering process in all production sites [1].

It is estimated that 8% (wet basis) of the plant corresponds to fiber, and the remaining 92% is composed of mucilage (cuticle and palisade and parenchyma tissue), fluff (short fibers), and sap - chlorophyllic sap [2]. Anaerobic digestion of sisal waste offers an opportunity to transform this byproduct into a valuable energy resource, contributing to sustainable resource management and the mitigation of environmental impacts [3-

6], including the potential use of the remaining residue after digestion as a biofertilizer to return to the soil [3].

Sisal was introduced to Brazil in the 19th century, and it originated from the African continent. Its production began in Ceará, later spreading to other states in the Northeast. Sisal production experienced its "Golden Age" in the 1950s, when Brazil became the world's largest producer, going into decline in the 1970s. However, Brazil is now the world's largest producer again, surpassing the African continent's total production and historically the most significant producer [7].

Table 1 presents the sisal production between 2020 and 2022 and the projected production in 2032 from the leading producers [7].

Given this context, this study aims to analyze available literature to identify advancements, applications, and trends in biogas production using byproducts from the industrial utilization of *Agave sisalana*.

## Materials and Methods

This systematic literature review employed scientific data from the Web of Science (WoS)

Received on 27 September 2024; revised 28 December 2024.

Address for correspondence: Julio C.A. Toqueiro. Av. Cândido Rondon, 501 - Cidade Universitária, Campinas - SP. Zipcode: 13083-875. E-mail: jctoqueiro@gmail.com.

J Bioeng. Tech. Health 2024;7(4):380-385  
© 2024 by SENAI CIMATEC. All rights reserved.



**Table 1.** Main sisal producers [7].

Country	Production 2020-2022 (kton)	Production 2032-projected (kton)
Brazil	88.2	98.7
China	63.5	65.3
United Republic of Tanzania	36.3	43.5
Kenya	31.6	37.5
Madagascar	6.0	7.0

(Clarivate Analytics®, Boston, USA) with a cutoff date of May 31, 2024. The search equation incorporated types/varieties of *Agave* with the potential for commercial energy applications and biogas production. The search within the WoS database was restricted to the topic (TS) field, which encompasses terms in the title, abstract, author, keywords, and keywords plus. The established equation was: TS=((*Agave* OR *tequilana* OR *sisal* OR *sisalana* OR "*agave americana*" OR *salmiana* OR *fourcroydes* OR "*agave angustifolia*" OR "*agave sp*") AND (biogas OR methane OR Anaerobic OR digestion OR CH<sub>4</sub>)). The search results were filtered to exclude literature reviews and specific research categories within WoS, such as food science and technology, agriculture and animal science, and polymer science, as these areas did not align with the selected topic focused primarily on biogas and energy generation.

Additionally, the language of the selected documents was limited to English, Spanish, and Portuguese, and the analysis timeframe encompassed the period from 1980 to 2024. The collected information was compiled using the open-source software VOSviewer 1.6.6, and using default settings, co-authorship, and keyword co-occurrence networks was generated. Finally, an analysis of the historical series identified, alongside future advancements and trends, is discussed and presented.

## Results and Discussion

The search for research on biogas production using byproducts from the *Agave* production chain

yielded 158 consolidated results distributed among review articles (7.6%), research articles (89.2%), and conference papers (3.1%). The terms "anaerobic digestion," "biogas," and "Agave," with 35, 30, and 27 citations, respectively, were the most frequently occurring in the selected database. Figure 1 illustrates the keyword co-occurrence network and clusters obtained using VOSviewer, considering 25 keywords with a minimum of 6 occurrences in the database. As depicted in Figure 1, five main clusters were identified based on color coding (green, red, blue, yellow, and purple). The green cluster, for instance, demonstrates a correlation between studies employing anaerobic digestion, sisal pulp, and anaerobic batch reactors, suggesting that continuous systems are limited, likely due to the need for pretreatment to adjust the physical properties of the residue. Similarly, the yellow cluster, associated with "bioethanol production," is linked to the blue and green clusters as ethanol production, particularly in the form of tequila and mescal, generates residues such as vinasse and agave bagasse, which possess the potential for biogas production, thereby enabling the generation of thermal and electrical energy. Finally, it is crucial to highlight the purple cluster, which features the word "Tanzania." Much of the research focusing on utilizing *Agave sisalana* residues was developed in the context of fiber production in Tanzania, one of the world's leading fiber producers alongside Brazil and China.

## Publications on Strategies for Optimizing

### Biogas Production

Anaerobic digestion is a biological process that occurs in the absence of oxygen, where microorganisms convert organic matter into biogas, mainly composed of methane (CH<sub>4</sub>) and carbon dioxide (CO<sub>2</sub>), along with other gases in smaller quantities, such as hydrogen sulfide (H<sub>2</sub>S).

The process is divided into four main stages [3]:

**Hydrolysis:** Degradation of complex macromolecules, such as carbohydrates, proteins, and lipids, into smaller, simpler molecules with higher solubility. This process produces sugars, amino acids, and fatty acids.

**Acidogenesis:** Fermentation of the molecules resulting from hydrolysis, generating volatile fatty acids (VFAs), such as acetic, propionic, butyric, and valeric acids. Carbon dioxide and hydrogen are also produced during this stage.

**Acetogenesis:** Conversion of VFAs into acetic acid, hydrogen, and carbon dioxide.

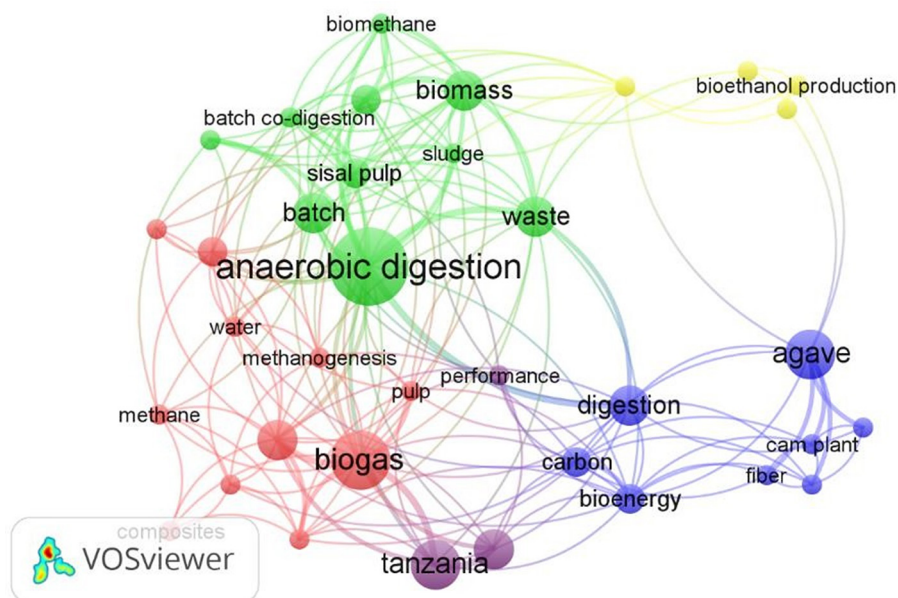
**Methanogenesis:** Production of methane from acetic acid, hydrogen, and carbon dioxide, a conversion carried out by methanogenic bacteria.

Several factors affect the anaerobic digestion process, such as temperature, pH, solids concentration, retention time (hydraulic and solids), agitation, the type of substrate and inoculum, and the possible presence of inhibitory agents. Numerous studies have been developed to evaluate the impact of changes in these factors on methane generation, with those listed below considered of most significant interest [3, 4, 8-13]:

**Pretreatment:** Sisal pretreatment aims to increase the material's biodegradability by facilitating the action of microorganisms and modifying the substrate's initial characteristics. Various pretreatment methods can be used, such as aerobic pretreatment, which involves the oxidation of organic matter by aerobic microorganisms, and treatment with fungi, which decomposes lignin and increases the accessibility of cellulose and hemicellulose [8-9].

**Co-digestion:** Co-digestion of sisal with other organic residues aims to improve the digester's

**Figure 1.** Network co-occurrence of keywords using the reported search equation.



nutrient balance, increase biogas production, and reduce digestion time [10-12].

**Particle size:** Reducing the size of sisal particles increases the surface area available for microorganisms, accelerating degradation and increasing methane production. Alterations to this factor have consequences similar to agitation for the digestion process [13].

The literature highlights two strategies for increasing methane production from sisal pulp pretreatment: aerobic pretreatment and fungal treatment.

The results for aerobic pretreatment were positive for short periods, with a peak in methane production for 9 hours, generating 24 m<sup>3</sup>/VS and a 26% increase compared to digestion without pretreatment. However, this process can reduce methane generation, as observed for 72 hours of pretreatment, where methane production was reduced to 12 m<sup>3</sup>/VS [8].

Pretreatment using fungi, developed in a previously published study using CCHT-1 and *T. reesei* fungi, varied the application sequence of the fungi for treatment. When CCHT-1 was applied initially, a 101% increase in methane generation was observed compared to production without pretreatment. In the reverse sequence, production increased by only 46% [9].

The co-digestion of sisal with other residues has been studied, with associations found in the literature

with fish waste, zebu manure, and palash leaves. Table 2 compares methane production from pure sisal residue and in the case of co-digestion [10-12].

As demonstrated in previous studies, particle size is directly related to methane production. For sisal fiber particles of 2 mm, a 23% increase in methane production was observed compared to production without size reduction, with a generation of 0.22 m<sup>3</sup> per VS. Figure 2 illustrates the methane production for different particle sizes studied [13].

While published studies present a wide range of methane production values, only the underlying concepts can be compared across different references. These experiments were conducted under varying conditions and should only be directly compared within the same study.

#### Typical Application of Biogas

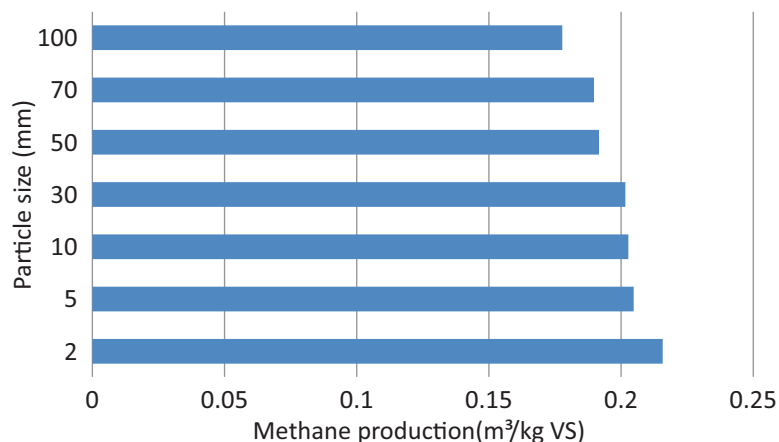
Biogas produced from the anaerobic digestion of sisal has been used in various ways globally, as listed below [3,4,14-16]:

**Power Generation:** Biogas can be directly used in internal combustion engines to generate electricity [3,4,14-16]. This is the primary application in Brazil currently, and it is widely used in sanitary landfills.

**Injection into Natural Gas Pipelines:** Biomethane, methane obtained through biogas

**Table 2.** Methane production through co-digestion of sisal [10-12].

Substrat	Configuration	Methane Production
Sisal + Palash co-digestion	Digestion of sisal	130 mL/day
	Co-digestion	320 mL/day
Sisal + Fish Residues	Digestion of sisal	0.32 m <sup>3</sup> /kg VS
	Co-digestion (67% sisal + 33% fish residues)	0.62 m <sup>3</sup> /kg VS
Sisal + Zebu Manure	Digestion of sisal	Uninformed
	Co-digestion	166 mL/g VS

**Figure 2.** Methane production for different particle sizes [13].

Source: Adapted from MSHANDETE, A. et al., 2006.

purification, can be injected into natural gas pipelines, providing a clean and sustainable alternative. However, the main limitation of this application is the presence of pipelines in the area of biogas production [15].

**Cooking Gas Supply:** Biogas can replace LPG (liquefied petroleum gas) for burning in stoves and cooking. This application is uncommon in Brazil but is more prevalent in lower-income countries.

In regions where this application is used, it is often not subject to strict controls, raising the possibility of accidents related to its use. Biogas can replace LPG, reducing dependence on fossil fuels and lowering energy costs for families and businesses. However, regulations, as well as the necessary infrastructure, must be defined to ensure safe utilization [3,4,14-16].

#### Challenges and Perspectives of Anaerobic Digestion of *Agave Sisalana*

Anaerobic digestion of sisal has been studied in various parts of the world, primarily in countries that are major producers. This results in a massive waste generation, typically without any use, making its disposal challenging. It is expected to increase due to projected production growth in the coming years. However, its digestion allows for the

production of biofuels, such as butanol, hydrogen, and primarily biogas, containing biomethane [7, 16]. Despite this potential, several for its large-scale implementation, challenges need to be overcome, such as the construction of necessary infrastructure, technological advancements, cost reduction for installation, and defining logistics for transporting sisal waste and delivering the generated biogas [1,17].

Research and development of innovative technologies, such as co-digestion, pretreatment, and the use of different types of support for biofilms, are crucial for enhancing the efficiency of anaerobic digestion of sisal and reducing biogas production costs [4, 8-12, 15].

It is essential to promote the implementation of pilot projects in various contexts to assess their technical, economic, and social feasibility. The biogas produced has several possibilities in the current Brazilian context, such as direct electricity generation, a process already widely utilized in sanitary landfills, and its purification for feeding and mixing into natural gas pipelines, which are expected to be encouraged in the coming years due to recent legislative changes.

Additionally, the increasing demand for green energy must be considered, driven by the numerous green hydrogen plants announced or under study in the country. These plants are currently linked to wind or solar generation, with their main parks in

the Northeast region. The use of biogas to generate green energy for these plants, besides allowing their installation in other regions of Brazil, would also solve the major drawback of dependence on solar and wind energy generation, which is its reliance on weather conditions, a factor not applicable to biogas generation.

## Conclusion

Anaerobic digestion of sisal emerges as a promising solution for renewable energy production in Brazil, leveraging the growing volume of residues generated by its production. Furthermore, studies indicate the potential of this technique to generate biogas, which can be used for various applications such as electricity generation, injection into gas pipelines, and supplying cooking gas.

As highlighted in this article, numerous strategies exist to optimize the utilization of this potential. However, challenges remain, such as investments in infrastructure, technological development, and process optimization. Continued research into potential applications and maximizing its energy potential is crucial for large-scale adoption.

## References

1. Vuorine I, Heiskanen J, Maghenda M, Mwangala L, Muukkonen P, Pellikka PKE. Allometric models for estimating leaf biomass of sisal in a semi- arid environment in Kenya. *Biomass and Bioenergy* 2021;155:106294.
2. Silva ORRF, Coutinho WM, Cartaxo WV, Sofiatti V, Silva JLF, Carvalho O, Costa LB. Cultivo do Sisal no Nordeste Brasileiro. *Embrapa Circular Técnica* 123. 2008. ISSN 0100-6460.
3. Oudshoorn L. Biogas from sisal waste – a new opportunity for the sisal industry in Tanzania. *Energy for Sustainable Development* 1995;2(4):46–49.
4. Kiarie E. Biogas as a potential alternative source of energy for industrial sector: case study of kilifi sisal plantation biogas plant. *International Journal of Advanced Research and Publications* 2019;3(7).
5. Díaz-Jiménez L, Hernandez SC, Rodríguez DJ García RR. Conceptualization of a biorefinery for guishe revalorization. *Industrial Crops and Products* 2019;138:111441.
6. Luengwattanapong K et al. Anaerobic digestion of Crassulacean acid metabolism plants: Exploring alternative feedstocks for semi-arid lands. *Bioresource Technology* 2020;297:122262.
7. Fao. Current market situation and medium-term outlook for Jute and Kenaf; Sisal and Henequen; Abaca and Coir – CCP: HF/JU 24/2, 2024.
8. Mshandete A et al. Anaerobic batch co-digestion of sisal pulp and fish wastes. *Bioresource Technology* 2004;95(1):19–24.
9. Kivaisi AK et al. The potential of agro-industrial residues for production of biogas and electricity in Tanzania. *Applied Microbiology* 1996:917–921.
10. Muthangya M et al. Two-stage fungal pre-treatment for improved biogas production from sisal leaf decortication residues. *International Journal of Molecular Sciences* 2009;10(11):4805–4815.
11. Arisutha S et al. Evaluation of methane from sisal leaf residue and palash leaf litter. *Journal of The Institution of Engineers (India): Series E* 2014;95(2):105–110.
12. Cundr O, Haladová D. Biogas yield from anaerobic batch co-digestion of sisal pulp and zebu dung. *Poljoprivredna Tehnika* 2012:111–117.
13. Mshandete A et al. Effect of particle size on biogas yield from sisal fibre waste. *Renewable Energy* 2006;31(14):2385–2392.
14. Varela Gonzalez C. Techno-economical analysis of the benefits of anaerobic digestion at a rural sisal processing industry in Tanzania. *Degree Project in Energy and Environment* 2017.
15. Oliva-Rodríguez AG et al. Biohydrogen gas/acetone-butanol-ethanol production from *Agave guishe* juice as a low-cost growing medium. *Fermentation* 2023;9(9).
16. Azadi P, Khosh-Khui M. Micropropagation of *Lilium ledebourii* (Baker) Boiss as affected by plant growth regulator, sucrose concentration, harvesting season and cold treatments. *Electronic Journal of Biotechnology* 2007;10(4):582–591.
17. Terrapon-Pfaff JC, Fischedick M, Monheim H. Energy potentials and sustainability-the case of sisal residues in Tanzania. *Energy for Sustainable Development* 2012;16(3):312–319.



## Sustainable AI Applied to Project Management: A Literature Review

Hérica de Souza Araújo<sup>1\*</sup>, Thiago Barros Murari<sup>1</sup>, Anusio Menezes Correia<sup>1</sup>, Erick G. Sperandio Nascimento<sup>1,2</sup>

<sup>1</sup>SENAI CIMATEC University; Salvador, Bahia, Brazil; <sup>2</sup>Surrey Institute for People-Centred AI, Faculty of Engineering and Physical Sciences, University of Surrey, Guildford, Surrey, UK

**Integrating sustainable practices with emerging technologies, such as Artificial Intelligence, has proven crucial to achieving new sustainable development goals. In the industrial context, project management is important in promoting sustainability. This work aims to review the literature on applying sustainable Artificial Intelligence in project management, focusing on optimizing resources and aligning with the SDGs. As a result, the research highlighted the good performance of the technological transformation of project management, combined with sustainability concepts, as an agent capable of generating the necessary transformations to guarantee a more sustainable future.**

**Keywords:** Project Management. Artificial Intelligence. Sustainable Development. Sustainable AI.

In recent years, sustainability has aroused great interest and has been the focus of numerous discussions and global initiatives. Much of the emphasis on the topic is due to the growing concern with maintaining economic, social, and environmental systems in alignment with the Sustainable Development Goals (SDGs).

Sustainability addresses the need to satisfy the current world's needs without compromising future generations' capacity, establishing a balance between economic development and sustainable pillars. Sustainable development, in turn, aims to achieve this balance, promoting economic growth that is inclusive, ecologically correct, and socially fair. Sustainable practices can generate business opportunities, drive innovation, and improve social well-being, contributing to long-term economic and social stability. Linking sustainability to new emerging technologies, such as Artificial Intelligence (AI), is a demand that arises in parallel to discussions on sustainable development and can contribute to achieving the goals established by the United Nations General Assembly.

Received on 11 September 2024; revised 21 December 2024.  
Address for correspondence: Hérica de Souza Araújo.  
Avenida Orlando Gomes, 1845, Piatã. Salvador, Bahia, Brazil.  
Zipcode: 41650-010. E-mail: herica.araujo@fieb.org.br.

In the industrial area, another practice emerges as an important ally in promoting the aforementioned changes: project management. Capable of offering the necessary guidance to meet a given scope, project management is a potential tool for ensuring good results and achieving goals. Incorporating new technologies into project management practices and integrating sustainability concepts can result in satisfactory organizational benefits, contributing significantly to the search for sustainable development. The main objective of this work is to carry out a literature review on the concept of sustainable AI applied to project management, focusing on resource optimization. The research is directly related to the Sustainable Development Goals, whose focus is SDG 9: Industry, innovation, and infrastructure, which aims to build resilient infrastructure, promote inclusive and sustainable industrialization, and foster innovation [1].

### Materials and Methods

The method applied in this research is based on a traditional narrative review methodology, which aims to synthesize and interpret existing knowledge on a specific topic through a coherent narrative. Below is a step-by-step guide:

**Scope Definition:** The research objective was

established, and the review scope delineated, involving selecting key concepts and formulating research questions responsible for guiding the narrative.

**Information Sources Identification:** Search strategies were defined (keywords and inclusion/exclusion criteria), and the leading scientific databases were identified (ScienceDirect, SciELO, Scopus, etc.).

**Study Selection and Inclusion:** The criteria were established, and the main works were identified and selected.

**Data Extraction and Synthesis:** Selected studies were analyzed, and relevant data were extracted and synthesized to highlight key themes, trends, and emerging debates in the literature reviewed. Study Analysis and Interpretation: A critical analysis of selected studies was conducted, discussing their contributions to understanding the topic and highlighting common patterns, discrepancies, and gaps in the literature.

**Narrative Structuring:** The review text was structured into a coherent narrative, beginning with a clear introduction to the topic, then developing key debate questions, and concluding with a synthesis of findings and future directions. Review and Editing: Finally, the work underwent a review and editing process to ensure clarity, coherence, and academic rigor.

## Literature Review

### Sustainability and Sustainable Development Goals

In recent years, discussions about sustainable development have grown exponentially due to numerous events highlighting economic, social, and environmental instability [2]. At the same time, as the demand for sustainability grows, the demand for the subsistence of industries in the current market also increases. This is mainly because

the concept of sustainability is directly linked to the idea of survival, and, in the long term, this perspective is translated into the economic capacity of organizations [3]. Sustainable development represents a dimension of sustainability that focuses primarily on promoting economic growth by the constraints of the planet's natural systems, maintaining the balance of the ecosystem [4]. In line with this need, the new technological era has required companies to adapt their development models to incorporate new sustainable approaches to business practices [2].

In this scenario, and to strengthen the search for sustainable development, many initiatives have encouraged the application of new technologies to address sustainability in different domains. Artificial Intelligence (AI), for example, is one of the recent technological advances that represent a potential resource for enabling sustainable growth [5], mainly if applied in alignment with the 17 Sustainable Development Goals (SDG).

The 17 Sustainable Development Goals were proposed in 2015 by the United Nations (UN) and include 169 targets to achieve the sustainable development agenda by 2030 [6]. These objectives cover issues that encompass different challenges, ranging from combating climate change to eradicating hunger, and the application of AI in this scenario has aroused the interest of several researchers. Analyzing and understanding the impact of AI on sustainable development has been a topic of growing interest in recent years [7]. The World Economic Forum reinforced the need to direct the use of Artificial Intelligence to contribute to the Sustainable Development Goals [8]. At the same time, the European Commission highlighted the fundamental role in AI's transformation, being a source of change towards a fairer, more prosperous, and sustainable future [9]. All of these factors reinforce the importance of understanding the concept of AI and the possible implications of its use.

### AI and Sustainable AI

The most widespread definition of AI today

consists of the relationship between the application of generative algorithms and the direct impact of this application on the efficiency of processes [10]. In the field of research, the application of AI focuses on optimizing processes, emphasizing reducing costs and increasing productivity [11]. Exploring the use of AI to optimize solutions for complex contemporary problems is one of the leading development paths in alignment with the SDGs [2]. According to Sulich and colleagues [10], Artificial Intelligence can drive innovation by addressing the priority dimensions of the Sustainable Development Goals, and it is crucial to understand the mutual relationship between the SDGs and ethical paradigms for technology implementation. Recognizing the role of Artificial Intelligence in building a sustainable future through its capacity for data analysis, expansion of the quantitative knowledge base, and optimization of human activities in terms of energy efficiency and costs is essential for disseminating technology [4]. Given the discussions presented, it is possible to affirm that the growing interest in sustainability issues has driven the demand for studies on integrating AI into sustainable business practices [12]. Sustainable AI emerges against this scenario based on the policies and practices associated with the Sustainable Development Goals [13].

Sustainable AI has been the subject of study by many researchers, and applying this technology to promote sustainability has become increasingly common, often in association with the SDGs [11]. Recent studies highlight the effectiveness of Artificial Intelligence in achieving sustainable development, especially in economics, agriculture, and business management, supporting the achievement of sustainable goals and the decision-making process [10]. Exploring AI's impact on a sustainable level is extremely important, especially from an economic point of view [14]. For this reason, the topic has been of interest in science and marketing [10]. Due to its ability to process and learn from large volumes of information, AI can be applied across various fields to optimize resource utilization [15]. If

applied to the management field, the technology can resolve managerial problems [16]. In the innovation sector, the application of Artificial Intelligence proves highly efficient, mainly due to its ability to work with large sets of data [14].

Reinforcing the aspects already highlighted, Li and Xu [16] point out that enterprises must adapt to the evolution of AI and the consequent emergence of new businesses to guarantee their survival. For Sipola and colleagues [12], the use of Artificial Intelligence can allow faster extraction of information and assist in the decision-making process, strengthening the competitive position of organizations, and Waltersmann and colleagues [17], in turn, reinforces that the application of sustainable AI in the search for resource efficiency has grown as the importance of sustainable values increases in manufacturing industries. The new needs that arise from the aspects mentioned so far reinforce the importance of disseminating the application of AI in the search for cost reduction and resource optimization [12]. In this way, sustainable AI can be understood as a potential tool for achieving the SDGs in different sectors of the world economy, contributing to advancing socioeconomic aspects in underdeveloped countries [18]. Organizations can employ AI to utilize available assets more efficiently, often allocating limited resources more effectively and improving oversight and data sharing. They will also focus on investigating key application-related aspects of sustainable AI in the field of project management.

### Sustainability AI in Project Management

In recent years, project management has gained significant notoriety, receiving attention for its essential role in different sectors of the global market, offering the structure and guidelines necessary to achieve good results. With the advent of AI, interest also arose in using new technologies available to improve project management practices [19]. As interest in the topic grows, the need to understand the concept of project management and

its different application possibilities also increases, with the main focus being the search for the satisfaction of interested parties and ensuring the expected financial return [20]. Despite this, recent data show that only 35% of projects executed are successful, and, in most cases, this low performance is attributed to the lack of technologies applied to project management [21]. Given this scenario, the application of Artificial Intelligence in this field of study emerged as a key factor in enabling the development of a management structure based on the historical experience of past projects, supporting the development of proactive strategies throughout the execution of new projects [18].

Faced with the competitiveness of the current market, organizations have been faced with new demands linked to project management, ranging from planning and effective control of trivial elements involved in conducting a project, such as scope, deadline, and cost, to other aspects focused on sustainable practices, covering the economic, social and environmental dimensions [20]. In this context, disseminating new technologies applied to project management, combined with adopting sustainability criteria, can represent a competitive differentiator capable of guaranteeing the prominence of organizations in the current market by increasing the probability of success of the projects developed [19]. To ensure sustainable development and strengthen the balance between the pillars of sustainability, organizations need to adapt their processes to enable risk reduction and cost optimization, adding value to the business [3]. This adaptation must require the adaptation and/or replacement of many production and management processes combined with implementing environmental and safety guidelines [22]. Seeing new sustainability challenges as opportunities for innovation is crucial for maintaining business competitiveness, and disseminating the application of sustainable AI in project management in large organizations is the first step towards this new scenario.

Project management plays a fundamental role in disseminating sustainability criteria within

organizations, and there are several possibilities for integrating sustainable aspects throughout project development, especially in promoting the optimization of available resources and ensuring projects' economic performance [23]. Considering that part of defining a project concept involves constraining time, cost, and resources [3], promoting conscientious use of these components is crucial for preventing failures and ensuring successful outcomes [22]. In this scenario, AI applied to project management may be able to increase task performance through the automation of operational functions, in addition to optimizing the allocation of available resources through the analysis of historical data and the establishment of standards that enable the targeting of resources based on demand forecast, allowing the implementation of a flexible and adaptable management model [24]. For Nieto-Rodriguez e Vargas [21], AI should be used with a focus on creating personalized project plans capable of directing efforts and available resources in an optimized and precise manner, ensuring the best use of resources and a balance between environmental, social, and economic dimensions. In this way, by incorporating AI techniques into project management, organizations can improve their internal processes by directing efforts, reducing costs, optimizing resources, and increasing the performance of their processes in alignment with the concept of sustainable development [20]. Combined with the sustainability criterion, the restructuring of project management practices may be capable of boosting new economic scenarios and promoting the modernization of the industry, contributing to the strengthening of the pillars of sustainability and the search for achieving the SDGs, especially SDG 9 (Industry, Innovation, and Infrastructure), which aims to build resilient infrastructure, promote inclusive and sustainable industrialization and foster innovation [1,25].

Prioritizing the efficient control of resources, which are almost always limited, must be understood as a strategic project management approach, an essential factor for sustainable growth



[20]. Therefore, capitalizing on all the knowledge already established in project management, incorporating additional concepts and attributes related to sustainability, and integrating new technologies can be the principal transformative agent for the future of organizations [3]. The dissemination of the use of Artificial Intelligence applied to project management, with a focus on optimizing resources, can be understood as an advance of great importance for the transformation of organizational processes, not only boosting the economic efficiency of businesses but also promoting the development sustainability and the subsistence of institutions [25].

## Conclusion

Promoting the development of countries without compromising the future of humanity is the great challenge of the 21st century, and investing in sustainable practices, aiming not only to preserve natural resources but also economic stability and social well-being, is a decisive factor capable of driving innovation and the creation of new business opportunities. As the demand for sustainability grows, the advancement of emerging technologies also intensifies, awakening the need for technological transformation of current processes. These discoveries represent opportunities for transformation, increasing the efficiency and quality of processes and fostering innovation. Organizations can stay competitive and ensure their continuity by adopting emerging technologies like AI.

In this scenario, the discussions presented throughout this work show that project management is a cross-sectional research field capable of encompassing different approaches. In the corporate world, project management plays an essential role, providing the necessary structure to achieve goals and enabling the appropriate allocation of resources and compliance with deadlines. This results in successful deliveries and greater competitiveness for organizations. Linking sustainability concepts to project

management through Artificial Intelligence with a focus on optimizing resources, reducing costs, and strategically directing efforts may generate the necessary transformations to guarantee a more sustainable future and alignment with SDG 9. Finally, the aspects discussed throughout this work are not just ethical recommendations but fundamental concepts for maintaining the economic, social, and environmental spheres. The main limitation found throughout this research is the scarcity of work related to AI and project management with practical applications.

Finally, future research will focus on developing and applying an AI model in a pilot project, focusing on planning and optimizing resources, including analyzing results and mapping the main benefits obtained.

## References

1. Instituto de Pesquisa Econômica Aplicada (IPEA). (s.d.). Objetivo de Desenvolvimento Sustentável 9 - Indústria, Inovação e Infraestrutura. Available at <https://www.ipea.gov.br/ods/ods9.html>.
2. Saturnino CB, Du S, Grewal D. Using artificial intelligence to advance sustainable development in industrial markets: A complex adaptive systems perspective. *Industrial Marketing Management*, 2024;116:145-157. <https://doi.org/10.1016/j.indmarman.2023.11.011>.
3. Morioka SN, Carvalho MM. Sustentabilidade e gestão de projetos: um estudo bibliométrico. *Production* 2016;26(3):656-674. <https://doi.org/10.1590/0103-6513.058912>.
4. Francisco M, Linnér B. AI and the governance of sustainable development. An idea analysis of the European Union, the United Nations, and the World Economic Forum. *Environmental Science & Policy* 2023;150:103590. <https://doi.org/10.1016/j.envsci.2023.103590>.
5. Davenport T, Guha A, Grewal D, Bressgott T. The impact of AI on marketing. *Journal of the Academy of Marketing Science* 2020;48(1):24-42.
6. United Nations. The 17 goals. Department of Economic and Social Affairs 2015. Accessed 02/2024 at: <https://sdgs.un.org/goals>.
7. Briscoe E, Fairbanks J. Artificial scientific intelligence and its impact on national security and foreign policy. *Orbis* 2020;64:544-554. <https://doi.org/10.1016/j.orbis.2020.08.004>.



8. World Economic Forum. Harnessing Artificial Intelligence for the Earth 2018:3–27.
9. European Commission. Communication from the Commission to the European Parliament, the European Council, the Council, the European Economic and Social Committee and the Committee of the Regions: Artificial Intelligence for Europe. 2018:1–20.
10. Sulich A et al. Artificial intelligence and sustainable development in business management context – Bibliometric review. *Procedia Computer Science* 2023;225:3727–3735. <https://doi.org/10.1016/j.procs.2023.10.368>.
11. Nasi O et al. Artificial intelligence and sustainable development goals nexus via four vantage points. *Technology in Society* 2023;72:102171. <https://doi.org/10.1016/j.techsoc.2022.102171>.
12. Sipola J, Saunila M, Ukko J. Adopting artificial intelligence in sustainable business. *Journal of Cleaner Production* 2023;426:139197, ISSN 0959-6526, <https://doi.org/10.1016/j.jclepro.2023.139197>.
13. Wilson C, Van der Vellen M. Sustainable AI: An integrated model to guide public sector decision-making. *Technology in Society* 2022;68:101926. ISSN 0160-791X. <https://doi.org/10.1016/j.techsoc.2022.101926>.
14. Kar et al. How can artificial intelligence impact sustainability: A systematic literature review. *Journal of Cleaner Production* 2022;376:134120. ISSN 0959-6526. <https://doi.org/10.1016/j.jclepro.2022.134120>.
15. Rolnick D et al. Tackling climate change with machine learning. *ACM Computing Surveys (CSUR)* 2022;55(2):1–96.
16. Li F, Xu G. AI-driven customer relationship management for sustainable enterprise performance. *Sustainable Energy Technologies and Assessments* 2022;52(Part B):102103. ISSN 2213-1388. <https://doi.org/10.1016/j.seta.2022.102103>.
17. Waltersmann L, Kiemel S, Stuhlsatz J, Sauer A, Mische R. Artificial intelligence applications for increasing resource efficiency in manufacturing companies—a comprehensive review. *Sustainability* 2021;13:6689.
18. Van Wynsberghe A. Sustainable AI: AI for sustainability and the sustainability of AI. *AI and Ethics* 2021;1(3):213–218.
19. Barcaui A, Monat A. Who is better in project planning? Generative artificial intelligence or project managers? *Project Leadership and Society* 2023;4:100101. ISSN 2666-7215. <https://doi.org/10.1016/j.plas.2023.100101>.
20. Lourenço N, Zambon MZ. Otimização de recursos de gerenciamento de projetos nas organizações. *Caderno Técnico de Administração Contemporânea* 2021;3.
21. Nieto-Rodriguez A, Vargas RV. How AI will transform project management. *Harv Bus Rev* 2023. Available at: <https://hbr.org/2023/02/how-ai-will-transform-project-management>.
22. Cavalcanti CT de A, Silva IRM. Contribuições e Desafios da Sustentabilidade na Gestão de Projetos. *Revista de Gestão e Projetos [S. l.]* 2016;7(3):20–28. doi: 10.5585/gep.v7i3.358. Available at <https://periodicos.uninove.br/gep/article/view/9649>.
23. Bocchini P et al. Resilience and sustainability of civil infrastructure: toward a unified approach. *Journal of Infrastructure Systems* 2014;20:1–16.
24. Prifti V. Optimizing project management using artificial intelligence. *European Journal of Formal Sciences and Engineering* 2022;5(1):29–37.
25. Wang Z et al. Achieving sustainable development goal 9: A study of enterprise resource optimization based on artificial intelligence algorithms. *Resources Policy* 2023;80:103212. ISSN 0301-4207. <https://doi.org/10.1016/j.resourpol.2022.103212>.

## Game Theory to Promote the Sustainable Development of the Pharmaceutical Industry

Rosivaldo Cardoso Santiago<sup>1,2\*</sup>, Aloísio Santos Nascimento Filho<sup>1</sup>, Bruna Aparecida Souza Machado<sup>3</sup>,  
Hugo Saba Pereira Cardoso<sup>4</sup>

<sup>1</sup>Postgraduate Program in Management and Industrial Technology, SENAI CIMATEC University; <sup>2</sup>Oswaldo Cruz Foundation; <sup>3</sup>Senai Institute of Innovation in Advanced Health Systems; <sup>4</sup>State University of Bahia; Salvador, Bahia, Brazil

**This study evaluated the application of game theory in sustainable development strategies in the pharmaceutical industry through a bibliometric analysis. Using databases such as Scopus, Web of Science, and Science Direct, the results indicate a lack of studies focused on applying game theory, specifically in the pharmaceutical industry, especially in sustainability. Gaps were identified in risk management, profitability, decision-making, and competition. It is concluded that game theory can model investment decisions in R&D, competitive scenarios, and sustainable medicine marketing practices, integrating economic, social, and environmental objectives. These insights stimulate future academic research in the area.**

**Keywords:** Game Theory. Pharmaceutical Industry. Sustainable Development. Cooperation. Sustainability. Competition.

The pharmaceutical sector has received increasing attention regarding its contribution to sustainable development. Companies in this segment face multidimensional challenges involving economic, social, and environmental objectives, often with conflicting interests and priorities among stakeholders. The industry's economic vision seeks financial returns through innovations and commercialization of medicines. In contrast, stakeholders in the social vision focus on promoting universal access to treatments, and environmentalists prioritize mitigating adverse environmental impacts [1].

In the pharmaceutical field, social objectives aim to guarantee access to medicines for as many people as possible, regardless of the regional economic context. The economic objectives seek to enable revenues and mitigate costs to create an attractive business model for ongoing investments. Environmental objectives involve implementing practices that minimize the negative externalities of pharmaceutical operations, making production processes more efficient and less polluting [2,3].

Although sustainability objectives are well-defined, practical implementation faces significant challenges. Economically, the industry faces pressure from affordability, high R&D costs, government regulations, and patent issues that impact innovation. Balancing profitability with social responsibility and equitable access to medicines is a significant challenge.

Environmentally, reducing energy and resource consumption and managing pharmaceutical waste are critical issues. Managing these tensions with decision-support tools that promote cooperation is essential to the long-term sustainable success of the pharmaceutical industry [2].

In this context, game theory emerges as a promising analytical approach to integrate economic, social, and environmental objectives, facilitating conflict resolution and cooperation between interested parties. This approach allows for formal model interactions between industry actors, identifying solutions that maximize mutual benefits and minimize conflicts. The application of game theory can facilitate negotiating and implementing policies that effectively align diverse interests, promoting truly sustainable pharmaceutical development. Furthermore, game theory can help identify Nash equilibria, where no player benefits from changing their strategy unilaterally, creating an environment of stability and predictability [4-7].

Received on 11 September 2024; revised 21 December 2024.  
Address for correspondence: Hérica de Souza Araújo.  
Avenida Orlando Gomes, 1845, Piatã. Salvador, Bahia, Brazil.  
Zipcode: 41650-010. E-mail: herica.araujo@fieb.org.br.

J Bioeng. Tech. Health 2024;7(4):392-398  
© 2024 by SENAI CIMATEC. All rights reserved.

This article aimed to understand the current state of application of game theory in sustainable development strategies in the pharmaceutical industry, exploring how this theory has been used in scientific literature. It focuses on identifying existing knowledge gaps and questions the strategies' effectiveness and innovation. We also investigate how these strategies can be improved to integrate economic, social, and environmental objectives.

## Materials and Methods

A bibliometric analysis was carried out to achieve its objectives based on scientific literature available in databases. These searches were conducted in the Scopus, Web of Science, and Science Direct databases, focusing on scientific articles and literature reviews. The descriptor was first used: ("game theory") and ("pharmaceutical industry" or "pharmaceutical laboratory"), to understand the profile of scientific research between Game Theory and the pharmaceutical industry or laboratories. Afterward, a second research was carried out with the descriptors ("game theory") and ("sustainable development" or "triple bottom line" or "TBL" or "Sustainable growth"), to understand the profile of scientific research between Game Theory and sustainable development. Next, to understand the development of research between Game Theory, sustainable development, and the pharmaceutical industry, the descriptor ("game theory," and ("pharmaceutical industry," or "pharmaceutical laboratory ") and ("sustainable development " or "triple bottom line" or "TBL" or "sustainable growth").

## Results and Discussion

Initially, we sought to identify the evolution of the number of scientific articles in a comparative way between Game Theory and Sustainable Development, Game Theory and the Pharmaceutical Industry, and the evolution of scientific articles that simultaneously address

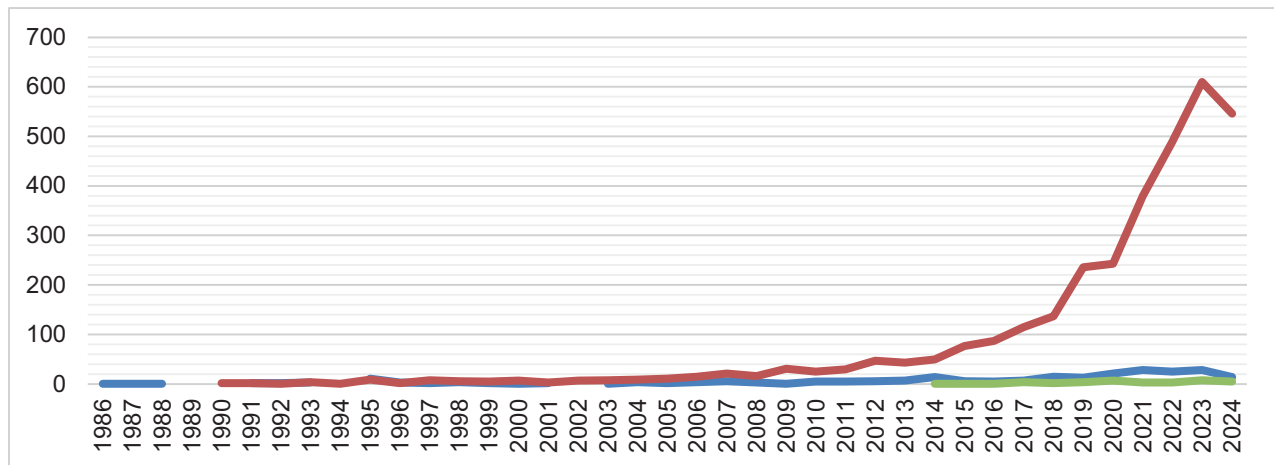
Game Theory, Sustainable Development, and the Pharmaceutical Industry. Table 1 and Figure 1 show this evolution.

Publications on Game Theory and Sustainable Development (orange-Figure 1) have grown exponentially in recent years, ranging from 0 to 610 annual publications. In contrast, articles on Game Theory and the Pharmaceutical Industry were sporadic before 2008 but have gradually increased since then, with a peak starting in 2020. The combination of Game Theory, Sustainable Development, and the Pharmaceutical Industry had few publications before 2006 but has seen a slight increase since 2018, reaching 8 articles in 2023. In 2023, 29 articles on Game Theory and the Pharmaceutical Industry and 610 articles on Game Theory and Sustainable Development were published, highlighting a growing academic interest in the association between Game Theory and Sustainable Development, Games and Sustainable Development. The scarcity of publications that combine the three themes reveals an underexplored area with great potential for discoveries and contributions.

When investigating the quality of journals linked to themes, the data in Table 2 is presented. Table 2 reveals the distribution of scientific articles classified by QUALIS for the research descriptors "Game Theory x Pharmaceutical Industry," "Game Theory x Sustainable Development," and "Game Theory x Sustainable Development x Pharmaceutical Industry." It is observed that most articles are published in high-quality journals (A1 and A2), with emphasis on the descriptors "Game Theory x Sustainable Development x Pharmaceutical Industry." In contrast, there are no articles in the A3 and A4 classifications for all descriptors, suggesting that research on these topics is often published in journals of more significant impact and quality. Furthermore, the combination of all descriptors ("Game Theory x Sustainable Development x Pharmaceutical Industry") presents a significantly smaller number of articles (12), with 58.33% of these in A1 journals, indicating an emerging area with

**Table 1.** Annual evolution of the number of scientific articles published in the research descriptor.

<b>Year</b>	<b>Game Theory x Pharmaceutical Industry</b>	<b>Game Theory x Sustainable Development</b>	<b>Game Theory x Pharmaceutical Industry x Sustainable Development</b>
1986	1		
1987	1		
1988	1	1	
1989			
1990		2	
1991	2	2	
1992	2	1	
1993	3	4	
1994		1	
1995	11	9	
1996	3	2	
1997	2	8	
1998	4	6	
1999	2	5	1
2000	1	7	
2001	2	3	
2002		7	
2003	1	8	
2004	4	9	
2005	2	11	
2006	4	15	1
2007	6	21	
2008	3	16	
2009	1	31	
2010	5	25	
2011	5	30	
2012	6	47	1
2013	7	43	
2014	14	50	1
2015	6	77	1
2016	5	87	1
2017	7	115	4
2018	15	137	2
2019	13	236	4
2020	21	243	7
2021	29	380	3
2022	25	489	3
2023	29	610	8
2024	14	546	5

**Figure 1.** Annual evolution of the number of scientific articles published according to research descriptor.**Table 2.** Research Descriptor x Qualis.

Qualis	Game Theory x Pharmaceutical Industry		Game Theory x Sustainable Development		Game Theory x Pharmaceutical Industry x Sustainable Development	
A1	54	52,43%	1047	57,40%	7	58,33%
A2	3G	37,86%	548	30,04%	3	25,00%
A3		0,00%		0,00%		0,00%
A4		0,00%		0,00%		0,00%
B1	8	7,77%	137	7,51%	1	8,33%
B2		0,00%	50	2,74%		0,00%
B3	1	0,97%	37	2,03%	1	8,33%
B4	1	0,97%	1	0,05%		0,00%
B5		0,00%	4	0,22%		0,00%
Total	103			1824	12	100,00%

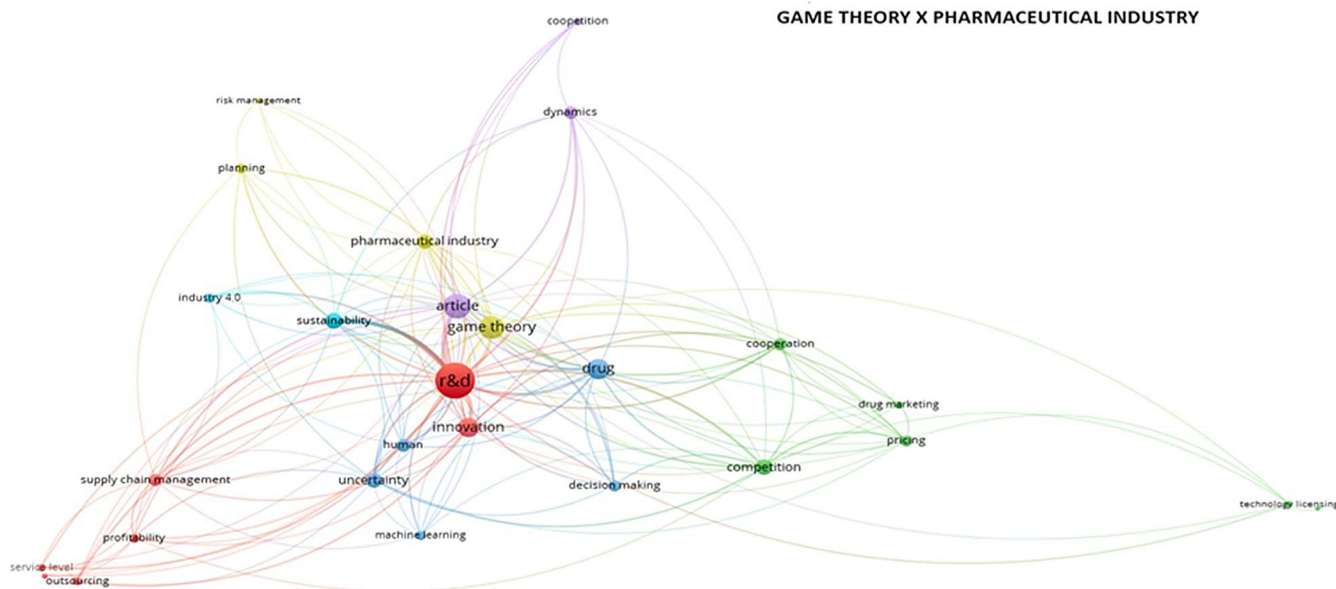
potential for future growth. The smaller presence of articles in lower QUALIS (B2, B3, B4, B5) reinforces the tendency for publication in more prestigious journals.

Some findings can be identified when conducting a semantic network analysis of the research using the specified descriptors (Figure 2). The figure shows the semantic network of the descriptor "game theory" in combination with

"pharmaceutical industry" or "pharmaceutical laboratory."

It is evident in this semantic network that Research and Development (R&D) occupies a central position, connecting to several other terms. This highlights its importance at the intersection between game theory and the pharmaceutical industry, which is in the same cluster as innovation, profitability, outsourcing, service



**Figure 2.** Semantic Network: Game Theory x Pharmaceutical Industry.

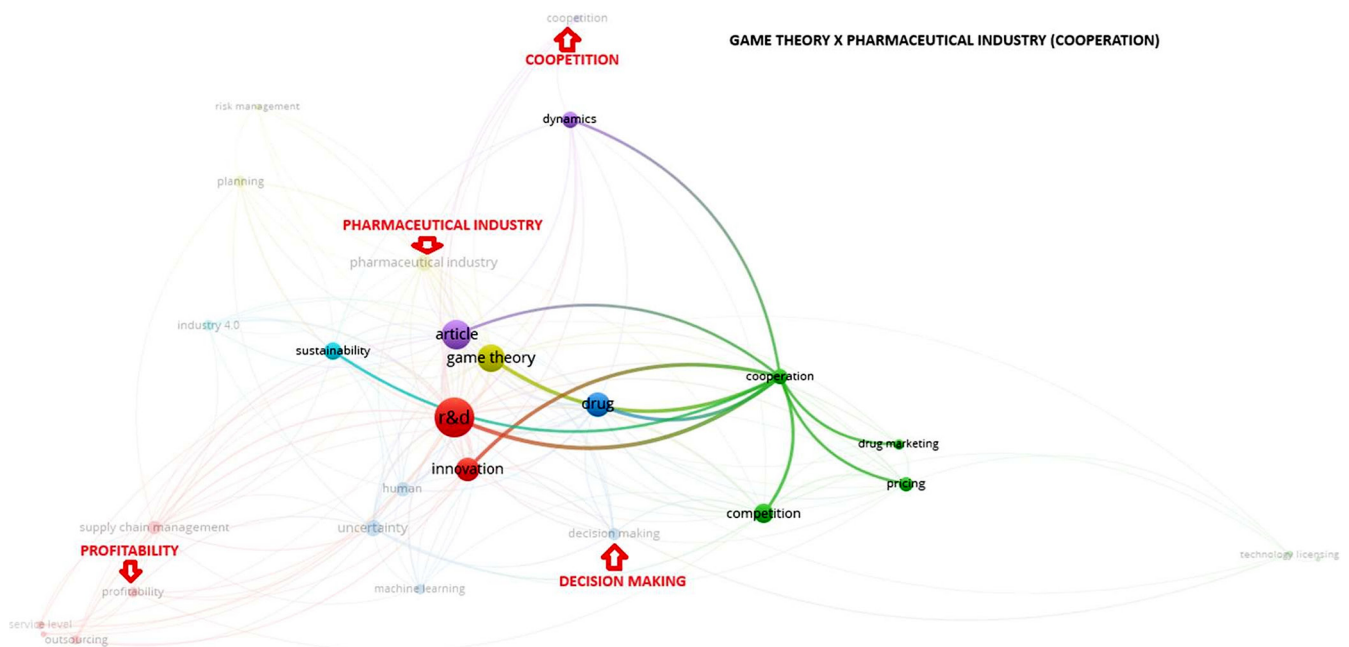
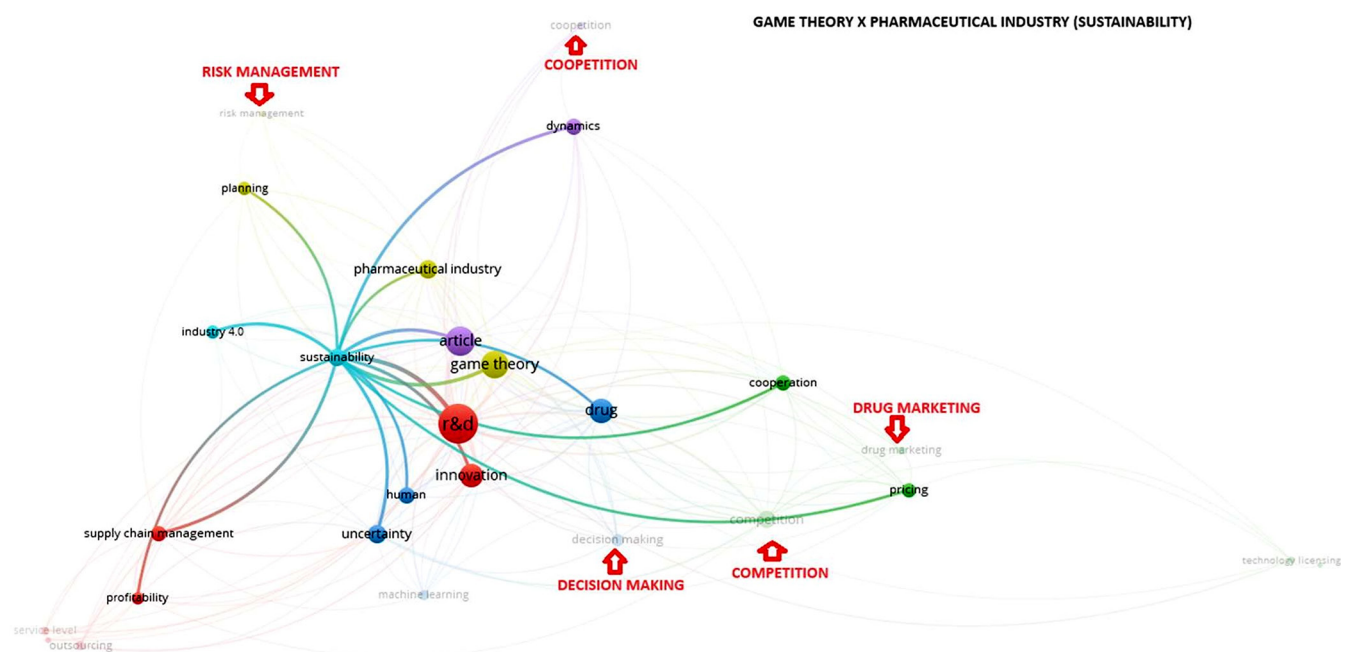
quality, level), Supply Chain Management, and Product Recall. This grouping suggests that game theory can be used to model investment decisions in R&D, considering competition and the need for innovation to maintain competitiveness.

Additionally, game theory can help determine the best strategies for increasing profitability by optimizing processes such as outsourcing and supply chain management. It can also be applied to improve interaction between different parts of the supply chain and to improve risk management, evidenced by the emphasis on product recalls, which must be managed effectively to minimize negative impacts on the company's reputation and finances. The proximity in the semantic network of cooperation, competition, pricing, and drug marketing suggests that these areas are closely related and often studied together in the context of game theory and the pharmaceutical industry. This indicates that medicine marketing strategies are influenced by both cooperation and competition between companies, reflecting the complexity of marketing decisions, where it is necessary to balance market rivalry and strategic partnerships to improve efficiency and innovation. To be more specific, Figure 3 shows the semantic network of Game Theory and the Pharmaceutical Industry, focusing on the word "cooperation."

Several connections can be identified through this semantic network that represent knowledge gaps and research opportunities.

Figure 3 identifies knowledge gaps (highlighted in red) related to research on Game Theory, the Pharmaceutical Industry, and Cooperation: risk management, competition, profitability, and decision-making. These gaps represent opportunities to explore how game theory, through cooperation, can model risk scenarios and develop effective mitigation strategies, improving operational resilience. Furthermore, it allows us to understand the balance between competition and cooperation, facilitating strategic partnerships that promote innovation. Pricing and operations optimization models based on game theory, linked to cooperation, can maximize profitability, while advanced modeling tools can improve strategic decision-making. These insights can guide the pharmaceutical industry to implement more effective and sustainable strategies and better adapt to complex market dynamics. Figure 4 highlights the semantic network of Game Theory x Pharmaceutical Industry x sustainability:

When relating Game Theory, the Pharmaceutical Industry, and Sustainability, some research gaps highlighted in red are identified: risk management,

**Figure 3.** Semantic Network: Game Theory x Pharmaceutical Industry: cooperation.**Figure 4.** Game Theory Semantic Network x Pharmaceutical Industry: sustainability.

coopetition, and competition, decision-making) and drug marketing. These gaps deserve investigation as they can explore how game theory can be used to model environmental risk scenarios in the pharmaceutical industry and develop effective mitigation strategies, promoting operational resilience. Additionally, competition analysis

can identify ways to balance competition and cooperation between pharmaceutical companies to foster innovation and sustainability. Game theory can also help optimize strategic decision-making, such as investments in research and development and marketing strategies, maximizing profitability, and minimizing environmental impacts. These

investigations can provide valuable insights into integrating economic, social, and environmental objectives, creating a more sustainable model for the pharmaceutical industry.

## Conclusion

This study used a bibliometric analysis to understand the current state of the application of game theory in sustainable development strategies in the pharmaceutical industry. The research identified that, despite the great academic interest in integrating game theory with sustainable development, there is a scarcity of studies focused on applying game theory specifically in the pharmaceutical industry and even less in the context of sustainable development in this industry. When examining the intersection between game theory and the pharmaceutical industry, emphasizing cooperative practices, important knowledge gaps were identified that integrate these practices with risk management, profitability, decision-making, and competition, for example. That game theory can be modeled using the logic of cooperative games, building the design of strategic alliances in R&D, where companies collaborate to share costs and benefits, focused on developing new medicines with less environmental impact in a faster and cheaper way. Furthermore, competitive Scenarios can be modeled, where pharmaceutical companies and public laboratories can collaborate in areas of basic research and innovation while competing in the commercialization of products, avoiding oligopolies.

This research is also identified as a knowledge gap, research on the use of game theory in the pharmaceutical industry with a focus on sustainability in which medicine marketing, cooperative practices, coopetition, risk management, and competition are articulated. In this case, game theory can model sustainable medicine marketing practices that are environmentally responsible, competitive, and cooperative.

This research, therefore, brought insights that allowed us to raise several questions,

such as: How can game theory be used to develop sustainable marketing strategies in the pharmaceutical industry? How can game theory balance cooperation and competition (coopetition) between pharmaceutical companies to promote sustainable innovation? How can game theory be used to model sustainable R&D resource allocation? How can game theory help prioritize economic, social, and environmental goals?

Both these questions and the knowledge that came to light in this article address the complexity and interdependence of economic, social, and environmental objectives in the pharmaceutical industry, which can find answers in Game Theory, providing a solid basis for future academic research, which can stimulate new research that also leads to exponential growth in academic interest in the theme of Game Theory to promote the sustainable development of the pharmaceutical industry.

## References

1. Milanesi M, Runfola A, Guercini S. Pharmaceutical industry riding the wave of sustainability: Review and opportunities for future research. *Journal of Cleaner Production* 2020;261:121204.
2. Bourcier-Béquaert B, Bañada-Hirèche L, Sachet-Milliat A. Cure or sell: how do pharmaceutical industry marketers combine their dual mission? An approach using moral dissonance. *Journal of Business Ethics* 2022;1-27.
3. Reinhardt UE. Perspectives on the pharmaceutical industry. *Health Affairs* 2001;20(5):136-149.
4. Bhuiyan BA. An overview of game theory and some applications. *Philosophy and Progress* 2018;59(1-2):111-128.
5. Fiani R. Game theory. 4th ed. – [4th printing] – Rio de Janeiro: GEN Grupo Editorial Nacional. Published by the Editora Atlas label, 2023. Elsevier Brasil, 2006.
6. Palafox-Alcantar PG, Hunt DVL, Rogers CDF. The complementary use of game theory for the circular economy: A review of waste management decision-making methods in civil engineering. *Waste Management* 2020;102:598-612.
7. Chew IML, Tan RR, Foo DCY, Chiu ASF. Game theory approach to the analysis of inter-plant water integration in an eco-industrial park. *Journal of Cleaner Production* 2009;17(18):1611-1619. <https://doi.org/10.1016/J.JCLEPRO.2009.08.005>.

### 3D Modeling of Hospital Environments: Case Study to Improve Patient Safety

Luciane Oliveira Lima<sup>1\*</sup>, Marcelly Ribeiro Bulcão Macêdo<sup>1</sup>, Laura Ferreira Morais de Souza<sup>1</sup>, Camille Pereira Guimarães<sup>1</sup>, Andressa Clara Barbosa de Araujo<sup>2</sup>, Sabrina Cortiana Rodrigues Lima<sup>2</sup>, Cristiane Agra Pimentel<sup>1</sup>

<sup>1</sup>Federal University of Recôncavo da Bahia; <sup>2</sup>Federal University of Bahia; Salvador, Bahia, Brazil

**Hospital environments require reconciling structuring with the National Health Surveillance Agency (ANVISA) standards. In this context, 3D modeling emerges as a tool for modernization and improvement. This article aims to describe its application in a children's physiotherapy room, seeking the best scenario for care and compliance with medical legislation. This case study was conducted in a mother and child complex between February and March 2024. 3D modeling at the studied location demonstrates that the changes made are by standards and promote everyone's satisfaction, efficiency, and well-being, that are inserted.**

**Keywords:** 3D Modeling. Children's Physiotherapy Room. ANVISA.

Hospital institutions have particularities in their architecture that require specific responsibilities to comply with rules and standards established by the National Health Surveillance Agency (ANVISA), seeking to avoid significant problems such as infections and accidents. Thus ensuring the safety and well-being of patients and staff at the site. Therefore, hospital environments still have a gap in structuring qualified patient care and an adequate environment for providing good care from professionals.

3D modeling is crucial in modernizing and improving hospital environments [1]. By offering the ability to visualize and design spaces in a three-dimensional way, this technology not only facilitates compliance with ANVISA's strict standards but also optimizes the arrangement of equipment and the functionality of spaces [2]. In a context where operational efficiency and patient safety are priorities, 3D modeling allows us to anticipate challenges and adjust projects before physical implementation, significantly saving time and resources.

Therefore, the justification for this study is the importance and relevance of using technologies such as three-dimensional modeling to structure

health units. The development of this technology saves time and money when simulating projects, anticipating potential errors to avoid rework and additional expenses [3], being an innovative tool for architects and engineers in the design of hospital facilities, and promoting a more functional and adaptable environment to demands dynamics of modern healthcare.

The study's objective is to apply 3D modeling in a children's physiotherapy room to simulate an environment that promotes satisfaction, efficiency, and well-being for those involved, following the regulations established by ANVISA.

#### Anvisa Resolutions in Hospital Settings

In Brazil, ANVISA establishes strict guidelines for the choice, acquisition, storage, and use of medical technologies, ensuring that devices meet the highest standards of safety and effectiveness [4]. The resolutions described below were used for the children's physiotherapy room studied.

**RDC N° 50/2002:** Provides technical regulations for planning, programming, elaboration, and evaluation of physical projects for healthcare establishments [5].

**RDC N° 63/2011:** This resolution establishes the requirements of good practices for operating health services, aiming to guarantee patient safety and quality of care [6].

Received on 28 September 2024; revised 20 December 2024.  
Address for correspondence: Luciane Oliveira Lima. T. José Lúcio de Oliveira Lima, 43 - Novo Horizonte. Zipcode: 48009-582. Alagoinhas, Bahia, Brazil. E-mail: luciane@aluno.ufrb.edu.br.

J Bioeng. Tech. Health 2024;7(4):399-404  
© 2024 by SENAI CIMATEC. All rights reserved.



**RDC N° 307/2002:** Provides minimum requirements for the operation of health services, including infrastructure and operation criteria to guarantee the quality and safety of the services provided [7].

**RDCN°36/2013:** Institutes actions for patients safety in health services and provides other measures, emphasizing risk prevention and control [8].

## Materials and Methods

This work was based on a case study, a methodology that makes it possible to study a place, a human being, or something specific in-depth [9]. The study was carried out between February and March 2024, and the research location was a child physiotherapy room in a maternal and child complex at the obstetric hospital in Feira de Santana. For this purpose, study hypotheses were raised, such as:

- What changes are generated from 3D modeling?

- Have ANVISA resolutions made the changes?
- Do the improvements impact patient safety and quality?

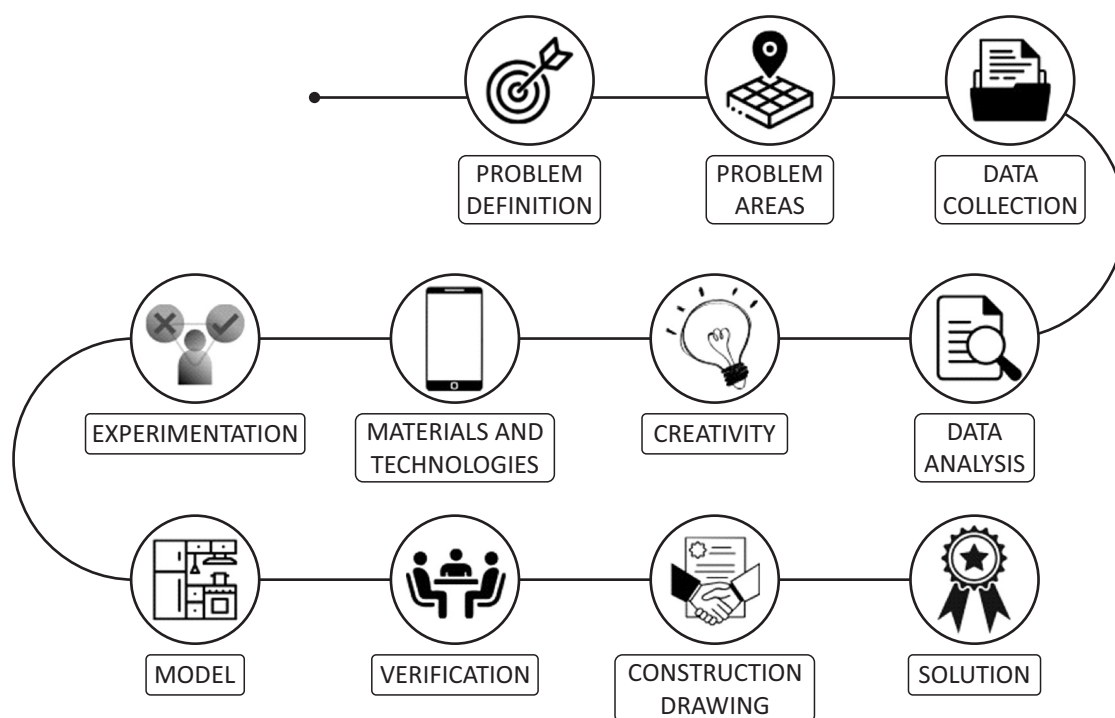
To create the three-dimensional model, a method was used based on 11 steps adapted from Munari [10], which will be presented and detailed below (Figure 1):

**Problem Definition:** The study focused on actions to physically adapt the children's physiotherapy room to ANVISA standards, aiming to meet the needs identified in audits and achieve the health unit's goals.

**Problem Areas:** The study, after the initial stage, was divided into specific subproblems to meet the needs of the hospital, focusing the analysis on the children's physiotherapy room.

**Data Collection:** Data collection was carried out by identifying critical points. Analyzing ANVISA

**Figure 1.** Research method.



Source: adapted Munari [10].



resolutions was essential to defining the specific needs to be met. The standards consulted were RDC 50/2002, RDC 63/2011, RDC 307/2002, AND RDC 36/2013.

**Data Analysis:** A detailed analysis of the content of each resolution and standard was carried out, seeking to identify the specific requirements that applied to the hospital environment under study.

**Creativity:** The analysis revealed that 3D modeling was a promising tool for visualizing spaces. Using this technique, it was possible to create intuitive and dynamic representations of spaces, facilitating the understanding of the characteristics and needs of each location.

**Materials and Technology:** Looking for an economical, accessible, versatile, and easy-to-use solution, the choice fell on the Room Planner application. The application is free and available for mobile devices. It offers a wide range of products (equipment and materials), information about stores and prices, and fidelity to the actual measurements of the environment and products.

**Experimentation:** Experimenting with the Room Planner application began the construction of the 3D modeling, following a few steps: first, the existing materials and equipment in the location were added, with their actual measurements, for an accurate visualization of the space. After adjustment, the items were placed in the desired locations. Finally, the remaining necessary products were researched, added to the modeling, and organized in the desired way.

**Model:** After creating the initial model, three other models with different layouts were developed to find the best solution. Once the alternatives were finalized, the final model was selected.

**Verification:** After finalizing the 3D model, a crucial validation step was carried out with the study's target audience. This stage involved

presenting the model to the coordination of the Quality and Patient Safety Center and the hospital board. The objective was to obtain feedback on the model, identify areas for improvement, and seek final approval.

**Construction Drawing:** A construction document was prepared to complete the work. This detailed the situation in the modeled environments, with comprehensive records and descriptions of all relevant aspects. The document included images and detailed descriptions of the 3D modeling and a complete list of necessary materials and equipment, with their respective measurements and specifications.

**Solution:** The finalized and validated 3D model solved the study's initial problem. The next step will be implementing the proposed solutions in the modeled environments and adapting them to ANVISA standards to guarantee a safe and quality environment for patients and healthcare professionals.

## Results and Discussion

In this study, the effects of using technology on the experience of patients and employees in the children's physiotherapy room were analyzed, making it possible to simulate the scenarios and identify and correct existing inadequacies in the location. According to Souza [2], the project is seen as a whole in a three-dimensional creation, enabling a broad view of the study site. In this context, the modeling in the children's physiotherapy room demonstrates that the changes made are by the RDC mentioned above; the improvements made and their relationship with the standards established by ANVISA are described in Table 1.

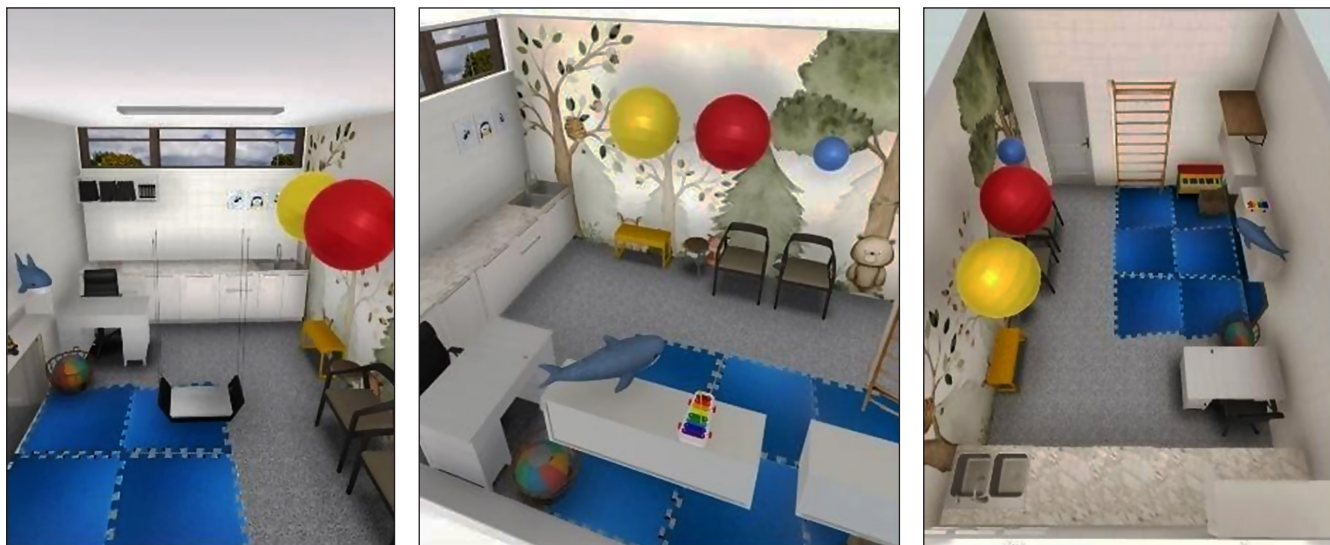
From these improvements, the construction of the future state was made; in Figures 2 and 3, it is possible to visualize the transformation to a space with more excellent safety, comfort, and compliance with ANVISA legislation for

**Table 1.** Improvements and their resolutions.

DRC	Standard Compliance	Improvement
Nº 50/2002	This resolution helps ensure the children's physiotherapy room has adequate dimensions, ventilation, lighting, and appropriate materials.	Exchange of old equipment for more modern ones; solutions for ceiling infiltration; space optimization and removal of equipment that does not belong on site
Nº 63/2011	This RDC considers implementing a quality policy to manage services according to rules and focusing on quality management, patient safety, organizational conditions, the physiotherapist's health protection, and the site's infrastructure management.	Improved workflow; positioning sockets close to the places and equipment required; removing cardboard boxes and photo walls; creating a hygiene policy.
Nº 307/2002	Ensures that the children's physiotherapy room provides a safe and efficient service.	Removing cracks in the ceiling.
Nº 36/2013	Contributes to children's safety during physiotherapy, preventing falls and accidents	Swings with ideal and fixed supports

**Figure 2.** Current status of the children's physiotherapy room.

**Figure 3.** 3D modeling of the children's physiotherapy room.



hospital environments. Providing more excellent quality of care for employees and patients through outstanding organization, efficiency, use of unused available materials, and acquisition of essential resources to provide greater satisfaction.

According to Lozado [11], public or private hospitals must adapt to established quality standards, thus aiming to improve performance and the provision of services offered to patients. Investment in infrastructure, equipment, and materials combined with policies and standards are essential to ensure patient safety [12]. Therefore, institutions that do not prioritize these investments contribute to risks and incidents related to patient care.

## Conclusion

Based on the above, 3D modeling is an indispensable tool in planning and optimizing hospital environments. Using architectural software, it is possible to create three-dimensional representations, allowing a complete visualization and better analysis of these spaces. Thus, adopting this proves to be an efficient tool, but it is essential to guaranteeing well-designed, functional, and adapted hospital settings to the needs of healthcare professionals and patients. It is concluded that the initial objective of the work

was achieved, and the application of 3D modeling in the planning of a children's physiotherapy room proved to be an effective tool to ensure compliance with ANVISA regulations and to create an environment that promotes satisfaction, efficiency, and well-being. The tool allows detailed visualization and adjustment of different aspects of the environment, resulting in a functional, safe, and welcoming space for children.

## References

1. Pinheiro CMP, Mota GE, Steinhaus C, Souza M. 3D printers: A change in the dynamics of consumption. *Signs of Consumption*, São Paulo 2018;10(1):15-22.
2. Souza X et al. 3D Modeling for architecture: A study applied to design teaching. *Social & Applied Humanities* 2019;9(26):163–171. Available at: <https://doi.org/10.25242/887692620191891>
3. Vilela J et al. 3D modeling of historic buildings: Digital technologies and international cooperation in the management of cultural, architectural and urban heritage. *Project Management and Technology*. São Paulo-SP 2021;16:148-162. Available at: <https://www.revistas.usp.br/gestaodeprojetos/article/view/174398/171770>.
4. ANVISA. Ministry of Health. National Health Surveillance Agency. Resolution-RDC No. 509, of May 27, 2011. Provides for the management of health technologies in health establishments. Published in the Official Gazette of the Union. Available at: <https://>

- bvsms.saude.gov.br/bvs/saudelegis/anvisa/2020/rdc0509\_27\_05\_2021.pdf.
5. ANVISA. Ministry of Health. National Health Surveillance Agency. Resolution RDC nº 50, of February 21, 2002. Provides for the Technical Regulation for planning, programming, preparation and evaluation of physical projects for healthcare establishments. Official Gazette of the Union, Brasília, DF. Available in: [https://bvsms.saude.gov.br/bvs/saudelegis/anvisa/2002/rdc0050\\_21\\_02\\_2002.html](https://bvsms.saude.gov.br/bvs/saudelegis/anvisa/2002/rdc0050_21_02_2002.html).
  6. ANVISA. Ministry of Health. National Health Surveillance Agency. Resolution-RDC nº 63, of November 25, 2011. Provides for the Requirements for Good Operating Practices for Health Services. Published in the Official Gazette of the Union. Available at: [https://bvsms.saude.gov.br/bvs/saudelegis/anvisa/2011/rdc0063\\_25\\_11\\_2011](https://bvsms.saude.gov.br/bvs/saudelegis/anvisa/2011/rdc0063_25_11_2011).
  7. Brazil. Ministry of Health. National Health Surveillance Agency. Resolution of the Collegiate Board – RDC No. 307, of November 14, 2002. Amends the Resolution - RDC No. 50 of February 21, 2002. Official Gazette of the Union: section 1, Brasília, DF. Available at: [https://bvsms.saude.gov.br/bvs/saudelegis/anvisa/2002/rdc0307\\_14\\_11\\_2002.html](https://bvsms.saude.gov.br/bvs/saudelegis/anvisa/2002/rdc0307_14_11_2002.html).
  8. Brazil. Ministry of Health. National Health Surveillance Agency. Resolution of the Collegiate Board – RDC No. 36, of July 25, 2013. Establishes actions for patient safety in health services and provides other measures. Official Gazette of the Union, Brasília, DF. Available at: [https://bvsms.saude.gov.br/bvs/saudelegis/anvisa/2013/rdc0036\\_25\\_07\\_2013.pdf](https://bvsms.saude.gov.br/bvs/saudelegis/anvisa/2013/rdc0036_25_07_2013.pdf).
  9. Freitas WRS, Jabbour JC. Using case study as a qualitative research strategy: good practices and suggestions. *Lajeado: Study & Debate, Lajeado, RS, Brazil* 2022;18(2):7-22. Available at: <http://www.meep.univates.br/revistas/index.php/estudoedebate/article/view/560/550>.
  10. Munari B. Things are born from things. São Paulo: Martins Fontes, 2000.
  11. Lozado LFP Health quality indicators: reality of a surgical clinical inpatient unit of a hospital in the interior of Rio Grande do Sul/RS. Completion of course work. University of Santa Cruz do Sul. Santa Cruz do Sul. 2017.
  12. Siqueira CL, Silva CC, Teles JKN, Feldman LB. Risk management: perception of nurses in two hospitals in the south of Minas Gerais, Brazil. *Revista Mineira de Enfermagem* 2015;19(4):919-26.



## Instructions for Authors

The Authors must indicate in a cover letter the address, telephone number and e-mail of the corresponding author. The corresponding author will be asked to make a statement confirming that the content of the manuscript represents the views of the co-authors, that neither the corresponding author nor the co-authors have submitted duplicate or overlapping manuscripts elsewhere, and that the items indicated as personal communications in the text are supported by the referenced person. Also, the protocol letter with the number should be included in the submission article, as well as the name of sponsors (if applicable).

Manuscripts may be submitted within designated categories of communication, including:

- Original basic or clinical investigation (original articles on topics of broad interest in the field of bioengineering and biotechnology applied to health). We particularly welcome papers that discuss epidemiological aspects of international health, clinical reports, clinical trials and reports of laboratory investigations.
- Case presentation and discussion (case reports must be carefully documented and must be of importance because they illustrate or describe unusual features or have important practice implications).
- Brief reports of new methods or observations (short communications brief reports of unusual or preliminary findings).

- State-of-the-art presentations (reviews on protocols of importance to readers in diverse geographic areas. These should be comprehensive and fully referenced).
- Review articles (reviews on topics of importance with a new approach in the discussion). However, review articles only will be accepted after an invitation of the Editors.
- Letters to the editor or editorials concerning previous publications (correspondence relating to papers recently published in the Journal, or containing brief reports of unusual or preliminary findings).
- Editor's corner, containing ideas, hypotheses and comments (papers that advance a hypothesis or represent an opinion relating to a topic of current interest).
- Innovative medical products (description of new biotechnology and innovative products applied to health).
- Health innovation initiatives articles (innovative articles of technological production in Brazil and worldwide, national policies and directives related to technology applied to health in our country and abroad).

The authors should checklist comparing the text with the template of the Journal.

Supplements to the JBTH include articles under a unifying theme, such as those summarizing presentations of symposia or focusing on a specific subject. These will be added to the regular publication of the Journal as appropriate, and will be peer reviewed in the same manner as submitted manuscripts.

## Statement of Editorial Policy

The editors of the Journal reserve the right to edit manuscripts for clarity, grammar and style. Authors will have an opportunity to review these changes prior to creation of galley proofs. Changes in content after galley proofs will be sent for reviewing and could be required charges to the author. The JBTH does not accept articles which duplicate or overlap publications elsewhere.

### Peer-Review Process

All manuscripts are assigned to an Associate Editor by the Editor-in-Chief and Deputy

Editor, and sent to outside experts for peer review. The Associate Editor, aided by the reviewers' comments, makes a recommendation to the Editor-in-Chief regarding the merits of the manuscript. The Editor-in-Chief makes a final decision to accept, reject, or request revision of the manuscript. A request for revision does not guarantee ultimate acceptance of the revised manuscript.

Manuscripts may also be sent out for statistical review ou *ad hoc* reviewers. The average time from submission to first decision is three weeks.



## Revisions

Manuscripts that are sent back to authors for revision must be returned to the editorial office by 15 days after the date of the revision request. Unless the decision letter specifically indicates otherwise, it is important not to increase the text length of the manuscript in responding to the comments. The cover letter must include a point-by-point response to the reviewers and Editors comments, and should indicate any additional changes made. Any alteration in authorship, including a change in order of authors, must be agreed upon by all authors, and a statement signed by all authors must be submitted to the editorial office.

## Style

Manuscripts may be submitted only in electronic form by [www.jbth.com.br](http://www.jbth.com.br). Each manuscript will be assigned a registration number, and the author notified that the manuscript is complete and appropriate to begin the review process. The submission file is in OpenOffice, Microsoft Word, or RTF document file format for texts and JPG (300dpi) for figures.

Authors must indicate in a cover letter the address, telephone number, fax number, and e-mail of the corresponding author. The corresponding author will be asked to make a statement confirming that the content of the manuscript represents the views of the co-authors, that neither the corresponding author nor the co-authors have submitted duplicate or overlapping manuscripts elsewhere, and that the items indicated as personal communications in the text are supported by the referenced person.

Manuscripts are to be typed as indicated in Guide for Authors, as well as text, tables, references, legends. All pages are to be numbered with the order of presentation as follows: title page, abstract, text, acknowledgements, references, tables, figure legends and figures. A running title of not more than 40 characters should be at the top of each page. References should be listed consecutively in the text and recorded as follows in the reference list, and must follow the format of the National

Library of Medicine as in Index Medicus and “Uniform Requirements for Manuscripts Submitted to Biomedical Journals” or in “Vancouver Citation Style”. Titles of journals not listed in Index Medicus should be spelled out in full.

Manuscript style will follow accepted standards. Please refer to the JBTH for guidance. The final style will be determined by the Editor-in-Chief as reviewed and accepted by the manuscript’s corresponding author.

## **Approval of the Ethics Committee**

The JBTH will only accept articles that are approved by the ethics committees of the respective institutions (protocol number and/or approval certification should be sent after the references). The protocol number should be included in the end of the Introduction section of the article.

## **Publication Ethics**

Authors should observe high standards with respect to publication ethics as set out by the International Committee of Medical Journal Editors (ICMJE). Falsification or fabrication of data, plagiarism, including duplicate publication of the authors’ own work without proper citation, and misappropriation of the work are all unacceptable practices. Any cases of ethical misconduct are treated very seriously and will be dealt with in accordance with the JBTH guidelines.

## Conflicts of Interest

At the point of submission, each author should reveal any financial interests or connections, direct or indirect, or other situations that might raise the question of bias in the work reported or the conclusions, implications, or opinions stated - including pertinent commercial or other sources of funding for the individual author(s) or for the associated department(s) or organizations(s), and personal relationships. There is a potential conflict of interest when anyone involved in the publication process has a financial or other beneficial interest in

the products or concepts mentioned in a submitted manuscript or in competing products that might bias his or her judgment.

### Materials Disclaimer

The opinions expressed in JBTH are those of the authors and contributors, and do not necessarily reflect those of the SENAI CIMATEC, the editors,

the editorial board, or the organization with which the authors are affiliated.

### Privacy Statement

The names and email addresses entered in this Journal site will be used exclusively for the stated purposes of this journal and will not be made available for any other purpose or to any other party.

### Brief Policies of Style

Manuscript	Original	Review	Brief Communication	Case Report	Editorial ; Letter to the Editor; Editor' s Corner	Innovative Medical Products	State-of-the-Art	Health Innovation Initiatives
Font Type	Times or Arial	Times or Arial	Times or Arial	Times or Arial	Times or Arial	Times or Arial	Times or Arial	Times or Arial
Number of Words – Title	120	90	95	85	70	60	120	90
Font Size/Space-Title	12; double space	12; double space	12; double space	12; double space	12; double space	12; double space	12; double space	12; double space
Font Size/Space-Abstracts/Key Words and Abbreviations	10; single space	10; single space	10; single space	10; single space	-	-	10; single space	10; single space
Number of Words – Abstracts/Key Words	300/5	300/5	200/5	250/5	-	-	300/5	300/5
Font Size/Space-Text	12; Double space	12; Double space	12; Double space	12; Double space	12; Double space	12; Double space	12; Double space	12; Double space
Number of Words – Text	5,000 including spaces	5,500 including spaces	2,500 including spaces	1,000 including spaces	1,000 including spaces	550 including spaces	5,000 including spaces	5,500 including spaces
Number of Figures	8 (title font size 12, double space)	3 (title font size 12, double space)	2 (title font size 12, double space)	2 (title font size 12, double space)	-	2 (title font size 12, double space)	8 (title font size 12, double space)	8 (title font size 12, double space)
Number of Tables/Graphic	7 title font size 12, double space	2 title font size 12, double space	2(title font size 12, double space)	1(title font size 12, double space)	-	-	7 title font size 12, double space	4 title font size 12, double space
Number of Authors and Co-authors*	15	10	5	10	3	3	15	10
References	20 (font size 10,single space	30(font size 10,single space	15 (font size 10,single space)	10 (font size 10,single space)	10 (font size 10,single space	5(font size 10,single space	20 (font size 10,single space	20

\*First and last name with a sequencing overwritten number. Corresponding author(s) should be identified with an asterisk; Type 10, Times or Arial, single space. Running title of not more than 40 characters should be at the top of each page. References should be listed consecutively in the text. References must be cited on (not above) the line of text and in brackets instead of parentheses, e.g., [7,8]. References must be numbered in the order in which they appear in the text. References not cited in the text cannot appear in the reference section. References only or first cited in a table or figures are numbered according to where the table or figure is cited in the text. For instance, if a table is placed after reference 8, a new reference cited in table 1 would be reference 9.1 would be reference 9.

## Checklist for Submitted Manuscripts

- ☐1. Please provide a cover letter with your submission specifying the corresponding author as well as an address, telephone number and e-mail.
- ☐2. Submit your paper using our website [www.jbth.com.br](http://www.jbth.com.br). Use Word Perfect/Word for Windows, each with a complete set of original illustrations.
- ☐3. The entire manuscript (including tables and references) must be typed according to the guidelines instructions.
- ☐4. The order of appearance of material in all manuscripts should be as follows: title page, abstract, text, acknowledgements, references, tables, figures/graphics/diagrams with the respective legends.
- ☐5. The title page must include a title of not more than three printed lines (please check the guidelines of each specific manuscript), authors (no titles or degrees), institutional affiliations, a running headline of not more than 40 letters with spaces.
- ☐6. Acknowledgements of persons who assisted the authors should be included on the page preceding the references.
- ☐7. References must begin on a separate page.
- ☐8. References must be cited on (not above) the line of text and in brackets instead of parentheses, e.g., [7,8].
- ☐9. References must be numbered in the order in which they appear in the text. References not cited in the text cannot appear in the reference section. References only or first cited in a table or figures are numbered according to where the table or figure is cited in the text. For instance, if a table is placed after reference 8, a new reference cited in table 1 would be reference 9.
- ☐10. Reference citations must follow the format established by the “Uniform Requirements for Manuscripts Submitted to Biomedical Journals” or in “Vancouver Citation Style”.
- ☐11. If you reference your own unpublished work (i.e., an “in press” article) in the manuscript that you are submitting, you must attach a file of the “in press” article and an acceptance letter from the journal.
- ☐12. If you cite unpublished data that are not your own, you must provide a letter of permission from the author of that publication.
- ☐13. Please provide each figure in high quality (minimum 300 dpi: JPG or TIF). Figure must be on a separate file.
- ☐14. If the study received a financial support, the name of the sponsors must be included in the cover letter and in the text, after the author’s affiliations.
- ☐15. Provide the number of the Ethics Committees (please check the guidelines for authors).